A study of Fluctuations and Transport in Non-equilibrium systems

by

Rahul Marathe

A Thesis submitted to the
Jawaharlal Nehru University
for the Degree of
Doctor of Philosophy

2008

Raman Research Institute
Bangalore 560 080
India

Certificate:

This is to certify that the thesis entitled **A study of Fluctuations and Transport in Non-equilibrium systems** submitted by **Mr. Rahul Marathe** for the award of the degree of Doctor of Philosophy of Jawaharlal Nehru University is his original work. This has not been published or submitted to any other University for any other Degree or Diploma.

Prof. Ravi Subrahmanyan
(Center Chairperson)
Director,
Raman Research Institute,
Bangalore 560 080, INDIA.

Prof. Abhishek Dhar
(Thesis Supervisor)
Raman Research Institute,
Bangalore 560 080, INDIA.

Declaration:

I hereby declare that the work reported in this thesis is entirely original. This thesis is composed independently by me at Raman Research Institute under the supervision of Prof. Abhishek Dhar. I further declare that the subject matter presented in this thesis has not previously formed the basis for the award of any degree, diploma, membership, associateship, fellowship or any other similar title of any university or institution.

(Prof. Abhishek Dhar) (Rahul Marathe)

Theoretical Physics,

Raman Research Institute,

Bangalore 560 080, INDIA.

Acknowledgement:

First and foremost my parents, aunt and my wife Shraddha are responsible for me being here. They always encouraged me to do something different than others and be confident about the same. Emotional support given by Shraddha was always helpful and encouraging.

It was a great experience to work with Prof. Abhishek Dhar, who was always very understanding, helpful in every respect and ever ready for discussions, who always let me do things which interests me and sometimes advice, threaten, suggest whenever needed. Lots of discussions mainly with Prof. Arun Jayannavar, Prof. Madan Rao, Dr. Kavita Jain and Prof. N. Kumar have led to good collaborative work during my PhD work. I surely wish to collaborate with all of them in future.

It has been a very good stay at RRI doing my PhD work. Lots of people are responsible for making this stay happening, interesting and enjoyable. Though "quite" busy in research many people, my batch mates, seniors, juniors were very helpful in every respect. We had lots of discussions, debates on many different subjects apart from physics and science.

Apart from research and studies, RRI and IISc campus has given me a lot to learn, in these campuses I have observed and photographed lots of birds and flowers. Though RRI is a small campus, it shows a surprisingly amazing variety of flora and fauna. Here I have enjoyed playing different games mainly football and badminton. Badminton yearly tournaments were just fantastic. I also have enjoyed playing carom with many people in hostel as well as in the campus.

Last but not the least, I wish to thank all the people in RRI, administrative as well as academic for making this stay enjoyable. Also I would like to thank all those restaurants and pubs around Bangalore for serving us "lots of times" good beer and food.

Dedicated to my late grandparents.....

Contents

Preface

There are very few general results in statistical physics which are valid for systems far from equilibrium. Among these are the non-equilibrium fluctuation theorems which put conditions on the probability distribution of entropy production in non-equilibrium systems. Another is the Jarzynski equality, which relates the non-equilibrium work done on a system to equilibrium free energy differences. Unlike linear response theory, these relations are valid for systems arbitrarily far away from equilibrium. These relations are exact no matter how far the system is driven out of equilibrium and are independent of the rate and strength of perturbation. In the first part of the thesis we look at some examples of non-equilibrium processes in the context of these new results.

A class of far from equilibrium systems are the so called ratchet models and microscopic models of pumps and engines. These models exhibit net directed transport of particles in the system in the presence of noise and driving and in the absence of any applied external bias. The first such construct of a miniature molecular engine was by Feynman. This is the Feynman ratchet and pawl engine, (discussed in *Feynman lectures on Physics*), which was first proposed as a microscopic mechanical model to explain the problem in constructing a Maxwell's demon. Similar models, based on the same principle, have recently been studied to understand the working of molecular motors and pumps in biological systems. These molecular motors (e.g. kinesin) move uni-directionally on the microtubules inside biological cells. Also, molecular pumps, like sodium or potassium pumps, maintain active transport across membranes against a concentration gradient. These motors and pumps are in a very noise environment but still they exhibit net uni-directional motion. The second part of the thesis includes studies on some new models of heat/particle pumps and engines.

In chapter 2 of the thesis we look at the validity of different fluctuation theorems for a simple system of a single Ising spin in contact with a heat bath and driven by an external time dependent magnetic field. We explicitly compute the distribution of the work done in driving the spin over a fixed time interval. The time evolution of the spin is modelled using Glauber dynamics. Monte-Carlo simulations are performed to find the work distributions

at different driving rates. We find that in general the work-distributions are broad with a significant probability for processes with negative dissipated work. The special cases of slow and fast driving rates are studied analytically.

In chapter 3 we look at some simple models of heat pumps. Motivated by recent studies on models of quantum particle and heat pumps, we study similar classical models and examine the possibility of heat pumping. Unlike many of the usual ratchet models of molecular engines, the models we study here do not have particle transport. We consider a two-spin system and a coupled oscillator system which exchange heat with multiple heat reservoirs and which are acted upon by periodic forces. The simplicity of our models allows accurate numerical and exact solutions and unambiguous interpretation of results. We demonstrate that while both our models seem to be built on similar principles, one is able to function as a heat pump (and also as an engine) while the other is not.

In chapter 4 we look at a model of a particle pump. We study a symmetric exclusion process in which the hopping rates at two (or more) chosen sites vary periodically in time and have a relative phase difference. This mimics a colloidal suspension subjected to external space and time dependent modulation of the diffusion constant. The two special sites act as a classical pump by generating an oscillatory current with a nonzero $\mathcal{DC}$ value whose direction depends on the applied phase difference. We analyze various features of this model through simulations and obtain an expression for the $\mathcal{DC}$ current via a novel perturbative treatment.

This work is done in collaboration with my thesis supervisor Prof. Abhishek Dhar and with Prof. Arun Jayannvar, Institute of Physics, Bhubaneshwar, Dr. Kavita Jain, JNCASR, Bangalore and Dr. Abhishek Chaudhury, Raman Research Institute, Bangalore.

Publications

- Work distribution functions for hysteresis loops in a single-spin system, Rahul Marathe and Abhishek Dhar, Phys. Rev. E **72**, 066112 (2005).
- Two simple models of classical heat pumps, Rahul Marathe, A. M. Jayannavar, and Abhishek Dhar, Phys. Rev. E **75**, 030103(R) (2007).

- Driving particle current through narrow channels using a classical pump, Kavita Jain, Rahul Marathe, Abhishek Chaudhuri, Abhishek Dhar, Phys. Rev. Lett., **99**, 190601 (2007).

- Particle current in symmetric exclusion process with time-dependent hopping rates, Rahul Marathe, Kavita Jain, Abhishek Dhar. Submitted to Journal of Statistical Mechanics (2008).

1 Introduction.

Any system in equilibrium can be fully described by the Boltzmann-Gibb's theory of ensembles. For a system in contact with a heat bath, the phase-space probability distribution is given by the canonical distribution. This expression is very general and can be applied to any given equilibrium system. One can then calculate the partition function and from this the free energy of the system. From this all equilibrium properties of a system can, in principle, be calculated. In practice of course this can be difficult and an explicit calculation of specific properties may not always be possible.

There is a large class of phenomena which cannot be described by the Boltzmann-Gibb's ensemble theory. These include non-equilibrium phenomena in glassy systems, granular material, electrical and thermal transport. The reasons that the equilibrium description breaks down in these systems can be various: for example there may be no Hamiltonian description; or the Hamiltonian is time-dependent; or relaxation times are extremely slow, etc.

There are few theories, such as those of non-equilibrium thermodynamics and theory of linear response, to describe some of these non-equilibrium phenomena. However, they work only in the linear regime where the perturbed system is slightly out of equilibrium. These theories thus have a very limited range of applicability. There is no general framework to treat non-equilibrium phenomena which is valid for systems far from equilibrium. In the absence of a general theory for such systems, one approach is to take simple but nontrivial model systems and understand their behaviour from first principles.

In the last decade the situation has changed somewhat. Certain general relations have been discovered which are valid independent of how far a system is driven out of equilibrium. These results include (1) the Jarzynski equality [3 – 6] and (2) the fluctuation theorems

[7 – 17]. These results are now being extended and shown to be valid for many different systems, dynamics (deterministic as well as stochastic) and ensembles. They have been verified for a variety of systems theoretically [18 – 20] as well as experimentally [21 – 24]. After the work by Crooks [10] and Seifert [11], it is now understood that many of these relations are closely related and are the manifestations of a single theorem, the theorem which connects the path probability of a thermostatted system to its time reversed trajectory. In Sec. (1.1) we will briefly describe these results on non-equilibrium fluctuations and state the new results obtained by us.

Another class of problems in non-equilibrium physics, which cannot be treated by conventional theories, is that of ratchet systems and of molecular pumps and engines. These are systems which are driven out of equilibrium by some external parameter and exhibit many interesting phenomenas like uni-directional current, resonances etc. Among their applications it has been proposed to model the behaviour of molecular motors and pumps in biological systems. There have also been many studies on the quantum version of such particle and heat pumps. So it is interesting to look at whether the quantum nature of a system is an essential requirement. In Sec. (1.2) we will briefly describe some known results on these systems and discuss our contribution.

1.1 The Jarzynski equality and the fluctuation theorems

Consider a system in contact with a heat reservoir. Let some parameter, λ, for example the external field on a magnet or the volume of a gas etc. be varied in time from an initial point λ_A to a final point λ_B (in general there can be many time-dependent parameters $\boldsymbol{\lambda} = \{\lambda_1, \lambda_2, ..., \lambda_n\}$ in the system). With this parameter variation, work is done on the system. Then, conventional thermodynamics tells us that the work done W, on the system is always greater than or equal to the free energy (Helmholtz free energy) difference. Thus:

$$W \geq \Delta F, \tag{1.1}$$

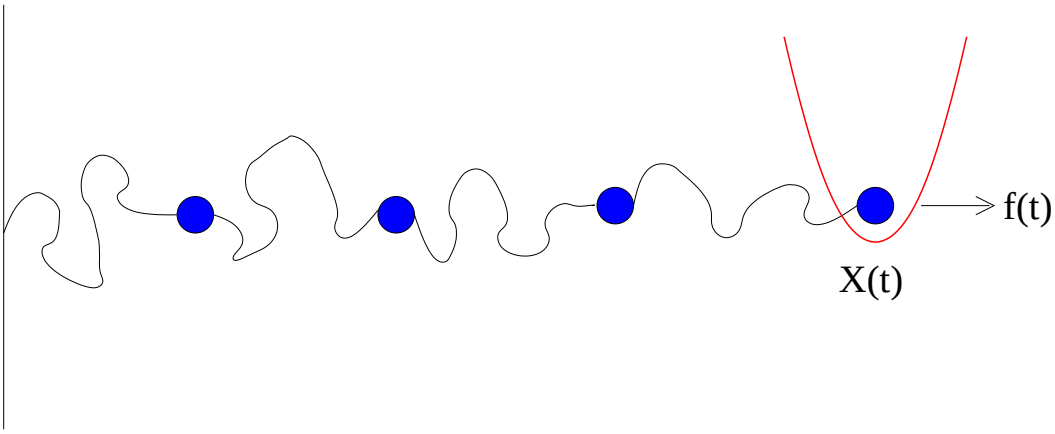

Figure 1.1: A polymer being stretched by an optical trap potential.

where, $\Delta F = F(\lambda_B) - F(\lambda_A)$. This result basically follows from the second law. The equality holds for a quasi-static, reversible process. For example consider a system as shown in Fig. (1.1). This is an example of a polymer placed in a bath at temperature T and stretched by an external time-dependent force $f(t)$ (thus $\lambda(t) = f(t)$ in this case) by means of, for example, an optical trap. The process is done in the following way. At time $t = 0$ the system is in equilibrium at a temperature T. Then the force is applied from time $t = 0$ to $t = \tau$. This stretching process is done for large number of times, every time starting the system in equilibrium and with the force following the same protocol $f(t)$. If such a process is done at a finite rate, then since we start with different initial equilibrium conditions and also because of the stochastic dynamics, we will get different amount of work done in different realizations. Hence we can find the distribution of work $P(W)$. Though the average work $\langle W \rangle$ is always greater than ΔF for all rates, the distribution may have a large negative part. This negative part implies that for some realizations of the experiment, system is doing work on the external agent while extracting heat from the reservoir. This contribution can be large if the system is non-thermodynamic, and can be viewed as transient violation of the second law. This observation of apparent violation of second law also startled early observers of Brownian motion. In his book [2], Perrin discusses this point. Here we give a paragraph from the same book:

It is clear that this agitation (of a Brownian particle) is not contradictory to the principle

of conservation of energy. It is sufficient that every increase in the speed of a granule is accompanied by a cooling of the liquid in its immediate neighbourhood, and like wise every decrease of speed by a local heating, without loss or gain of energy.

Perrin also stresses the following point that the Brownian motion (or motion at small scales) is not reconcilable with rigid enunciations too frequently given to Carnot's principle, because in a given realization a particle can spontaneously do work at the expense of the surrounding medium (heat bath).

So it must not any longer be said that perpetual motion of the second sort is impossible, but one must say: " On the scale of size (macroscopic) which interests us practically, perpetual motion of the second sort is in general so insignificant that it would be absurd to take into account."

But at the microscopic scales this fluctuations about the most probable behaviour are important and their study might provide us with a better understanding of the second law.

Let us now go back to our discussion of the Jarzynski equality. We consider a general Hamiltonian of a system given by $H_\lambda(\mathbf{x},\ \mathbf{p})$, where $\mathbf{x} = \{x_1, x_2, ...x_n\}$ and $\mathbf{p} = \{p_1, p_2, ...p_n\}$ are usual phase-space variables and λ is the parameter which is varied in time from λ_A to λ_B in time τ following a fixed protocol $\lambda(t)$. Then Jarzynski considers the following definition of work done on the system:

$$W_J = \int_0^\tau \frac{\partial H_\lambda(\mathbf{x},\ \mathbf{p})}{\partial t}\, dt = \int_0^\tau \frac{\partial H_\lambda(\mathbf{x},\ \mathbf{p})}{\partial \lambda}\, \frac{d\lambda}{dt}\ dt. \tag{1.2}$$

We take an ensemble of such processes, with initial conditions for the system generated from a canonical distribution at temperature T. Then the work done W_J can be calculated for every trajectory in the phase-space given by $(\mathbf{x}(t),\ \mathbf{p}(t))$. This work is a fluctuating quantity because of two reasons:

1. The initial conditions are generated from a canonical distribution, hence we get different work for different initial conditions.

2. The heat bath generates stochastic forces, which cause fluctuations in the phase-space

paths taken by the system.

It was proved by Jarzynski, that the distribution $P(W_J)$ satisfies the following equality:

$$\langle \exp\{-\beta W_J\} \rangle = \int_{-\infty}^{\infty} dW_J \exp\{-\beta W_J\} P(W_J) = \exp\{-\beta \Delta F\}, \tag{1.3}$$

where $\beta = 1/k_B T$. We now give a proof that of the Jarzynski equality, for the case where the system is in contact with a heat bath at time $t = 0$ and in equilibrium, but the heat bath is then removed during the driving process. Then the evolution of the system is deterministic and described by the phase-space trajectory $(\mathbf{x}(t),\ \mathbf{p}(t))$ which evolves according to $H_\lambda(\mathbf{x}(t),\ \mathbf{p}(t))$, with λ taken from λ_A to λ_B in time τ. Let the ensemble of such trajectories be described by the initial phase-space density given by:

$$\rho_{\lambda_A}(\mathbf{x}(0),\ \mathbf{p}(0)) = \frac{1}{Z_{\lambda_A}} \exp\{-\beta H_{\lambda_A}(\mathbf{x}(0),\ \mathbf{p}(0))\}, \tag{1.4}$$

where $Z_\lambda = \int exp\{-\beta H_\lambda\}\ d\mathbf{x}\ d\mathbf{p}$. For a particular phase-space trajectory starting from $(\mathbf{x}(0),\ \mathbf{p}(0))$ at time $t = 0$, the work done in time τ is given by Eq. (1.2). The probability of the initial state is $\rho_{\lambda_A}(\mathbf{x}(0),\ \mathbf{p}(0))$. Hence we get the following average:

$$\langle \exp\{-\beta W_J\} \rangle = \int \rho_{\lambda_A}(\mathbf{x}(0),\ \mathbf{p}(0))\ \exp\{-\beta W_J\}\ d\mathbf{x}(0)\ d\mathbf{p}(0). \tag{1.5}$$

Since the system is isolated, we can write $\partial H/\partial t = dH/dt$, and hence the work done, Eq. (1.2) on the system is nothing but the change in the total energy of the system, i.e., $W_J = H_{\lambda_B}(\mathbf{x}(\tau),\ \mathbf{p}(\tau)) - H_{\lambda_A}(\mathbf{x}(0),\ \mathbf{p}(0))$. This gives us:

$$\begin{aligned} &\langle \exp\{-\beta W_J\} \rangle \\ &= \frac{1}{Z_{\lambda_A}} \int_0^\tau \exp\{-\beta H_{\lambda_A}(\mathbf{x}(0),\ \mathbf{p}(0))\}\ \exp\{-\beta[\ H_{\lambda_B}(\mathbf{x}(\tau),\ \mathbf{p}(\tau)) - H_{\lambda_A}(\mathbf{x}(0),\ \mathbf{p}(0))\ ]\}\ d\mathbf{x}(0)\ d\mathbf{p}(0). \end{aligned} \tag{1.6}$$

Using Liouville's theorem, giving conservation of phase-space volume we get $d\mathbf{x}(0)\ d\mathbf{p}(0) = d\mathbf{x}(\tau)\ d\mathbf{p}(\tau)$ and the above equation then gives:

$$\langle \exp\{-\beta W_J\} \rangle = \frac{1}{Z_{\lambda_A}} \int \exp\{-\beta H_{\lambda_B}(\mathbf{x}(\tau),\ \mathbf{p}(\tau))\}\ d\mathbf{x}(\tau)\ d\mathbf{p}(\tau) = \frac{Z_{\lambda_B}}{Z_{\lambda_A}}\ . \tag{1.7}$$

Since $F_\lambda = -k_B T \ln(Z_\lambda)$, we then get the Jarzynski equality, given by Eq. (1.3). This equality can also be proved for the situation where system remains in contact with the heat bath during the driving process. In this case, the system and the reservoir are considered to be a larger isolated system, with Hamiltonian given by, $\mathcal{H}_\lambda = H_\lambda + H_B + h_I$, where H_λ is the system Hamiltonian, H_B is the reservoir Hamiltonian and h_I is the coupling between the system and the reservoir. The result in Eq. (1.3) was proved for weak coupling between the system and reservoir in [3] then for the general case in [6]. This relation can also be proved for discrete Markovian process [10], with heat bath dynamics and for Langevin dynamics [15] (we will outline this proof later in this section). It is remarkable that the result in Eq. (1.3) is valid independent of the rate at which the external parameter is varied. The only requirement is that the system should be in the equilibrium when the driving process starts. Unlike Eq. (1.1), this is an *equality* which relates a non-equilibrium quantity to an equilibrium free energy difference.

We will now give a simple example of a driven system with Langevin dynamics, where one can explicitly calculate the work distribution function and verify the Jarzynski equality. Consider a Brownian particle in a harmonic trap, which is moved with a constant velocity u. The Hamiltonian of the system is given by:

$$H = \frac{p^2}{2m} + \frac{1}{2}\, k(x - \alpha(t))^2, \tag{1.8}$$

where $\alpha(t) = ut$ is now the external control parameter. We consider the over-damped limit in which case the inertial term drops out and the Langevin equation of motion is given by:

$$\gamma \dot{x} = -k\,[x - \alpha(t)] + \eta(t), \tag{1.9}$$

where $\eta(t)$ is a Gaussian white noise, satisfying, $\langle \eta(t) \rangle = 0$ and $\langle \eta(t)\eta(t') \rangle = 2k_B T \gamma \delta(t - t')$. Using the Jarzynski definition of work, Eq. (1.2), we get for the work done in time τ:

$$\begin{aligned} W_J &= \int_0^\tau \frac{\partial H}{\partial \alpha}\, \dot{\alpha}\, dt = -k \int_0^\tau \dot{\alpha}\, [\, x \, - \, \alpha(t)\,]\, dt \\ &= \frac{k}{2}\, [\alpha^2(\tau) - \alpha^2(0)] - k \int_0^\tau \dot{\alpha}\, x\, dt. \end{aligned} \tag{1.10}$$

The general solution of Eq. (1.9) is given by:

$$x(t) = e^{-(k/\gamma)\ t}\ x_0 + \frac{1}{\gamma}\ \int_0^t e^{-(k/\gamma)\ (t-t')}\ [\ k\alpha(t')\ +\ \eta(t')\ ]\ dt'. \tag{1.11}$$

We choose $x_0 = x(t = 0)$ from the initial equilibrium distribution $P(x_0) = \exp\{-\beta H_{\alpha(0)}\}/Z_{\alpha(0)}$. It can be seen from Eq. (1.10) that W_J is linear in x, while x itself is linear in both, x_0 and $\eta(t)$ which are Gaussian variables. Hence it follows that the distribution of W_J will also be Gaussian. We thus just need to find the first and second moments of this distribution. We have:

$$P(W_J) = \frac{1}{\sqrt{2\pi\sigma^2_{W_J}}}\ \exp\Big[\ -\frac{(\ W_J - \langle W_J\rangle\ )^2}{2\sigma^2_{W_J}}\ \Big]. \tag{1.12}$$

Using Eqs. (1.10) and (1.11), it is straightforward to calculate $\langle W_J\rangle$ and $\sigma^2_{W_J} = \langle (W_J - \langle W_J\rangle)^2\rangle$, where we note that $\langle ...\rangle$ denotes an average over initial conditions as well as over noise. We find:

$$\begin{aligned} \langle W_J\rangle &= \gamma u^2\tau\ [1 + \frac{\gamma}{k\tau}\ (e^{-(k/\gamma)\tau} - 1)\ ], \\ \sigma^2_{W_J} &= 2\ k_B\ T\ \gamma u^2\tau\ [1 + \frac{\gamma}{k\tau}\ (e^{-(k/\gamma)\tau} - 1)\ ] = 2k_BT\langle W_J\rangle. \end{aligned} \tag{1.13}$$

For this particular Hamiltonian given by Eq. (1.8), it is easy to show that the free energy is independent of α and hence $\Delta F = 0$. Using Eqs. (1.12, 1.13), we immediately get:

$$\langle \exp\{-\beta W_J\}\rangle\ =\ 1\ =\ \exp\{-\beta\Delta F\}. \tag{1.14}$$

Thus we have verified that the Jarzynski equality Eq. (1.3) is satisfied.

Now we will discuss the fluctuation theorems which are somewhat more general than the Jarzynski equality and give information about the fluctuations of the entropy production in a non-equilibrium system. In fact we will see that the Jarzynski equality can be derived from one of the fluctuation theorems. There are various versions of the fluctuation theorems. All of them start with some definition of the entropy produced S in a particular realization of a non-equilibrium process in time τ. As discussed earlier (for the work done W), we

expect this entropy S to be also a fluctuating quantity with a distribution, say $P(S)$. The transient fluctuation theorem (TFT) [8, 12 − 15], states that for a system initially in thermal equilibrium, $P(S)$ satisfies the following equation:

$$\frac{P(S)}{P(-S)} = e^{S/k_B}. \tag{1.15}$$

This result is valid for any time interval τ. Another version of TFT, due to Crooks [10] gives:

$$\frac{P_F(S)}{P_R(-S)} = e^{S/k_B}, \tag{1.16}$$

where $P_F(S)$ and $P_R(S)$ are the probabilities in forward and time reversed processes respectively. This theorem is also true for all times τ. The steady state fluctuation theorem (SSFT) looks at the case where the initial state is chosen from a non-equilibrium steady state, rather from an equilibrium state as in TFT. In this case, the statement of the theorem as obtained by Cohen and Gallavotti [9] is

$$\frac{P(\sigma)}{P(-\sigma)} = e^{\tau\sigma}, \tag{1.17}$$

where $\sigma = S/(k_B\tau)$ is rate of entropy production and one looks at the limit $\tau \to \infty$.

Here we will give a proof of Crooks' fluctuation theorem for a single particle following Langevin dynamics. Then we will also show how to obtain the Jarzynski equality from this theorem. Consider a Brownian particle in the presence of an external potential $U(x)$. The Hamiltonian of the system is given by:

$$H = \frac{p^2}{2m} + U(x). \tag{1.18}$$

This particle is driven by an external time-dependent force $f(t)$, doing work on the particle. We also assume that the system is in contact with a heat bath at temperature T and it's time evolution is described by Langevin dynamics. The Langevin equation of motion is thus given

by:

$$\begin{aligned} m\ddot{x} &= -\frac{\partial U}{\partial x} + f(t) - \gamma\dot{x} + \eta(t) = -\frac{\partial H_f}{\partial x} - \gamma\dot{x} + \eta(t), \\ \text{with} \quad H_f &= H - f(t)x, \end{aligned} \tag{1.19}$$

where $\eta(t)$ is a Gaussian noise satisfying $\langle\eta(t)\rangle =$ and $\langle\eta(t)\eta(t')\rangle = 2k_BT\gamma\delta(t-t')$. For such stochastic systems the proof of Crooks' fluctuation theorem and the Jarzynski equality can be shown to follow from the principle of microscopic reversibility. For discrete systems, evolving for example through Monte Carlo dynamics, this principle has been proved by Crooks. Here we give a proof for Langevin dynamics [15].

We first state the principle of microscopic reversibility. Consider the evolution of the system from time $t = 0$ to $t = \tau$, through a path in phase-space given by $\{x(t), p(t), f(t)\}$. This path will correspond to a particular realization of the noise $\eta(t)$. The probability of this path is then given by:

$$P_+ = \mathcal{N}\ \exp\{-\frac{1}{4k_BT\gamma}\ \int_0^\tau \eta_+^2\ dt\} = \mathcal{N}\ \exp\Big\{-\frac{1}{4k_BT\gamma}\ \int_0^\tau (\ m\ddot{x} + \frac{\partial U}{\partial x}\ - f(t) + \gamma\dot{x}\ )^2\ dt\ \Big\}, \tag{1.20}$$

where $\mathcal{N}$ is a normalization factor. Now consider the time reversed trajectory given by $\{x'(t), p'(t), f'(t)\} = \{x(\tau-t), -p(\tau-t), f(\tau-t)\}$. The probability of this path is:

$$\begin{aligned} P_- &= \mathcal{N}\ \exp\{-\frac{1}{4k_BT\gamma}\int_0^\tau \eta_-^2\ dt\} = \mathcal{N}\ \exp\Big\{-\frac{1}{4k_BT\gamma}\ \int_0^\tau (\ m\ddot{x}' + \frac{\partial U}{\partial x'}\ - f'(t) + \gamma\dot{x}'\ )^2\ dt\ \Big\} \\ &= \mathcal{N}\ \exp\Big\{-\frac{1}{4k_BT\gamma}\ \int_0^\tau (\ m\ddot{x} + \frac{\partial U}{\partial x}\ - f(t) - \gamma\dot{x}\ )^2\ dt\ \Big\}. \end{aligned} \tag{1.21}$$

We then get after some simplification:

$$\frac{P_+}{P_-} = \exp\Big\{-\frac{1}{k_BT}\ \int_0^\tau (-\gamma\dot{x} + \eta)\ \dot{x}\ dt\ \Big\} = \exp\{\ -\beta Q\ \}, \tag{1.22}$$

where $Q = \int_0^\tau (-\gamma\dot{x}+\eta)\ \dot{x}\ dt$, is the amount of heat transferred from the heat bath to the system in time τ. The identification of Q as heat transferred follows from the fact that $(-\gamma\dot{x} + \eta)$ is the force from the heat bath on the particle.

Eq. (1.22) is the principle of microscopic reversibility. This principle is similar to that of detailed balance principle. The principle of microscopic reversibility relates the probability of a specified path in phase-space to the probability of the time reversed path. The detailed balance condition refers to the probability of transition between two points in phase-space say C and C' and states that $P(C \to C') = P(C' \to C)\, e^{-\beta\,[E(c')-E(c)]}$ and does not make reference to any specific path in phase-space.

Now we proceed to prove Crooks' fluctuation theorem. Following Crooks we will first motivate the definition of the entropy produced, S, for a given trajectory. This entropy S consists of two parts: a contribution from change in entropy of the bath which is $-\beta Q$ and another contribution coming from the change in entropy of the system. The entropy change of the system is found in the following way. Let some parameter $f(t)$, be switched from an initial value $f_A = f(0)$ to a final value $f_B = f(\tau)$. Let the equilibrium distributions corresponding to the parameters f_A and f_B be ρ_{f_A} and ρ_{f_B} respectively, where $\rho_f = e^{-\beta H_f}/Z_f$. Then the equilibrium entropy of the ensemble is given by:

$$\mathcal{S} = -k_B \int \rho_f(x,p) \ln \rho_f(x,p)\, dx\, dp. \tag{1.23}$$

One can think of $-k_B \ln \rho_f(x,p)$ as the entropy of a micro-state and the change in entropy of the system is given by $-k_B \ln \rho_{f_B} + k_B \ln \rho_{f_A}$. Thus for a given path, Crooks' definition of the *total* entropy generated is:

$$S/k_B = \ln \rho_{f_A} - \ln \rho_{f_B} - \beta Q. \tag{1.24}$$

Then $P_F(S)$, the probability of entropy S generated in time τ, in time forward process is given as:

$$\begin{aligned} P_F(S) &= \int D[x,p]\, dx(0)\, dp(0)\, dx(\tau)\, dp(\tau)\, \rho_{f_A}\, P_+\, \delta(S_F - S) \\ &= \int D[x,p]\, dx(0)\, dp(0)\, dx(\tau)\, dp(\tau)\, \rho_{f_A}\, P_-\, e^{-\beta Q}\, \delta(S_F - S), \end{aligned} \tag{1.25}$$

where S_F is the entropy generated for a given forward trajectory and $D[x,p]$ denotes a sum over all paths $\{x(t), p(t)\}$ between $\{x(0), p(0)\}$ and $\{x(\tau), p(\tau)\}$. Also from Eq. (1.24) we can

write $\rho_{f_A}\, e^{-\beta Q} = e^{S_F/k_B}\, \rho_{f_B}$. Note that under time reversal S changes sign hence we can write $S_R = -S_F$. Substituting these relations in Eq. (1.25), we get:

$$P_F(S) = \int D[x,p]\, dx(0)dp(0)\, dx(\tau)dp(\tau)\, \rho_{f_B}\, P_-\, e^{-S_R/k_B}\, \delta(S_R + S) = e^{S/k_B}\, P_R(-S), \tag{1.26}$$

thus proving Eq. (1.16).

Now we show how the Jarzynski equality can be derived from the Crooks' fluctuation theorem. To do this we note that, $\rho_{f_A} = \exp\{-\beta H_{f_A}\}/Z_{f_A}$ and $\rho_{f_B} = \exp\{-\beta H_{f_B}\}/Z_{f_B}$, where $H_f(x,p) = p^2/2m + U(x) - f(t)x$. This implies, using Eq. (1.24):

$$\begin{aligned} S/k_B &= \beta\, H_{f_B} + \ln Z(f_B) - \beta\, H_{f_A} - \ln Z(f_A) - \beta\, Q \\ &= -\beta\,(F_{f_B} - F_{f_A}) + \beta\,(H_{f_B} - H_{f_A}) - \beta\, Q, \end{aligned} \tag{1.27}$$

where, H_{f_A} and H_{f_B} are initial and final Hamiltonians, F_{f_A} and F_{f_B} are initial and final free energies. Using the equation of motion Eq. (1.19) and the definition of $H_f(x,p)$, it is easily seen that:

$$\frac{dH_f(x,p)}{dt} = \frac{\partial H_f(x,p)}{\partial t} + \frac{dQ}{dt}\,. \tag{1.28}$$

Which then gives $H_{f_B} - H_{f_A} = W_J + Q$. Hence from Eq. (1.27) we get:

$$S/k_B = -\beta\,\Delta F + \beta\, W_J = \beta\, W_d, \tag{1.29}$$

where we have defined $W_d = W_J - \Delta F$ as the dissipated work. Thus from the Crooks' identity we have:

$$\frac{P_F(W_d)}{P_R(-W_d)} = e^{\beta W_d}. \tag{1.30}$$

This is the Crooks' fluctuation theorem for work distribution and from this we get:

$$\int_{-\infty}^{\infty} P_F(W_d)\, e^{-\beta W_d}\, dW_d = \int_{-\infty}^{\infty} P_R(-W_d)\, dW_d = 1. \tag{1.31}$$

Thus

$$\langle \exp\{-\beta W_d\} \rangle = \langle \exp\{-\beta(W_J - \Delta F)\} \rangle = 1, \tag{1.32}$$

which is the Jarzynski equality in Eq. (1.3).

Let us see the validity of this Crooks' fluctuation theorem for the example we considered previously, namely a Brownian particle in a moving harmonic trap. In this example we proved that the distribution of work W_J is Gaussian. For Gaussian distribution it can be shown that [15] the distribution for forward trajectory $P_F(W_J)$ is same as that for time reversed trajectory $P_R(W_J)$ and therefore the Crooks' fluctuation theorem also implies the transient fluctuation theorem. Since $\Delta F = 0$ for this system, dissipated work W_d is nothing but the Jarzynski work W_J. Hence from the distribution given in Eqs. (1.12) and (1.13), we get:

$$\frac{P(W_J)}{P(-W_J)} = \exp\Big[\frac{2\,\langle W_J \rangle\, W_J}{\sigma^2_{W_J}}\Big] = e^{\,\beta W_J}, \tag{1.33}$$

which is the transient fluctuation theorem.

Contribution of this thesis: The fluctuation theorems have been proved for a large class of systems. However, their general validity has not been established and is still an open question. Here we look at the validity of these relations, namely the Jarzynski equality and the fluctuation theorems, for a single classical spin in the presence of a time-dependent magnetic field and where the dynamics of the spin is modeled by Glauber dynamics. Also, we note that the Jarzynski equality and the fluctuation theorems are general relations satisfied by the probability distribution function of some non-equilibrium quantity like work, and do not make any reference to the actual form of these distributions. There have been very few earlier studies which have explicitly looked at the form of the distribution functions, except in linear systems where the distributions are Gaussian. We have performed Monte-Carlo simulations to obtain the distributions for different driving protocols such as ramped magnetic field and periodically varied fields which can be symmetric or asymmetric. In general we find that the distributions are broad and have non-trivial forms. In some special limits, namely fast and

slow driving rates we show that the work distributions can be analytically calculated. We verify that Crooks' fluctuation theorem is always satisfied while the usual TFT and a steady state version is not.

1.2 Ratchets, heat engines and molecular motors

Ratchet models have been studied for a long time to examine how directed motion occurs in non-equilibrium systems even in the absence of any net external bias. Among its applications it has been proposed that Brownian ratchets could provide a possible mechanism of transport of motors in biological cells. An example of a molecular motors is kinesin which moves uni-directionally on microtubules inside the cell. Also molecular pumps, like sodium or potassium pumps maintain active transport across membranes against a concentration gradient. Note that these motors and pumps work in a very noisy environment and still they exhibit directed motion. It is thus of interest to understand the functioning of these highly complex systems by studying simple microscopic models. In this context several ratchet models like flashing ratchets, rocking ratchets, correlation ratchets, frictional ratchets etc. have been proposed [75]. In all these models one tries to get a net motion, by combining the effects of thermal (or a-thermal) fluctuations, spatial or temporal anisotropy and external non-directed driving. In some cases, the system is in contact with several thermal baths (thermal ratchets) at different temperatures. One of the first example of a ratchet is in fact Feynman's ratchet and pawl machine [49], where the machine is kept in contact with two baths at different temperatures, and is able to extract work from the heat transferred. In many of these models, one is interested in the dependence of the particle current on system parameters like temperature, diffusion constant, amplitude of external driving etc. Also one is interested in finding out the efficiency of these motors, a question which is of obvious practical interest. Many studies have been done to understand these aspects [64 – 66, 79]. The efficiency has mainly been studied as a function of temperature and external load in rocking, frictional ratchets. There have been lot of studies on improving the efficiency of such ratchet models. It turns out that this efficiency is small due to the non-equilibrium and irreversible

nature of the system. Questions like whether irreversibility can be suppressed, and whether a system can be made to achieve Carnot efficiency, have also been studied [69, 74]. To study efficiency of such ratchets models one usually uses the method of stochastic energetics developed by Sekimoto [64]. In this framework all the quantities like work done, input energy, output energy etc. can be understood and computed by the Langevin equation approach.

In the following sections we discuss a few ratchet models. We begin with the well known Feynman's ratchet and pawl model and then we look at some other models of externally driven ratchets, namely flashing, rocking and inhomogeneous ratchets.

1.2.1 Feynman's ratchet and pawl model

In this section we will look at a model discussed in *Feynman lectures on Physics, Vol. 1*. This model was devised to understand, from a molecular or kinetic point of view, how much maximum amount of work could be extracted from a heat engine. As we know from thermodynamics, there is a maximum limit to this efficiency, given by the Carnot efficiency. Feynman was trying to understand this through a microscopic mechanical model and using statistical mechanics. Feynman's ratchet and pawl device is shown in Fig. (1.2). This consists of two compartments containing gases at temperatures T_1 and T_2. The compartment (**I**), at temperature T_1, contains vanes which are able to rotate freely in both directions. The compartment (**II**), at temperature T_2, contains a ratchet and a pawl as shown. This ratchet with the pawl (with a spring) pressing on its teeth is an *asymmetric* object. With the pawl pressing on it, the ratchet can move only in one direction. The ratchet and the vanes are connected by a rigid rod. Let us consider a situation where both the temperatures are same, i.e., $T_1 = T_2 = T$. In compartment (**I**), gas molecules bombard on the vanes and make it rotate randomly. When the vanes try to move in one direction it is allowed but the other direction appears to be forbidden due to the presence of ratchet and pawl to which it is connected. Thus we should see the vanes moving only in one direction and the load moves up. It apparently looks like we get a directed motion out of random motion in thermal equilibrium. The flaw in above argument lies in the fact that, in our analysis we haven't considered the motion

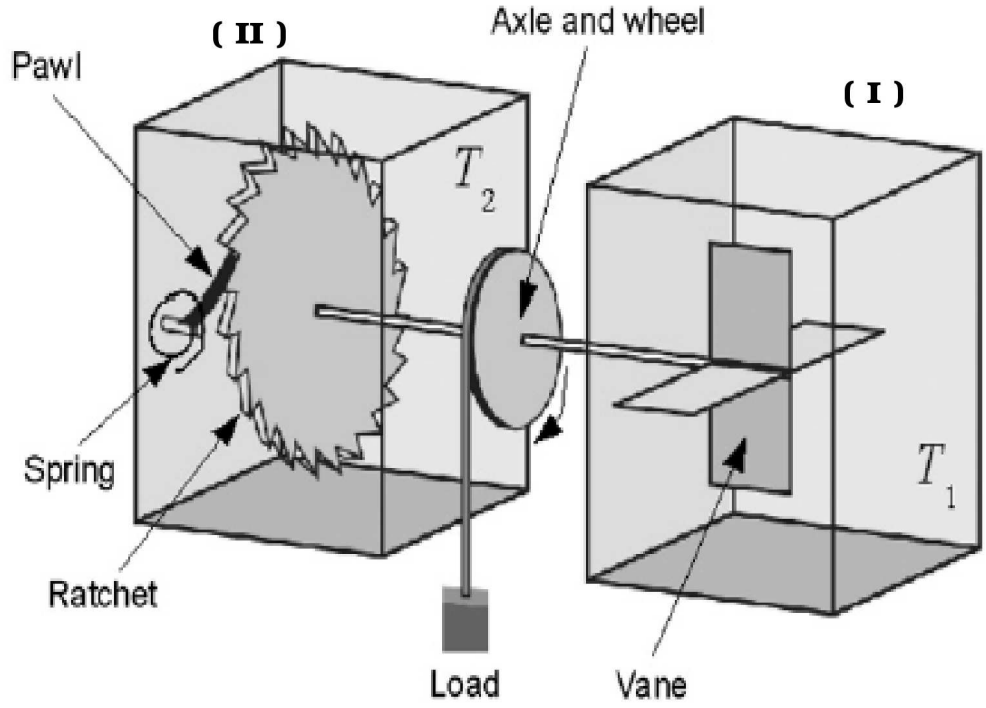

Figure 1.2: Feynman's ratchet and pawl engine.

of the pawl at all. Just as the vanes are getting kicks from the gas molecules, the pawl in the other compartment is also getting bombarded by the gas molecules in its compartment. Due to these kicks the pawl could be pressing against the ratchet, but it can also get lifted above the ratchet once in a while. At this particular instant when the pawl is lifted, if vanes get the kick in other direction (so called *forbidden*) then the ratchet is free to rotate. Thus we can see that in fact there can be motion in both the directions. Hence if we look at the load tied to the rigid rod, we will see it moving up and down at various instances, but on an average there will be no net motion.

Now let us see what happens when the temperatures are different. Let $T_1 > T_2$, that is the pawl is colder than the vanes. In this case, Feynman shows that directed motion is possible. Roughly the argument is as follows. The probability of a forward motion, by one tooth of the ratchet is $e^{-\epsilon/k_B T_1}$, where ϵ is the energy required to lift the pawl. On the other hand the probability of a reverse motion is $e^{-\epsilon/k_B T_2}$. Hence, as the rate of these jumps are no longer

equal, when $T_1 > T_2$, there can be a net forward motion of the ratchet. This can be used to do work, thus working as an engine.

Feynman then argues that in the reversible mode of operation, the efficiency of this model reaches a Carnot efficiency. In this analysis there are some flaws, which were pointed out by Parrondo [50] and Magnasco [51]. The point of their criticism was that, this system unlike other usual heat engines, is in contact with two heat baths at two different temperatures *simultaneously*, thus it can never work in a reversible way.

Actual analysis, of the Feynman's ratchet and pawl system turns out to be quite difficult, so different models have been proposed to model this engine [48 – 52]. A simple way of modeling is that given by Magnasco [51]. Consider a system with two degrees of freedom, x and y, where x is a cyclic coordinate representing the ratchet motion and y representing the pawl. These two coordinates are in contact with heat baths, at different temperatures T_1 and T_2 respectively, corresponding to the two compartments with gas in Feynman's model, and modelled by Langevin equation. An asymmetric periodic potential $U(x, y)$ is included to represent the asymmetry and periodicity of ratchet tooth and the interaction of ratchet and pawl degree of freedom. When the pawl is pressing against the ratchet, this potential is infinite. For a particular choice of $U(x, y)$ considered by Magnasco [51], the system works as an engine depending on the two temperatures, similar to Feynman's model. Also it was shown that the efficiency of this model is quite low, and it doesn't reach Carnot efficiency.

In such devices it is important to note the following points. A difference between such microscopic engines and thermodynamic engines like Carnot engines is that here effects of thermal fluctuations are important. The second important difference is that the system is simultaneously in contact with two (or more) heat baths at different temperatures and hence is essentially always a non-equilibrium system.

1.2.2 Other ratchet models

In the last section we discussed the ratchet and pawl model which is an example of an engine driven by temperature differences, with no external driving. Work is extracted solely from the

heat baths at different temperatures. There are other class of ratchets where an external time-dependent driving drives the system into a non-equilibrium steady state, and useful work is done. These models usually look at particle transport. In such models the general situation is as follows. Consider a Brownian particle placed in an asymmetric periodic potential such as shown in Fig. (1.3). Then, even if the potential is asymmetric, the system equilibrates at the temperature of the bath and reaches Boltzmann distribution. In this equilibrium situation there will be no net particle current. Thus we need to make the system non-equilibrium, and this can be done by various means and below we will discuss three examples.

I. Flashing ratchet: Suppose now that the asymmetric potential is made time-dependent [55]. This will drive the system into a non-equilibrium state and in such a situation we can have a uni-directional current in the system. In general such a system can be described by a Langevin equation as follows:

$$m\ddot{x} = -\frac{\partial U(x,t)}{\partial x} - \gamma\dot{x} + \eta(t), \tag{1.34}$$

where, m is the mass of the particle, γ is the dissipation in the bath, $U(x,t)$ is the external asymmetric time-dependent periodic potential. For flashing ratchets one takes $U(x,t) = U(x)f(t)$. Also $\eta(t)$ is the noise due to the heat bath. This noise is usually taken to be a Gaussian white noise satisfying $\langle\eta(t)\rangle = 0$ and $\langle\eta(t)\eta(t')\rangle = 2k_BT\gamma\delta(t-t')$. A simple example of a time-dependent potential is one shown in Fig. (1.3). In this case this potential is switched on (for time T_{on}) and off (for time T_{off}) and this is repeated periodically.

When the potential is off (during T_{off}), then particles are free to diffuse. Suppose we choose, $T_{off} \sim X_s^2/2D$, where D is the diffusion constant. Then, during this time, many particles starting from close to the potential minima would have diffused to the peak on the left hand side while few particles would have reached the peak on the right. Now when we switch on the potential, the particles on the left will slide down the slope to the next minima while those on the right return to the same minima (see Fig. (1.4)). Hence we get a net motion to the left. It is important to note that *we require diffusion* in order to get a directed motion.

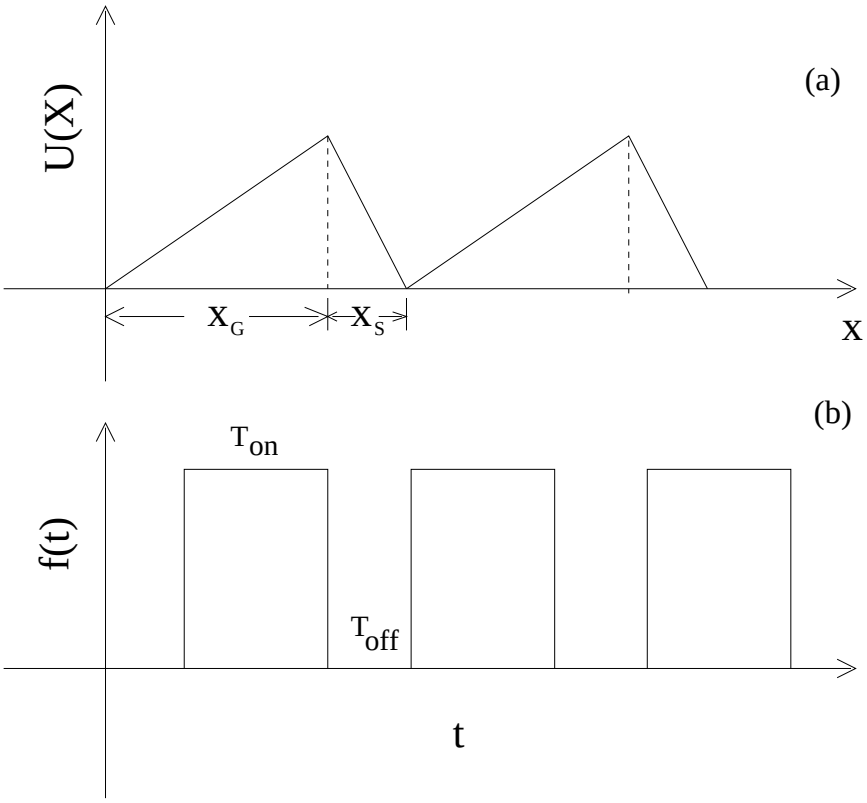

Figure 1.3: Part (*a*) of the figure shows a saw-tooth potential, an example of an asymmetric potential. Part (*b*) shows a switching function used to generate a time-dependent potential $U_t(x) = U(x)f(t)$, where $V(x)$ is as given in part (*a*). For time T_{on} potential in on and for time T_{off}, $U(x) = 0$. Such a driving can lead to an uni-directional particle current.

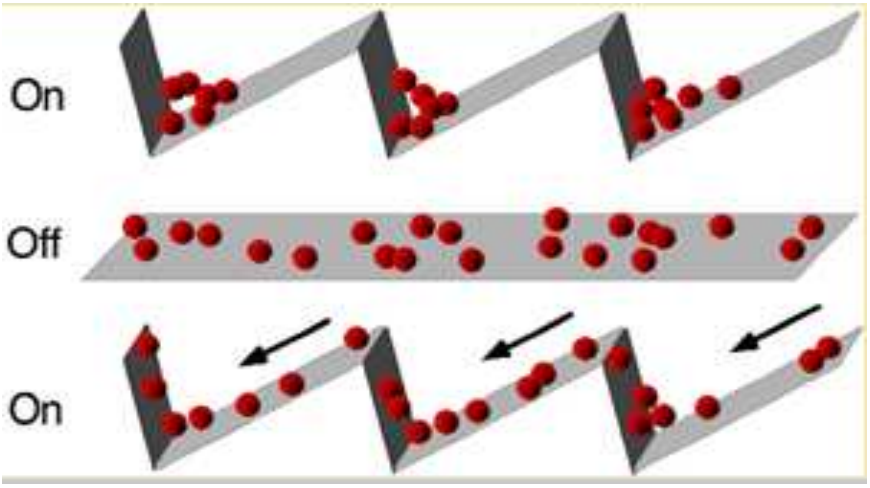

Figure 1.4: Brownian particles are trapped in a periodic, asymmetric potential that can be turned on and off. The random diffusion when the potential is off is converted into net motion to the left when the ratchet is switched on.

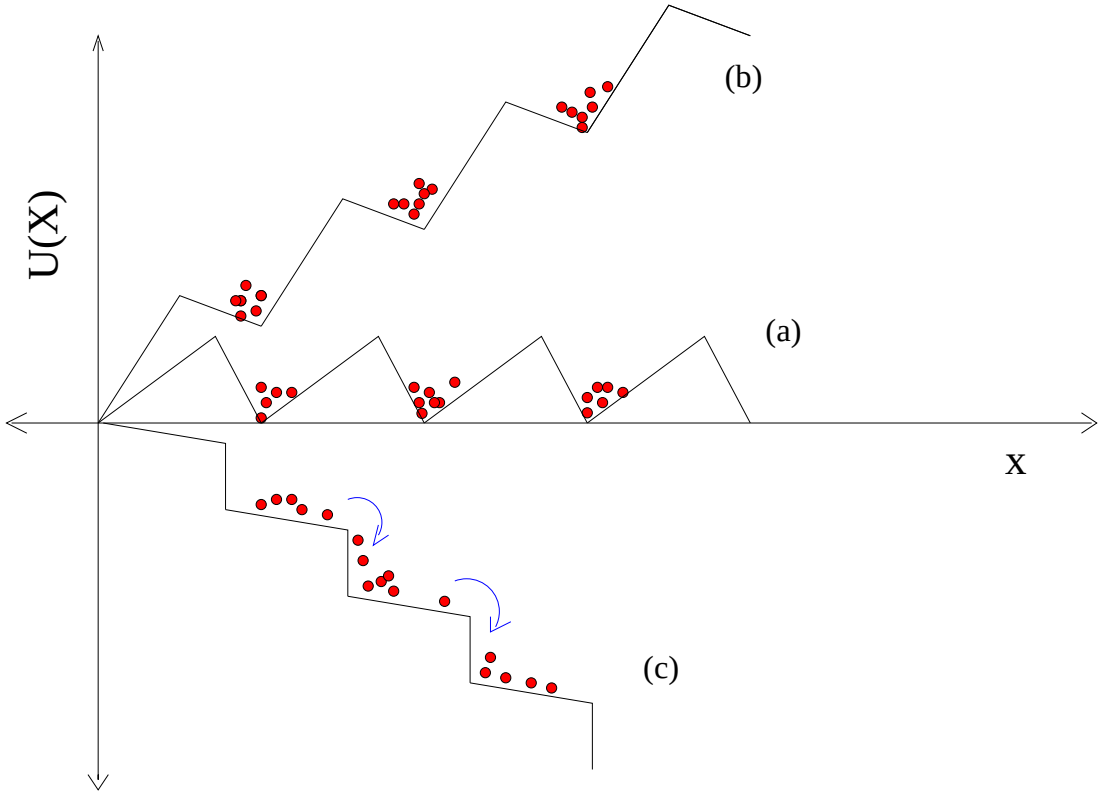

Figure 1.5: A rocking ratchet model where the external force is varied periodically in time. Because of the asymmetry of the potential, the situation (*b*) is not same as that of (*c*). In this case we get a motion in the direction of steeper slope.

Now suppose there is a gradient in the potential (which opposes the current, usually called as *load*). Then till some maximum load called as *stalled* load, the particles are able to move against this gradient and thus useful work can be done.

II. Rocking ratchet: In the case of flashing ratchets, discussed above, the potential fluctuates between on and off states. In another class of ratchets known as rocking ratchets [56], where one applies a time-dependent force with zero mean (see Fig. (1.5)). For example such a potential can be given by $U(x,t) = U(x) - \sin(\omega t)x$. This corresponds to a situation where the slope of the saw-tooth potential is periodically varied in time. More generally, this variation of slope can be done in a random or periodic way, the only requirement being that the average slope is zero. Consider the zero temperature case. Then, when the force is negative, (part (*b*) in Fig. (1.5)), particles can remain trapped in the valley of the potential, where local force there is positive. On the other hand, when the external force is positive (part (*c*)

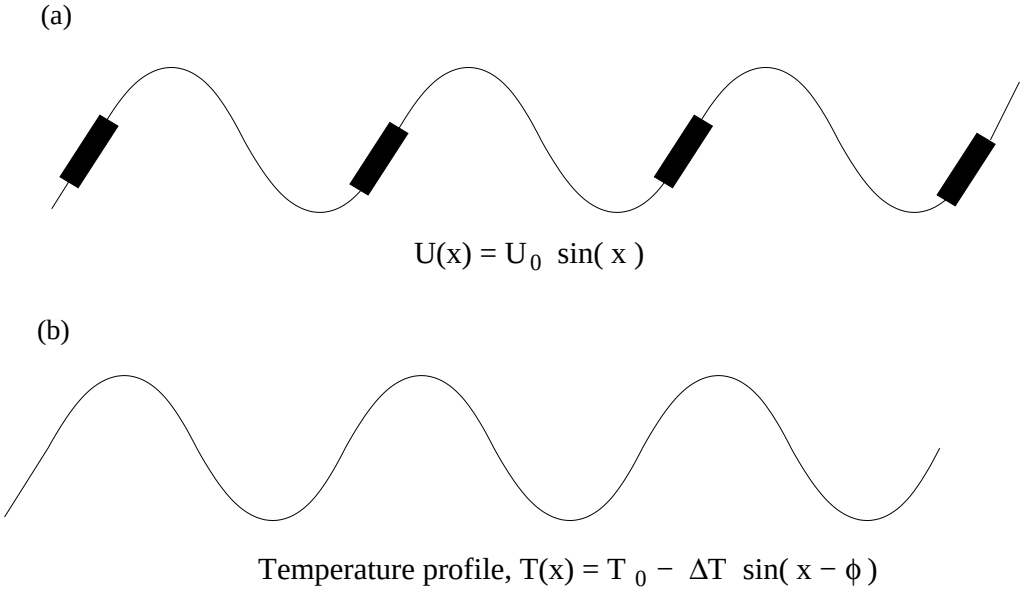

Figure 1.6: Inhomogeneous ratchet model where a periodic potential (*a*), and a temperature profile (*b*), is separated by a phase difference ϕ. Dark regions in (*a*) correspond to the higher temperature regions. Direction of the current depends on this phase difference.

in Fig. (1.5)), then particles slide down the slope. Thus the situations $+F$ and $-F$ are not equal and opposite to each other, which happens due the asymmetry of the potential, and we get a net current. This can be shown to be true even for finite temperatures. Unlike the case of flashing ratchets, the direction of the current in this case is in the direction of the steeper slope. Note that the flashing and rocking ratchets can be thought of as examples where a $\mathcal{DC}$ current is generated by applying an $\mathcal{AC}$ field.

III. Inhomogeneous ratchet: A third type of ratchet is the inhomogeneous ratchets [57, 58], which unlike flashing and rocking ratchets, have spatially symmetric periodic potential $U(x)$. They show directional transport due to the presence of space dependent diffusion coefficient $D(x)$. This space dependence can arise, for example from a spatially varying temperature $T(x)$ [57 – 60], since the diffusion constant is given by $D(x) = k_B T(x)/\gamma$. These systems are common in nature. For example, colloidal particles diffusing near any surface have space dependent diffusion coefficient, molecular motors moving on the microtubules experience space dependent mobility [63]. In this case, the ratchet effect arises because the system dissipates energy differently at different places due to the space dependent temperature $T(x)$. In this case the only criterion to be satisfied is that both the potential $U(x)$ and the

temperature $T(x)$ have to be periodic, and should be separated by a phase difference other than 0 or π.

Consider part (a) in Fig. (1.6), where dark regions corresponds to higher temperature (this is sometimes called as Landauer torch) corresponding to the maxima of temperature profile. Particles try to settle at the minima of the potential but, all the time they fluctuate around this minima due to noise from the bath. Thus when particles come into the contact with these higher temperature regions they get enough energy to cross the barrier and jump to next valley on the right. Thus particles in any minima will find it easier to jump to the right than to the left. Hence this temperature anisotropy produces a net particle transport in the system, whose direction and magnitude depends on the phase ϕ.

Contribution of this thesis: Here we look at models of both heat and particle pumps. These models are somewhat different from various ratchet models which we have described above and are motivated by models of quantum pumps. Unlike the flashing and rocking ratchets, there is no asymmetric potential in the examples we study. These models have external time-dependent magnetic field, forces etc. doing work on the system and driving the system in to non-equilibrium steady state. The ratchet effect is achieved through the fact that the external driving is both time, as well as space dependent.

In chapter (3) we study following two classical models of heat pump,

1. A spin system consisting of two coupled Ising spins each driven by periodic magnetic fields with a phase difference, and connected to two heat reservoirs.

2. An oscillator system of two interacting particles driven by periodic forces with a phase difference and connected to two reservoirs.

In both these models we drive the system by external periodic time-dependent magnetic fields or forces, with a phase difference and connected to multiple reservoirs. We find that though these models are based on same designing principles, one of them (Ising system) is able to work both as a heat pump and as an engine but the other is not. As discussed earlier for ratchet systems, to work, require spatial or temporal asymmetry. In these models there is

no built-in asymmetry but the phase different driving leads to an overall symmetry breaking.

In chapter (4) we study a model of a particle pump. We look at the symmetric exclusion process (SEP), with time-dependent hop-out rates at two or more sites. These hop-out rates are periodic in time and with a phase difference. We find that in this system, in the steady state we get a non zero $\mathcal{DC}$ current. Unlike previous models studied in chapter (3), here there is a particle transport. The hop-out rate is related to the diffusion constant and the modulation of this diffusion constant can be thought of as arising from a spatial and temporal modulation of the temperature or friction coefficient. We study this model by simulations and also analytically by doing a perturbation theory in driving strength around the exactly known time-independent SEP. We calculate general current expression and study its behaviour in few special cases. We look at the behaviour of this current as a function of driving frequency and the phase difference and also get a formal expression in adiabatic and fast driving limits.

2 Work distribution functions for Hysteresis loops in a single spin system.

2.1 Introduction

Consider a magnetic system in a time-dependent magnetic field. Assume that the magnetic field is varied periodically. Then plotting the magnetization of the system against the instantaneous magnetic field we get the well-known hysteresis curve. The area enclosed by the hysteresis loop gives the work done on the system by the external field and this leads to heating of the magnet. In the usual picture, that one has of hysteresis, one expects that the work done is positive. However if the magnetic system is small (*i*.e contains small number of magnetic moments) then this is no longer true. For a small magnet, one finds that the work is a fluctuating quantity, and in a particular realization of the hysteresis experiment one could actually find that the magnet cools and does work on the driving force.

In general, for a small system driven by time-dependent forces whose rates are not slow compared to relaxation times, one typically finds that various non-equilibrium quantities, such as the work done or the heat exchanged, take values from a distribution. Recently there has been a lot of interest in the properties of such distributions. Part of the reason for the interest is that it leads us to examine the question as to how the usual laws of thermodynamics, which are true for macroscopic systems, need to be modified when we deal with mesoscopic systems [1].

For instance in our example of the magnet with a small number of spins, there is a finite probability that all the spins could suddenly spontaneously flip against the direction of the

field by drawing energy from the heat bath. Intuitively this gives one the feeling that there has been a violation of the second law. In fact historically early observers of Brownian motion had the same feeling when they saw the "perpetual" motion of the Brownian particles [2]. However if one looks at the precise statement of the second law one realizes that there is no real violation.The second law is a statement on the most probable behavior while here we are looking at fluctuations about the most probable values. These become extremely small for thermodynamic systems. On the other hand, for small systems these fluctuations are significant and a study of the properties of these fluctuations could provide us with a better understanding of the meaning of the second law in the present context. This will be necessary for an understanding of the behavior of mesoscopic systems such as molecular motors, nanomagnets, quantum dots etc. which are currently areas of active experimental interest.

Much of the recent interest on these non-equilibrium fluctuations has focused on two interesting results on the distribution of the fluctuations. These are (1) the Jarzynski relation [3–6] and (2) the fluctuation theorems [7 – 17]. A large number of studies, both theoretical and experimental [19 – 24] have looked at the validity of these theorems in a variety of systems and also their implications. At a fundamental level both these theorems give some measure of "second law violations". At a practical level the possibility of using these theorems to determine the equilibrium free energy profile of systems using data from non-equilibrium experiments and simulations has been explored [25 – 29].

In this chapter we will be interested in the fluctuations of the area under a hysteresis loop for a small magnet. We look at the simplest example, namely a single Ising spin in a time-dependent magnetic field and evolving through Glauber dynamics. Hysteresis in kinetic Ising systems have been studied earlier [30 – 33] where the main aim was to understand various features such as dependence of the average loop area on sweeping rates and amplitudes, system size effects and dynamical phase transitions . The area distribution was also studied in [33] but the emphasis was on different aspects and so is quite incomplete from our present viewpoint.

A two state model with Markovian dynamics was earlier studied by Ritort *et al.* [34] to analyze experiments on stretching of single molecules. Systems with more than two states have also been studied [35] in the context of single-molecule experiments. However, the detailed forms of the work-distributions have not been investigated and that is the main aim of this study. These distributions are of interest since there are only a few examples where the explicit forms of the distributions have actually been worked out [37 – 40]. Most of the experiments so far, for example those in the RNA stretching experiments of Liphardt *et al.* [19] or the more recent experiment of Douarche *et al.* [25] on torsionally driven mirrors, are in regimes where the work-distributions are Gaussian.

We perform Monte-Carlo simulations to obtain the distributions for different driving rates. We consider different driving protocols and look at the two cases corresponding to the transient and the steady state fluctuation theorems. It is shown that the limiting cases of slow and fast driving rates can be solved analytically. We also point out that the problem of computing work-distributions is similar to that of computing residence-time distributions.

2.2 Definition of model and dynamics

Consider a single spin, with magnetic moment μ, in a time-dependent magnetic field $h(t)$. The Hamiltonian is given by

$$H = -\mu h\sigma \qquad \sigma = \pm 1 \tag{2.1}$$

We assume that the time-evolution of the spin is given by the Glauber dynamics. Let us first consider a discretized version of the dynamics. Let the value of the magnetic field at the end of the $(n-1)$th time step be h_{n-1} and let the value of the spin be σ_{n-1}. The discrete dynamics consists of two distinct process during the nth time step:

1. The field is changed from h_{n-1} to $h_n = h_{n-1} + \Delta h_n$. During this step an amount of work $\Delta W = -\mu\sigma_{n-1}\Delta h_n$ is done on the system.

2. The spin flips with probability $p(e^{-\beta\mu h_n\sigma_{n-1}}/Z)$ where $Z = e^{\beta\mu h_n} + e^{-\beta\mu h_n}$ is the equilibrium partition function at the instantaneous field value. The factor p is a parameter that is required

when we take the continuum time limit and whose value will set equilibration times. At the end of this step the spin is in the state σ_n. During this step the system takes in an amount of heat $\Delta Q = -\mu h_n(\sigma_n - \sigma_{n-1})$ from the reservoir.

Given the microscopic dynamics we can derive time-evolution equations for various probability distributions. These are standard results but we reproduce them here for completeness.

Time-evolution equation for spin distribution: First let us consider the spin configuration probability $P_n(\sigma)$ which gives the probability that at time n the spin is in the state σ. We write the field in the form $h_n = h_0 f_n$ where f_n is dimensionless and let us define $\epsilon = \beta\mu h_0$. Then we get the following evolution equation:

$$\begin{pmatrix} P_{n+1}(\uparrow) \\ P_{n+1}(\downarrow) \end{pmatrix} = \begin{pmatrix} 1 - p\frac{e^{-\epsilon f_n}}{Z} & p\frac{e^{\epsilon f_n}}{Z} \\ p\frac{e^{-\epsilon f_n}}{Z} & 1 - p\frac{e^{\epsilon f_n}}{Z} \end{pmatrix} \begin{pmatrix} P_n(\uparrow) \\ P_n(\downarrow) \end{pmatrix}$$

To go to the continuum-time limit we take the limits $p \to 0$, $\Delta t \to 0$, with $p/\Delta t \to r$ and $f_n \to f(t)$, $P_n(\sigma) \to P(\sigma, t)$. Using the dimensionless time $\tau = rt$ we then get:

$$\begin{aligned} &\frac{\partial \hat{P}}{\partial \tau} = -\mathcal{T}\hat{P} \qquad \text{where} \\ &\hat{P} = \begin{pmatrix} P(\uparrow,\tau) \\ P(\downarrow,\tau) \end{pmatrix}, \quad \mathcal{T} = \begin{pmatrix} \frac{e^{-\epsilon f(\tau)}}{Z} & -\frac{e^{\epsilon f(\tau)}}{Z} \\ -\frac{e^{-\epsilon f(\tau)}}{Z} & \frac{e^{\epsilon f(\tau)}}{Z} \end{pmatrix}. \end{aligned} \tag{2.2}$$

The magnetization $m(\tau) = \langle\sigma(\tau)\rangle = 2P(\uparrow,\tau) - 1$ thus satisfies the equation

$$\frac{dm(\tau)}{d\tau} = -m(\tau) + tanh[\epsilon f(\tau)] \tag{2.3}$$

whose solution is

$$m(\tau) = e^{-\tau}m(0) + \int_0^\tau d\tau' e^{-(\tau-\tau')} \tanh[\epsilon f(\tau')]. \tag{2.4}$$

Time-evolution equation for Work distribution: The total work done at the end of the nth time step is given by:

$$W = -\mu \sum_{l=1}^{n} \sigma_{l-1}\Delta h_l \tag{2.5}$$

To write evolution equations for the work-distribution it is necessary to first define $Q_n(W, \sigma)$,

the joint probability that at the end of the nth step the spin is in the state σ and the total work done on it is W. Then $Q_n(W,\sigma)$ will satisfy the following recursions:

$$Q_{n+1}(W,\uparrow) = (1 - p\frac{e^{-\epsilon f_{n+1}}}{Z_{n+1}}))Q_n(W + \mu\Delta h_n, \uparrow) + p(\frac{e^{\epsilon f_{n+1}}}{Z_{n+1}})Q_n(W - \mu\Delta h_n, \downarrow)$$
$$Q_{n+1}(W,\downarrow) = p(\frac{e^{-\epsilon f_{n+1}}}{Z_{n+1}})Q_n(W + \mu\Delta h_n, \uparrow) + (1 - p(\frac{e^{\epsilon f_{n+1}}}{Z_{n+1}}))Q_n(W - \mu\Delta h_n, \downarrow).$$

We take the limits $\Delta t \to 0$, $p \to 0$ with $p/(\Delta t) \to r$, $h_n \to h(t)$ and $\Delta h_n/(\Delta t) \to \dot{h}$. Then using the dimensionless variable τ defined earlier, and the total work done upto time τ, $w = \beta W = -\epsilon \int_0^\tau d\tau' \sigma(\tau')\, df/d\tau'$ we finally get

$$\begin{aligned} \frac{\partial \hat{Q}}{\partial \tau} &= -\mathcal{T}.\hat{Q} + \epsilon \frac{df}{d\tau}\sigma_z.\frac{\partial \hat{Q}}{\partial w} \quad \text{where} \\ \hat{Q} &= \begin{pmatrix} Q(w,\uparrow,\tau) \\ Q(w,\downarrow,\tau) \end{pmatrix}, \ \sigma_z = \begin{pmatrix} 1 & 0 \\ 0 & -1 \end{pmatrix} \end{aligned} \tag{2.6}$$

From Eq. (2.6) we get the following equation for $Q(w,\tau) = Q(w,\uparrow,\tau) + Q(w,\downarrow,\tau)$:

$$\frac{\partial^2 Q}{\partial \tau^2} + (1 - \frac{\ddot{f}}{\dot{f}})\frac{\partial Q}{\partial \tau} = \epsilon \dot{f} \tanh(\epsilon f)\frac{\partial Q}{\partial w} + (\epsilon \dot{f})^2 \frac{\partial^2 Q}{\partial w^2} \tag{2.7}$$

We have not been able to solve these equations analytically except in the limiting cases where the rate of change of the magnetic field is very slow or very fast. In a recent study done by Chvosta *et al.* [38, 39], this kind of evolution equation for a two level system is solved analytically, and their results match with our simulation results.

In the next two sections we will first present results from Monte-Carlo simulations which give accurate results for any rates and then discuss the special cases.

2.3 Results from Monte-Carlo simulations

We have studied three different driving processes:

(A) The system is initially in equilibrium at zero field and the field ($\beta\mu h$) is then increased linearly as a function of time from 0 to ϵ. The total time duration of the process is t_m (or τ_m in dimensionless units). By changing τ_m while keeping ϵ fixed we can control the rate at which the magnetic field sweep takes place.

(B) The system is initially in equilibrium and the field, which is taken to be piecewise linear, is changed over one cycle. The total time duration of the cycle is $4\tau_m$ for a symmetric cycle and is $2(\tau_m + \tau_n)$ for an asymmetric cycle.

(C) The system is run through many cycles till it reaches a non-equilibrium steady state. We measure work fluctuations in this steady state.

In cases (A) and (B) we will be interested in testing the transient fluctuation theorem (TFT) while in case (C) we will look at the steady state fluctuation theorem (SSFT). Let us briefly recall the statements of these theorems for work distributions in systems with Markovian dynamics.

Crooks' Fluctuation Theorem: Let us quickly recall the various definitions of the fluctuation theorems with our present notation. Consider our spin system, initially in thermal equilibrium and then external magnetic field $h(t)$, is changed from an initial value h_i, at time $t = 0$, to a final value h_f in a finite time t_m. Suppose the work done on the system during this process is W and the change in equilibrium free energy is ΔF. Let the dissipated work $W_d = W - \Delta F$, have a distribution $Q(W_d)$. Now consider a time-reversed path for the external field $h_R(t) = h(t_m - t)$ for which the work distribution is $Q_R(W_d)$. The fluctuation theorem of Crooks' then states:

$$\frac{Q(W_d)}{Q_R(-W_d)} = e^{\beta W_d}. \tag{2.8}$$

For Gaussian processes it can be shown that $Q_R(W_d) = Q(W_d)$ [15] and hence we get the usual form of the transient fluctuation theorem (TFT)

$$\frac{Q(W_d)}{Q(-W_d)} = e^{\beta W_d}. \tag{2.9}$$

Another situation where TFT is satisfied is the case where the field is kept constant or if the process is time-reversal symmetric. Finally we note that the Jarzynski relation

$$\langle e^{-\beta W_d} \rangle = \int dW_d e^{-\beta W_d} Q(W_d) = 1 \tag{2.10}$$

follows immediately from Crooks' theorem Eq. (2.8) and so will be satisfied in all cases

where Crooks' holds.

In the following sections we will verify that Crooks' FT is always satisfied but that TFT does not hold whenever the distributions are non-Gaussian processes and the process does not have time-reversal symmetry. We will also test the validity a particular version of the steady state fluctuation theorem (SSFT), which differs from the Cohen-Gallavotti theorem in that we consider a finite time τ. Thus, this version of SSFT has the same form as Eq. (2.9) with the difference that the initial state is chosen from a non-equilibrium steady state distribution instead of an equilibrium distribution.

In the simulations we used the discrete time dynamics specified in the beginning of Sec. (2.2). To get results corresponding to the continuum time limit we took the parameter values $\Delta t = t_m/10000$ and $p = \Delta t$. The distribution functions for a given rate were obtained by generating 2×10^6 realizations.

2.3.1 Field increased linearly from 0 to ϵ

In this case $f(\tau) = \tau/\tau_m$ and we have chosen $\epsilon = 0.5$. We note that with a static field, the equilibrium relaxation time is given by $t_r = 1/r$ or $\tau_r = 1$. The rate of change of magnetic field $\sim 1/t_m$ and comparing this with the relaxation time we find that slow and fast rates correspond, respectively, to large and small values for $t_m/t_r = \tau_m$. In Fig. (2.1) we plot the work distributions for various values of τ_m. We have plotted the distribution of the dissipated work $w_d = w - \beta\Delta F$ (Here $\beta\Delta F = -\ln\cosh\epsilon$). In Fig. (2.2) we plot the average magnetization as a function of field, again for different rates. Some interesting features of the work-distributions are:

(i) The distributions are in general broad. This is true even at the slowest driving rates where the average magnetization (Fig. (2.2)) itself is close to the equilibrium prediction. Note that the allowed range of values of w_d is $[-\epsilon - \beta\Delta F, \epsilon - \beta\Delta F] \approx [-0.38, 0.62]$. Also we see that the probability of negative dissipated work is significant.

(ii) For slow rates the distributions are Gaussian and this can be understood in the following way. Imagine dividing the time range into small intervals. Because the rate is slow, there

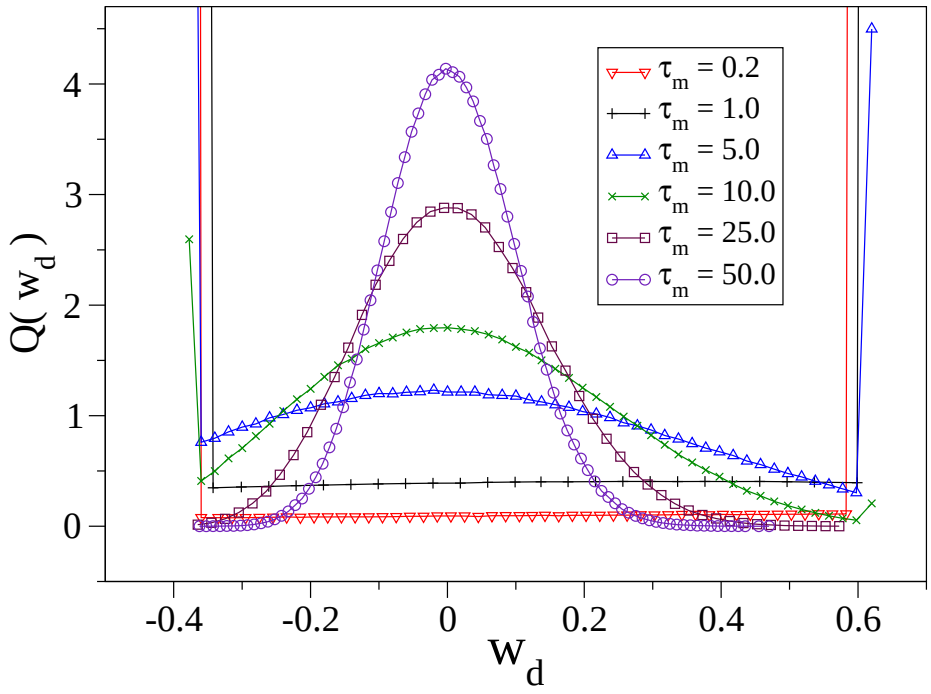

Figure 2.1: Distributions of the work done in driving a magnet at different rates when magnetic field is changed linearly.

are a large number of spin flips within each such interval, and so the average magnetization from one interval to the next can be expected to be uncorrelated. Since the work is a weighted sum of the magnetization over all the time intervals we can expect it to be a Gaussian.

(iii) For fast rates we get $\delta-$function peaks at $w = \pm\epsilon$. This again is easy to understand since the spin doesn't have time to react and stays in its initial state. In Sec. (2.4) we will work out analytic expressions for the the work distributions by considering probabilities of $0-$spin flip and $1-$spin flip processes.

For slow rates we have verified (see Fig. (2.3)) that the fluctuation theorem is satisfied. For faster rates we see that the probability of negative work processes is higher than what is predicted by the TFT.

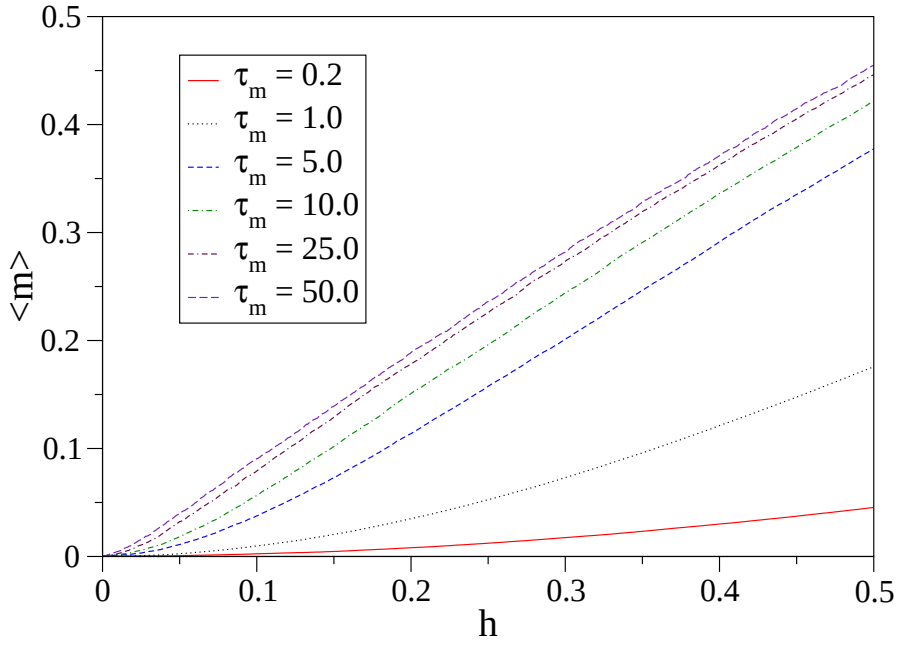

Figure 2.2: Average magnetization $m(\tau)$ for different rates, when magnetic field is changed linearly.

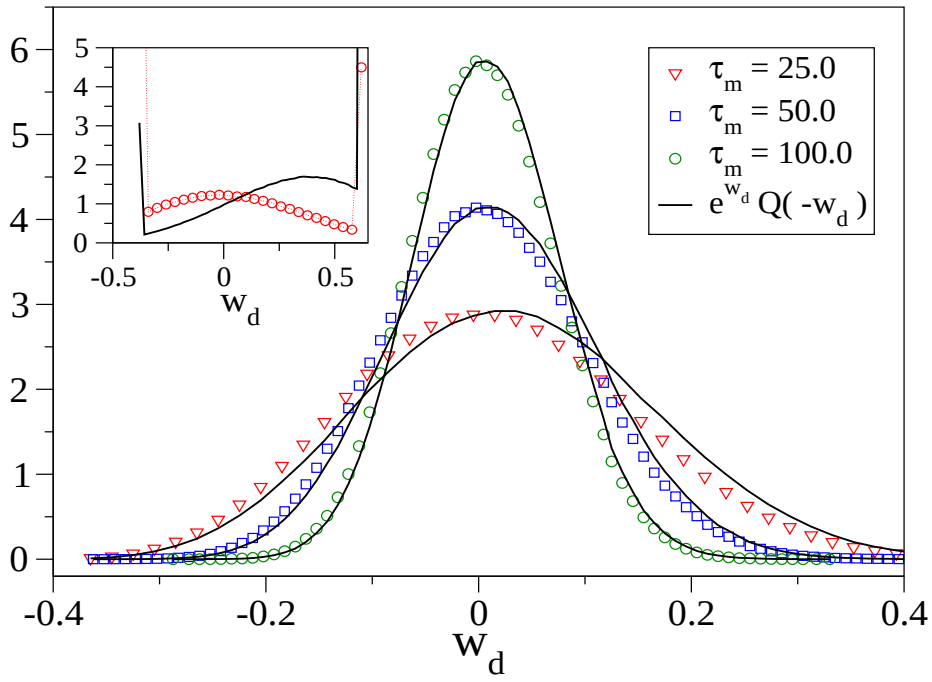

Figure 2.3: Plot shows that the fluctuation theorem is valid for slow processes with Gaussian work-distributions. Inset shows that for a fast rate ($\tau_m = 5.0$) the probability of negative work is much larger than that predicted by the FT.

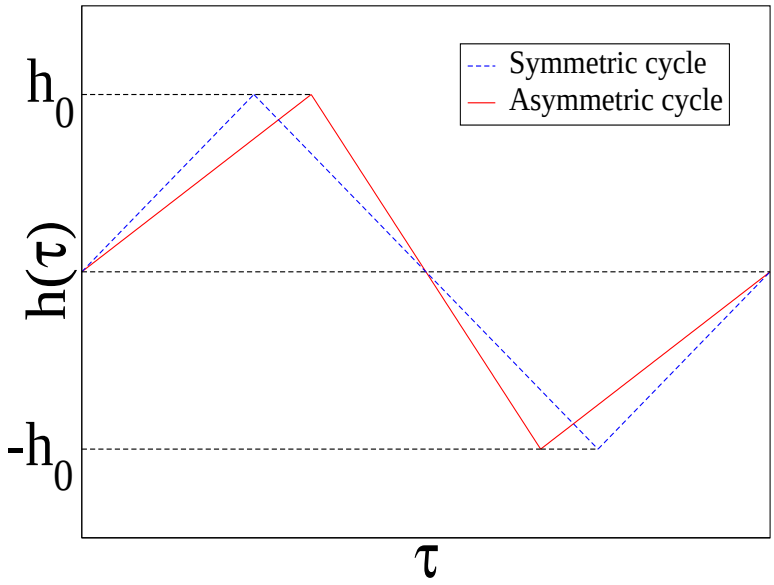

Figure 2.4: Magnetic field changed over a cycle. In the symmetric case the total cycle time is $4\tau_m$ while in the asymmetric case it is $2(\tau_m + \tau_n)$.

2.3.2 Field is taken around a cycle

As shown in Fig. (2.4) we consider two different cyclic forms for $f(\tau)$. One is a symmetric cycle and the other a asymmetric one. For these two cases the work-distributions are plotted in Fig. (2.5) and Fig. (2.6) respectively. For the symmetric cycle we plot the average magnetization as a function of the field in Fig. (2.7). This gives the familiar hysteresis curves.

As before we again find that the work-distributions are broad. For slow rates we get Gaussian distributions while for fast rates we get a $\delta-$function peak at the origin which correspond to a $0-$spin flip process. The slow and fast cases are treated analytically in Sec. (2.4).

As expected we can verify the transient fluctuation theorem for both the symmetric and asymmetric processes. That TFT should be satisfied follows from Crooks FT and noting that the time reversed process has the same distribution as the forward process because of the additional $h \to -h$ symmetry that we have in this case. We have also studied an asymmetric *half-cycle* for which $Q_R(w_d) \neq Q(w_d)$. Consequently we find that the usual TFT is not satisfied while the more general form of TFT of Crooks holds. We show this in Fig. (2.8) where we have plotted $Q(w_d)$, $e^{w_d}Q(-w_d)$ and $e^{w_d}Q_R(-w_d)$.

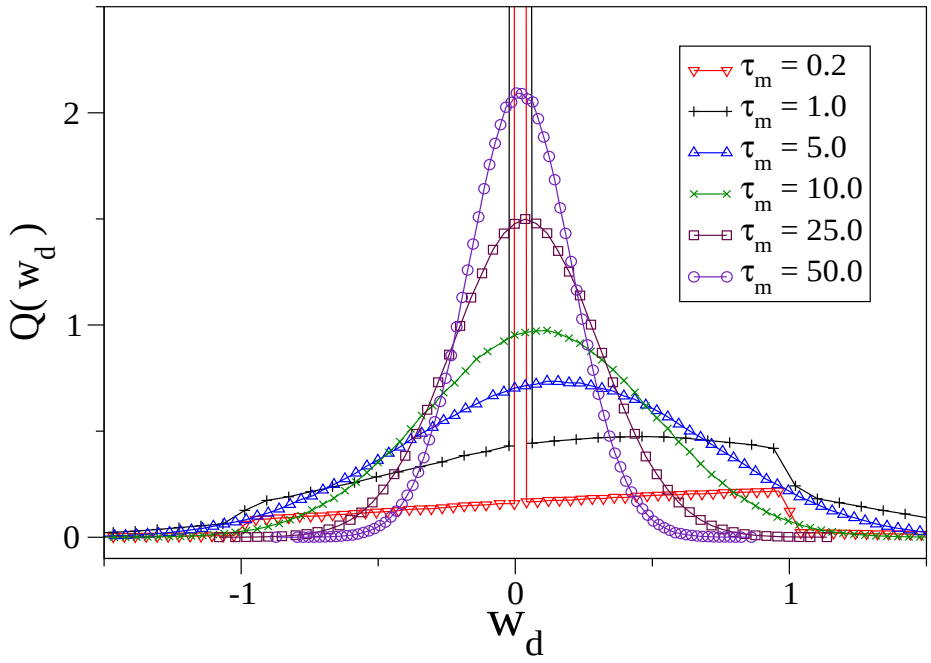

Figure 2.5: Plot of work-distributions for different driving rates when magnetic field is changed in a symmetric cycle.

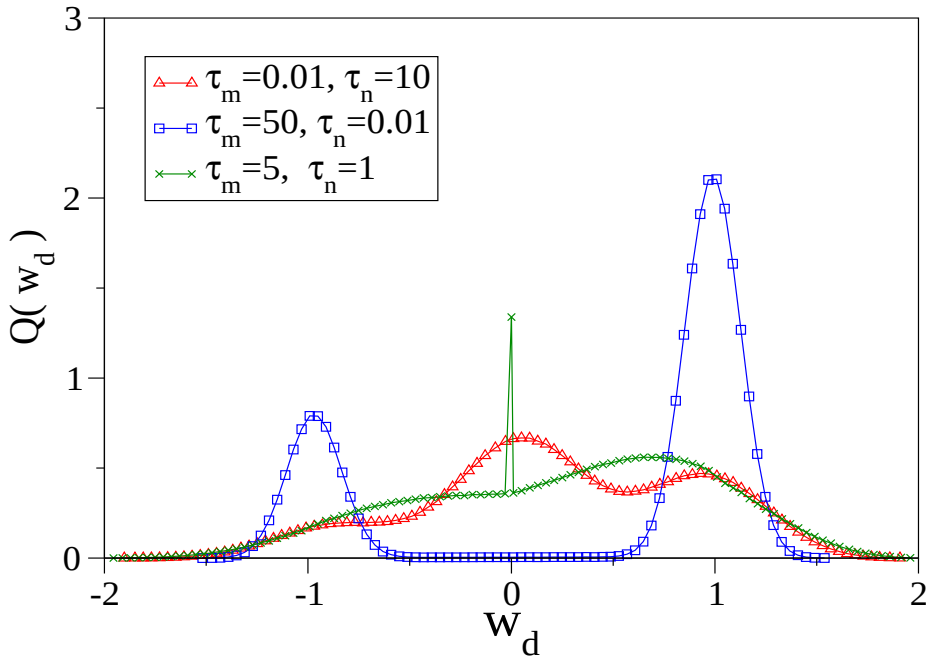

Figure 2.6: Plot of work-distributions obtained for different asymmetric cycles of the magnetic field.

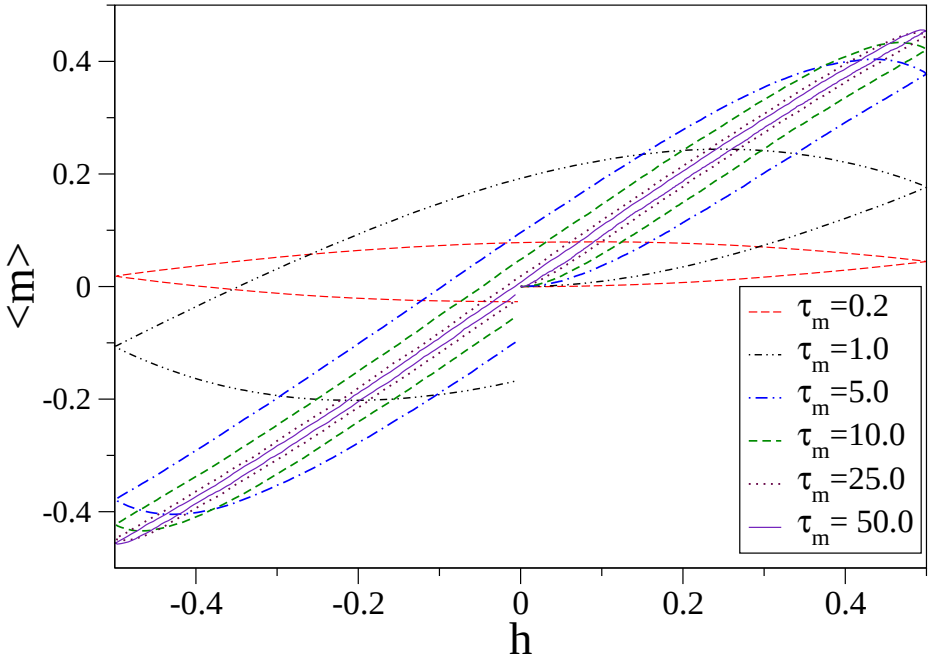

Figure 2.7: Hysteresis curves in driving a magnet at different rates when magnetic field is changed in a symmetric cycle and with the spin initially in equilibrium.

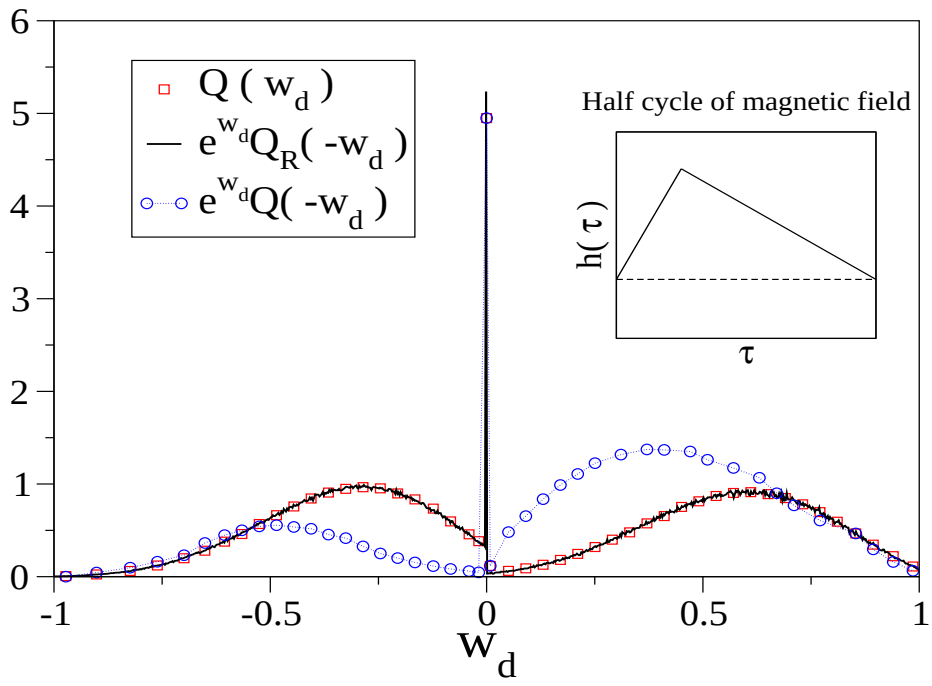

Figure 2.8: Plot showing the work-distribution for an asymmetric half-cycle and the validity of Crook's fluctuation theorem. Note that the probability of negative work processes is much higher than that predicted by usual TFT.

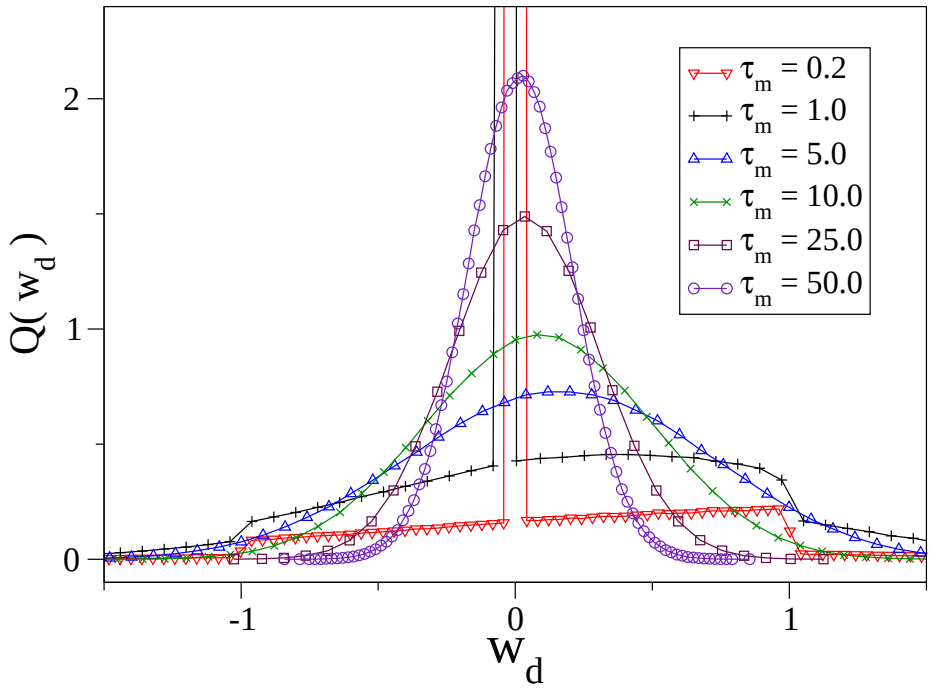

Figure 2.9: Work-distributions in the non-equilibrium steady state.

2.3.3 Properties in the non-equilibrium steady state

We now look at the case when the spin is driven by the oscillating field into a non-equilibrium steady state and we measure fluctuations in this steady state. In this case the work distributions (over a cycle) have the same forms as in the transient case (Fig. (2.9)). The joint distribution function $Q(w, \sigma, \tau)$ satisfies the same equation Eq. (2.6) but now the initial conditions are different. In Fig. (2.10) we plot the steady state hysteresis curves. Note that unlike the transient case the hysteresis curves are now closed loops.

Finally we test the validity of the steady state fluctuation theorem (SSFT). This theorem has been proved for dynamical systems evolving through deterministic equations but there exists no proof that a similar result holds for stochastic dynamics. From Fig. (2.11) it is clear that SSFT does not hold.

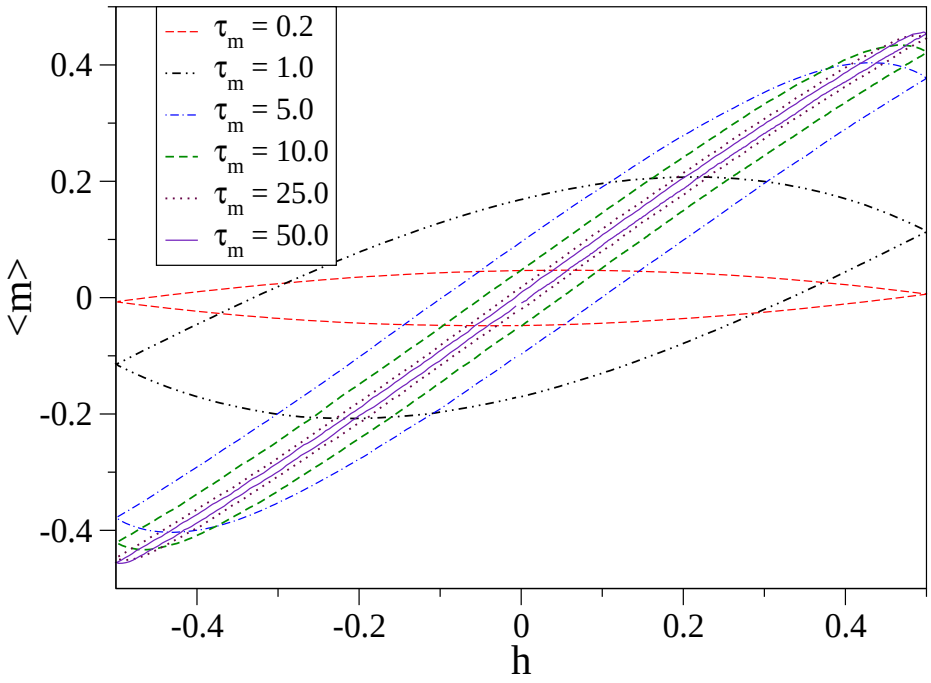

Figure 2.10: Hysteresis curves in the non-equilibrium steady state.

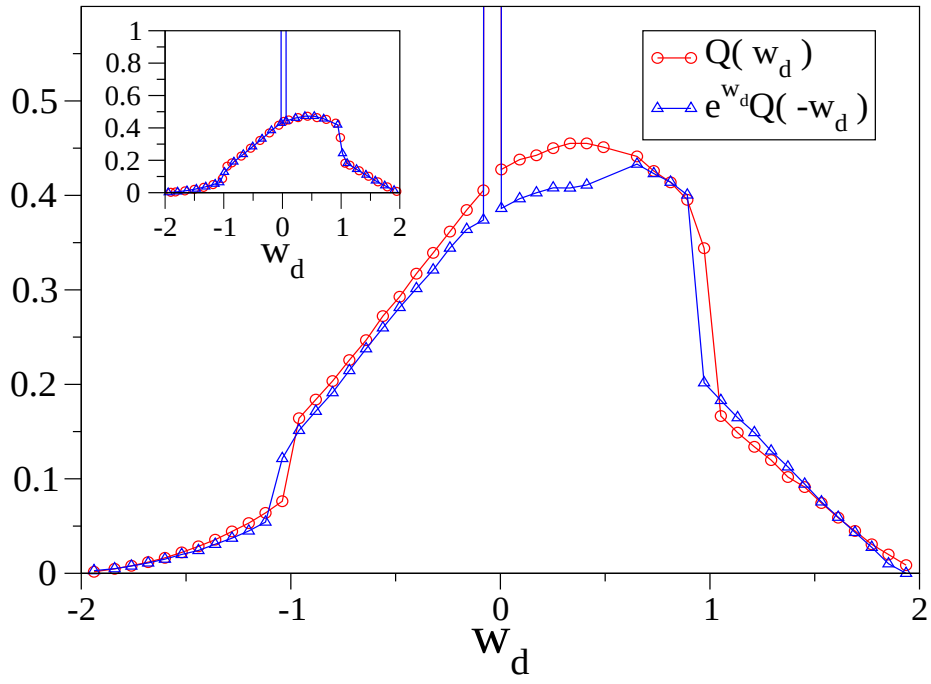

Figure 2.11: Violation of the fluctuation theorem for the steady state work-distribution corresponding to $\tau_m = 1.0$. Inset shows the same plots for the transient case where FT is clearly satisfied.

2.4 Analytic results for slow and fast rates

2.4.1 Field increased linearly from 0 to ϵ

(i) Slow case: $\tau_m >> 1$

As argued in the previous section we expect that the work-distributions to be Gaussians which will be of the general form

$$Q(w) = \frac{1}{\sqrt{2\pi\sigma_w^2}} e^{\frac{-(w-\langle w\rangle)^2}{2\sigma_w^2}} \quad . \tag{2.11}$$

where $\langle w\rangle$ and σ_w^2 are the mean and the variance of the distribution $Q(w)$. Since the distribution satisfies the Jarzynski equality, it follows at once that they are related by

$$\sigma_w^2 = 2(\langle w\rangle - \beta\Delta F). \tag{2.12}$$

Hence we just need to find the mean work done. The mean work done is given by $\langle w\rangle = -(\epsilon/\tau_m)\int_0^{\tau_m} d\tau m(\tau)$. In the strict adiabatic limit $\tau_m \to \infty$ we have $m_{ad}(\tau) = tanh(\epsilon\tau/\tau_m)$ and the mean work done $\langle w\rangle = -\log(\cosh(\epsilon)) = \beta\Delta F$. For large τ_m we try the perturbative solution

$$m(\tau) = m_{ad}(\tau) + \frac{1}{\tau_m} g(\tau) \tag{2.13}$$

Substituting in Eq. (2.3) we get an equation for $g(\tau)$ whose solution gives

$$g(\tau) = -\frac{\epsilon}{\tau_m} sech^2(\frac{\epsilon\tau}{\tau_m}) + O(\frac{1}{\tau_m^2}) \tag{2.14}$$

For the work done we then get

$$\langle w\rangle = \beta\Delta F + \frac{\epsilon}{\tau_m} tanh(\epsilon) \tag{2.15}$$

In Fig. (2.12) we compare the simulations for slow rates with the analytic results.

(ii) Fast case: $\tau_m << 1$.

If we change the field very fast then the spin is not able to respond and so there are few spin flips during the entire process. At the lowest order there is no flip and this gives rise to

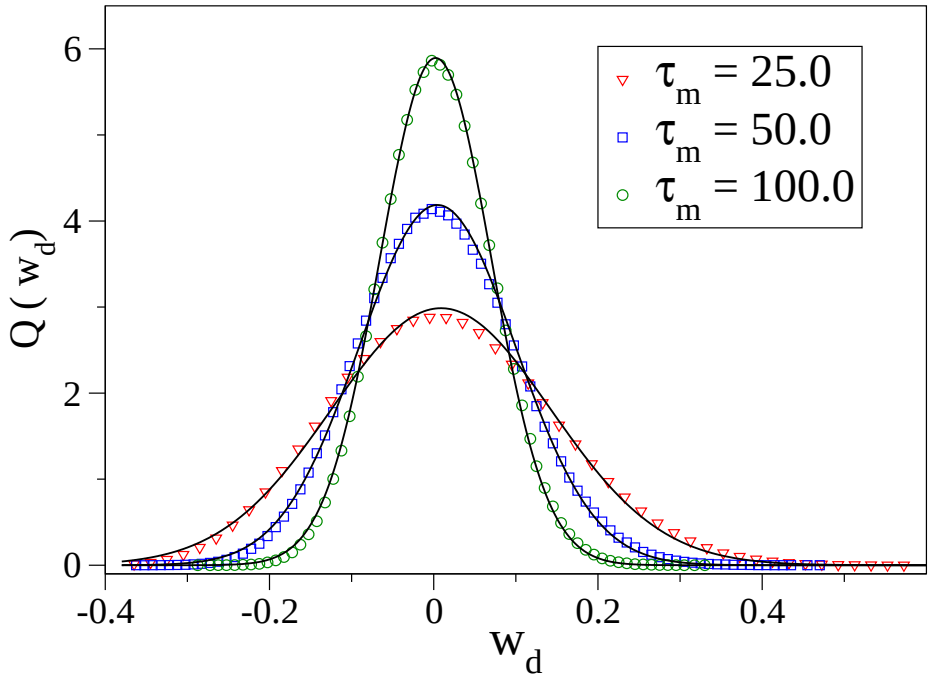

Figure 2.12: Comparison of work-distributions for slow rates obtained from simulations and from the analytic form. Solid lines show the analytic results.

the $\delta-$functions peaks at $\pm\epsilon$ seen in the distribution. We now calculate the work-distribution by looking at contributions from $0-$spin flip and $1-$spin flip processes. Let $S(\uparrow, \tau_0, \tau)$ be the probability that, given that the spin is $\uparrow$ at time τ_0, it remains in the same state till time τ. It is easy to see that $S(\uparrow, \tau_0, \tau)$ satisfies the equation

$$\frac{\partial S(\uparrow, \tau_0, \tau)}{\partial \tau} = -\frac{e^{-\epsilon f(\tau)}}{Z} S(\uparrow, \tau_0, \tau) \tag{2.16}$$

Solving we get, for the linear case $f(\tau) = \tau/\tau_m$,

$$S(\uparrow, 0, \tau) = e^{-\int_0^\tau \frac{e^{-\epsilon \frac{\tau'}{\tau_m}}}{Z(\tau')} d\tau'} = e^{\frac{-\tau}{2}} (\cosh(\frac{\epsilon\tau}{\tau_m}))^{\frac{\tau_m}{2\epsilon}} \tag{2.17}$$

Putting $\tau = \tau_m$ corresponds to the process for which the work done is $w = -\epsilon$. Hence, since the probability of the spin being initially in $\uparrow$ state is $1/2$, we get

$$Prob(w = -\epsilon) = \frac{1}{2} e^{-\frac{\tau_m}{2}} [\cosh(\epsilon)]^{\frac{\tau_m}{2\epsilon}} \tag{2.18}$$

Proceeding in a similar fashion by starting with a $\downarrow$ spin we get

$$Prob(w = \epsilon) = \frac{1}{2}\, e^{\frac{-\tau_m}{2}} (\cosh(\epsilon))^{-\frac{\tau_m}{2\epsilon}} \tag{2.19}$$

Next let us consider 1−spin flip processes which (for fast rates) are the major contributors to the part of the distribution between the two peaks. Let $S_1(\uparrow, \tau)d\tau$ be the probability that the spin starts in the $\uparrow$ *state,* flips once between times τ to $\tau + d\tau$, and stays $\downarrow$ till time τ_m. This is given by

$$S_1(\uparrow, \tau)d\tau = S(\uparrow, 0, \tau)(e^{-\epsilon\tau/\tau_m}/Z)d\tau S(\downarrow, \tau, \tau_m) \tag{2.20}$$

The work done during such a process is given by

$$w = -\frac{\epsilon}{\tau_m}\,(2\tau - \tau_m) \tag{2.21}$$

Similarly the case where the spin starts from a $\downarrow$ state gives

$$S_1(\downarrow, \tau)d\tau = S(\downarrow, 0, \tau)(e^{\epsilon\tau/\tau_m}/Z)d\tau S(\uparrow, \tau, \tau_m) \tag{2.22}$$

and the work done in this case is

$$w = \frac{\epsilon}{\tau_m}\,(2\tau - \tau_m) \tag{2.23}$$

Adding this two contributions and plugging in the form of $S(\sigma, \tau_0, \tau)$ obtained earlier we get the following contribution to the work-distribution:

$$Q_1(w) = \frac{\tau_m}{8\epsilon} e^{\frac{-(\tau_m - w)}{2}} \left(\frac{e^{\frac{-\epsilon}{2}} (\cosh(\epsilon)^{\frac{\tau_m}{2\epsilon}})}{\cosh(\frac{\epsilon - w}{2})} + \frac{e^{\frac{\epsilon}{2}} (\cosh(\epsilon)^{\frac{-\tau_m}{2\epsilon}})}{\cosh(\frac{\epsilon + w}{2})}\right)$$

The full distribution is given by

$$Q(w) = \frac{1}{2} e^{-\frac{\tau_m}{2}} [\cosh(\epsilon)]^{\frac{\tau_m}{2\epsilon}} \delta(w + \epsilon) + \frac{1}{2} e^{-\frac{\tau_m}{2}} [\cosh(\epsilon)]^{-\frac{\tau_m}{2\epsilon}} \delta(w - \epsilon) + Q_1(w) \tag{2.24}$$

for $-\epsilon < w < \epsilon$, and zero elsewhere. In Fig. (2.13) we show a comparison of this analytic form with simulation results for $\tau_m = 0.01$. The strengths of the $\delta-$functions at $w = \pm\epsilon$ are accurately given by Eqs. (2.18), (2.19).

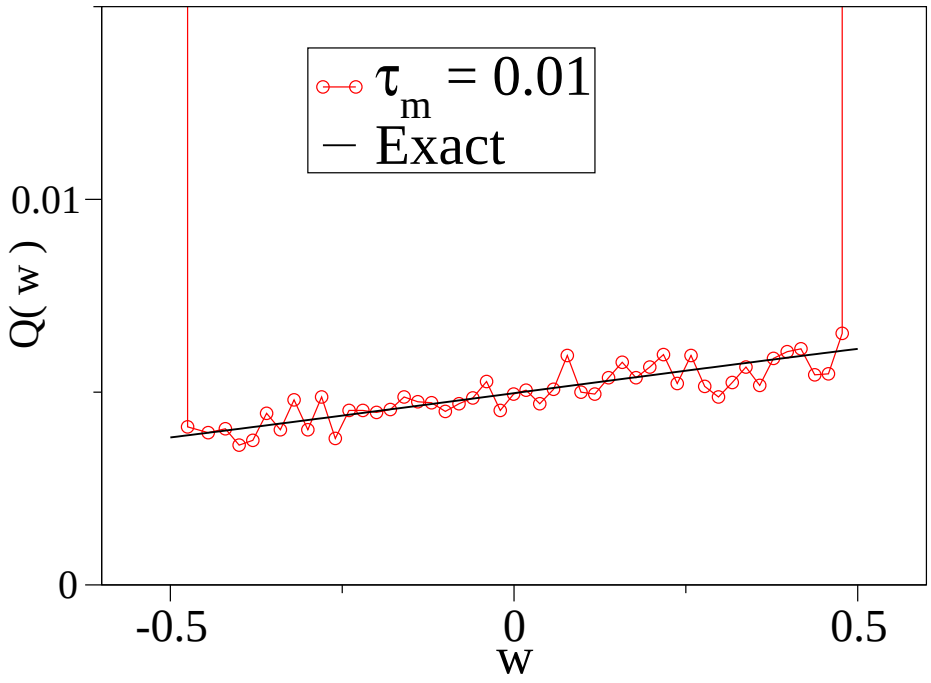

Figure 2.13: Comparison of work-distribution for a fast rate obtained from simulation and from the analytic form.

2.4.2 Field is taken around a cycle

(i) Slow case: $\tau_m >> 1$

We again expect a Gaussian distribution and since $\Delta F = 0$ for a cyclic process, hence the mean and variance of the distribution are related by $\sigma_w^2 = 2\langle w \rangle$. As before we compute the mean work to order $1/\tau_m$ and find

$$\langle w \rangle = \frac{4\epsilon}{\tau_m} tanh(\epsilon). \tag{2.25}$$

In Fig. (2.14) we show the comparison of analytical and simulation results.

(ii) Fast case: $\tau_m << 1$. In this case the work distribution gives a $\delta-$function peak at the origin for $0-$spin flip processes. To find the probability of this, we solve Eq. (2.16) with $f(\tau)$

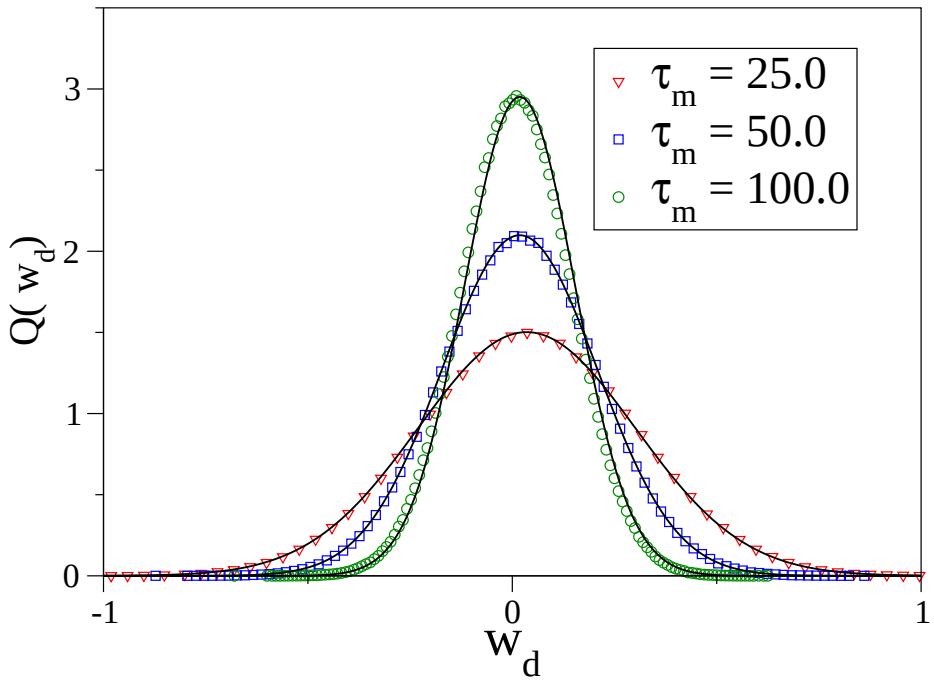

Figure 2.14: Comparison of work-distributions for slow rates obtained from simulations of the cyclic case and from the analytic form. Solid lines show the analytic results.

for the cycle given by

$$\begin{aligned} f(\tau) &= \frac{\epsilon}{\tau_m}\tau \qquad\qquad , 0 \le \tau \le \tau_m \\ f(\tau) &= \frac{\epsilon}{\tau_m}(2\tau_m - \tau) \ , \tau_m \le \tau \le 3\tau_m \\ f(\tau) &= \frac{\epsilon}{\tau_m}(\tau - 4\tau_m) \ , 3\tau_m \le \tau \le 4\tau_m \end{aligned}$$

This has the solution

$$S(\uparrow, 0, \tau_m) = e^{-2\tau_m} \tag{2.26}$$

Adding up an equal contribution from $S(\downarrow, 0, \tau_m)$, and since both initial conditions occur with probability half, we finally get

$$Prob(w = 0) = e^{-2\tau_m} \tag{2.27}$$

Next we look at the contribution of 1−spin flip processes. Let the spin flip occur between

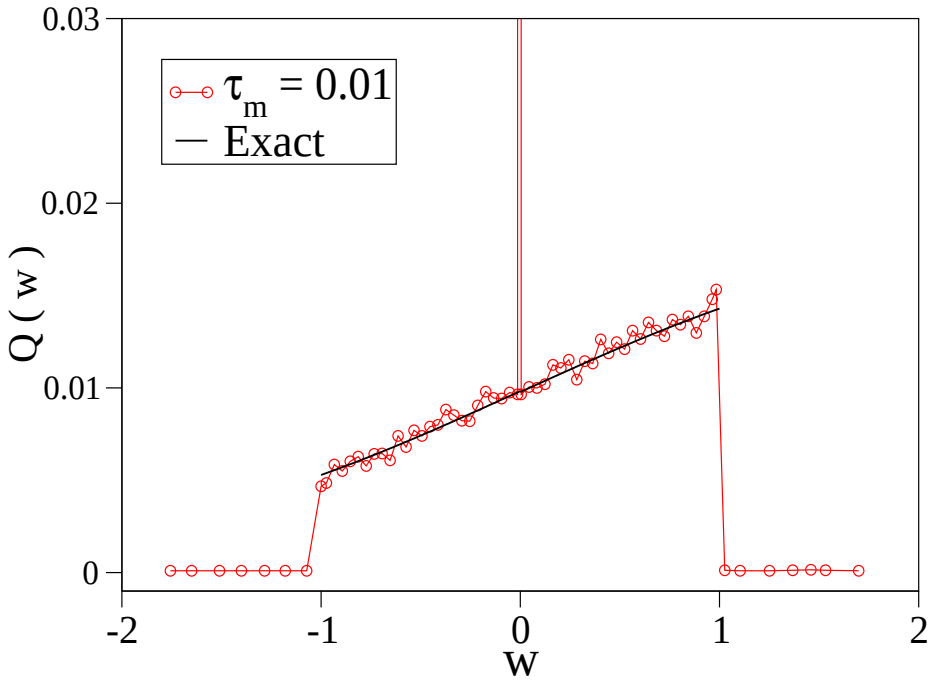

Figure 2.15: Comparison of work-distribution, for the symmetric cycle with a fast rate, obtained from simulations and from the analytic results.

times τ and $\tau + d\tau$. It is convenient to divide the total time $4\tau_m$ into four equal intervals, the dependence of w on τ being different in each of the intervals. Thus if we start with the spin initially in an $\uparrow$ state then we have

$$\begin{aligned} w &= -\frac{2\epsilon\tau}{\tau_m} && ,0 < \tau < \tau_m \\ &= \frac{2\epsilon}{\tau_m}(\tau - 2\tau_m) && ,\tau_m < \tau < 2\tau_m \\ &= \frac{2\epsilon}{\tau_m}(2\tau_m - \tau) && ,2\tau_m < \tau < 3\tau_m \\ &= \frac{2\epsilon}{\tau_m}(\tau - 4\tau_m) && ,3\tau_m < \tau < 4\tau_m. \end{aligned}$$

The probabilities of each of these processes is again given by:

$$S_1(\uparrow,\tau)d\tau = S(\uparrow,0,\tau)(e^{-\epsilon f(\tau)}/Z)d\tau S(\downarrow,\tau,4\tau_m) \tag{2.28}$$

Using the relations between w and τ and summing up the four different possibilities we

finally get (for initial spin state ↑)

$$Q_1^{\uparrow}(w) = \frac{\tau_m}{8\epsilon} e^{-2\tau_m} e^{\frac{w}{2}} [(\cosh(\frac{w}{2}))^{\frac{\tau_m}{\epsilon}-1} + (\cosh(\frac{w}{2}))^{-\frac{\tau_m}{\epsilon}-1} (\cosh(\epsilon))^{\frac{2\tau_m}{\epsilon}}] \tag{2.29}$$

for $-1 < w < 1$ and zero elsewhere. Note that the allowed range of w is $[-2, 2]$ but single spin-flip processes only contribute to work in the range $[-1, 1]$. Similarly if we start with spin state ↓ we get

$$Q_1^{\downarrow}(w) = \frac{\tau_m}{8\epsilon} e^{-2\tau_m} e^{\frac{w}{2}} [(\cosh(\frac{w}{2}))^{-\frac{\tau_m}{\epsilon}-1} + (\cosh(\frac{w}{2}))^{\frac{\tau_m}{\epsilon}-1} (\cosh(\epsilon))^{-\frac{2\tau_m}{\epsilon}}] \tag{2.30}$$

for $-1 < w < 1$. The full work-distribution (contribution from $1-$spin flip processes) is thus:

$$Q(w) = e^{-2\tau_m} \delta(w) + Q_1^{\uparrow}(w) + Q_1^{\downarrow}(w) \tag{2.31}$$

In Fig. (2.15) we compare the analytic and simulation results. The strength of the $\delta-$function at $w = 0$ is accurately given by Eq. (2.27).

2.5 Conclusions

We have computed probability distributions of the work done when a single spin, with Markovian dynamics, is driven by a time-dependent magnetic field. We find that work fluctuations are quite large (even for slow driving rates) and there is significant probability for processes with negative dissipated work. For slow driving the number of spin flips during the entire process is very large and the total work is effectively a sum of random variables. Hence the distributions are Gaussian with widths proportional to the driving rate. On the other hand for very fast driving the probability of flipping is low and we can compute the work-distributions perturbatively from probabilities of zero-flip, one-flip, etc. processes. While the two special cases of slow and fast rates can be solved, we have not been able to obtain a general solution valid for all rates even in this single particle problem. An exact solution of this problem was recently obtained by Chvosta *et al.* [38, 39].

Recently [40], work distribution functions for a charged colloidal particle placed in a time-dependent magnetic field has also been studied by Langevin equation approach. Where the

work distributions were Gaussian. Distributions of work and heat in a driven double well potential have been studied [41, 42] and also experimentally realised [43, 44], where non-Gaussian work distributions have been obtained. This system resembles to the two state Ising spin model discussed by us here.

We note that the problem of calculating the work-distribution is similar to that of calculating residence-time distributions in stochastic processes [43 – 45]. In fact for the case in Sec. (2.4.1) the work done is proportional to the average magnetization which is easily related to the residence time (time spin spends in $\uparrow$ state). For stationary stochastic processes, such as the random walk, the residence time distribution can be obtained exactly. However for non-stationary processes this becomes difficult and no exact solutions are available [47]. In our spin-problem too it appears that the non-stationarity of the process makes an exact solution difficult.

For a system with N spins the total work done on the system is simply a sum of the work done on each of the spins. For the case where the spins are non-interacting we thus get a sum of N independent random variables. For large N the distribution will be a Gaussian with a mean that scales with N and variance as $N^{1/2}$. For interacting spins the properties of the work-distribution is an open problem. Especially of interest is the question as to what happens as we cross the transition temperature. This has been studied by Chatelain *et al.* [48], who found that the Jarzynki equality do hold in different temperature regions. Finally we note that the large fluctuations in the area under a hysteresis curve should be experimentally observable in nano-scale magnets.

3 Simple models of heat pumps.

3.1 Introduction

The idea of constructing miniature versions of engines, motors and pumps has been an interesting one. The earliest theoretical construct of such a device is probably Feynman's ratchet and pawl model discussed in [49]. In this article Feynman uses this simple microscopic model to demonstrate why a Maxwell's demon cannot work. In the same article he also shows how this model can be used to construct a microscopic heat engine and discusses its efficiency. There have been a number of recent detailed studies on the pawl-and-ratchet model and some subtle flaws in Feynman's original arguments have been pointed out [48 – 50, 62, 63, 68, 69]. A different class of ratchet models have also been studied in [70 – 77]. In these models Brownian particles, kept in an asymmetric periodic potential and acted upon by periodic time-dependent forces, are found to exhibit directed motion. A number of variations of this model has been studied [78 – 82]. Among its applications it has been proposed that this could provide a mechanism of transport of motors in biological cells [85].

Ratchet models which work on somewhat different principles are models of quantum pumps which are recently being studied theoretically [84 – 90] and have also been experimentally realized [93, 94]. Since these pumps also work at zero temperature it appears that noise is not an essential feature, which is unlike the case for usual ratchet models. Motivated by the quantum particle pump model, Segal and Nitzan have proposed a model for a heat pump [95]. In this model a molecule with two allowed energy levels interacts with two heat reservoirs kept at different temperatures. The energy level difference is modulated in a periodic way. Thus unlike the other particle pump models here only a single parameter is

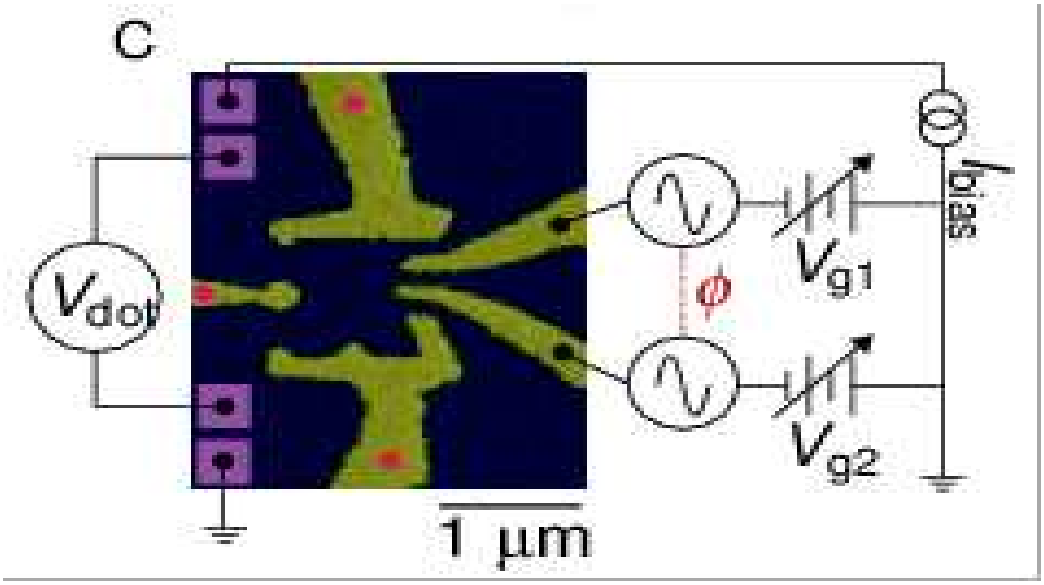

Figure 3.1: Schematic representation of the experimental assembly by Switkes *et al.* [93].

varied. An asymmetry is incorporated by taking reservoirs with different spectral properties and different couplings to the molecule. This seems to lead to the desired pumping of heat from the cold to the hot reservoir.

We will briefly discuss few of the experiments done on the quantum pump. One of the first experiment was by Switkes *et al.* [93], who used the quantum pumping mechanism to produce a $\mathcal{DC}$ current in response to the cyclic deformation of the confining potentials in an open quantum dot. The assembly of the the experiment is as shown in the Fig. (3.1). Three gates marked with red circles control conductance of point-contact leads that connect the dot to electronic reservoirs. In this experiment two coupled quantum dots are separately in contact with particle reservoirs which are at the same chemical potential. One applies $\mathcal{AC}$ gate voltages $V_{g_1} = V_0 \cos(\omega t)$ and $V_{g_2} = V_0 \cos(\omega t + \phi)$ to the two dots respectively. This leads to a net flow of particle current between the two reservoirs whose sign depends on the phase ϕ. This can be seen in Fig. (3.2) where the voltage across the dot which is proportional to the current is plotted as a function of phase difference ϕ. A sinusoidal dependence on ϕ is observed.

The physical picture of such processes can be understood as follows. In Fig. (3.3) we show

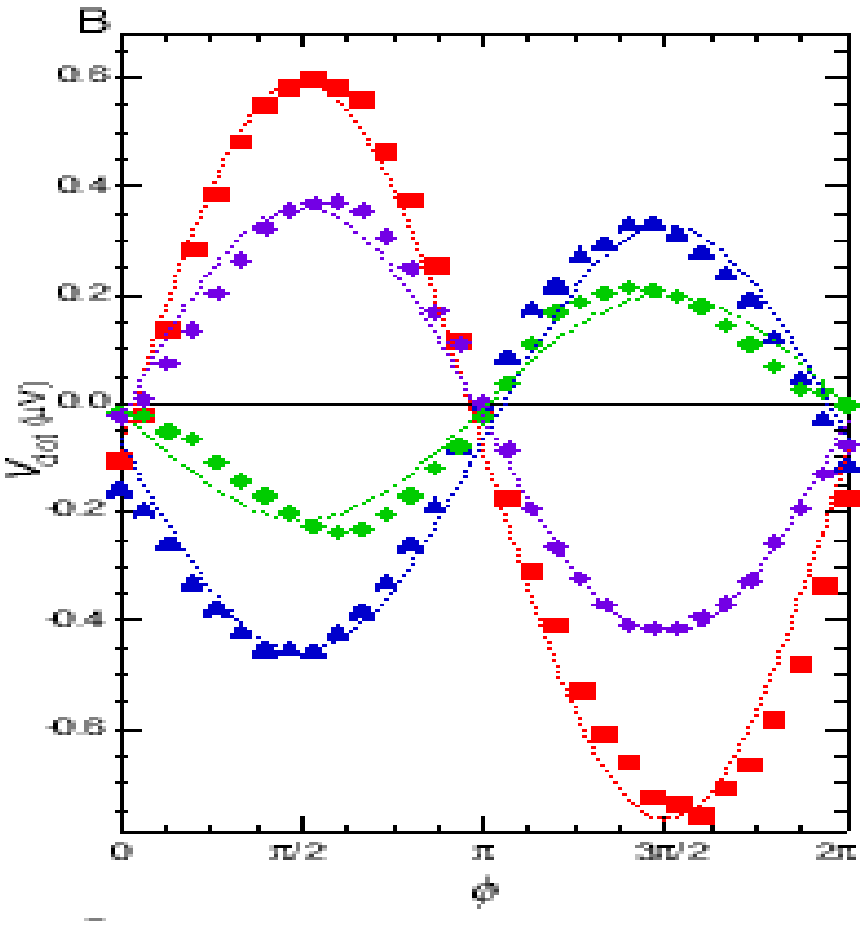

Figure 3.2: Plot of $V_{dot}(\phi)$ as a function of phase ϕ.

a schematic representation of the quantum pump model. Let the phase difference between the voltages be $\phi = \pi/2$. In step (a), a particle from right reservoir is trapped in a potential well $V_2 = -V_0$, in the next step (b), $V_1 = -V_0$ and $V_2 = 0$, so particle goes to the left hand side well. In step (c), $V_2 = V_0$, hence particle cannot go back to the right hand side hence it hops to left reservoir and in step (d), since $V_1 = V_0$, particle cannot hop back. Hence it can be seen that a net charge is transferred from right to left bath, as the potentials vary periodically in time. Also the direction of current depends upon the phase difference ϕ. Another experiment by Leek *et al.* [94] looked charge pumping across a carbon nanotube. The experimental set up is as shown in the Fig. (3.4). A carbon nanotube is attached to the surface of a quartz crystal and connected to reservoirs (source (S) and the drain (D)). A surface acoustic wave

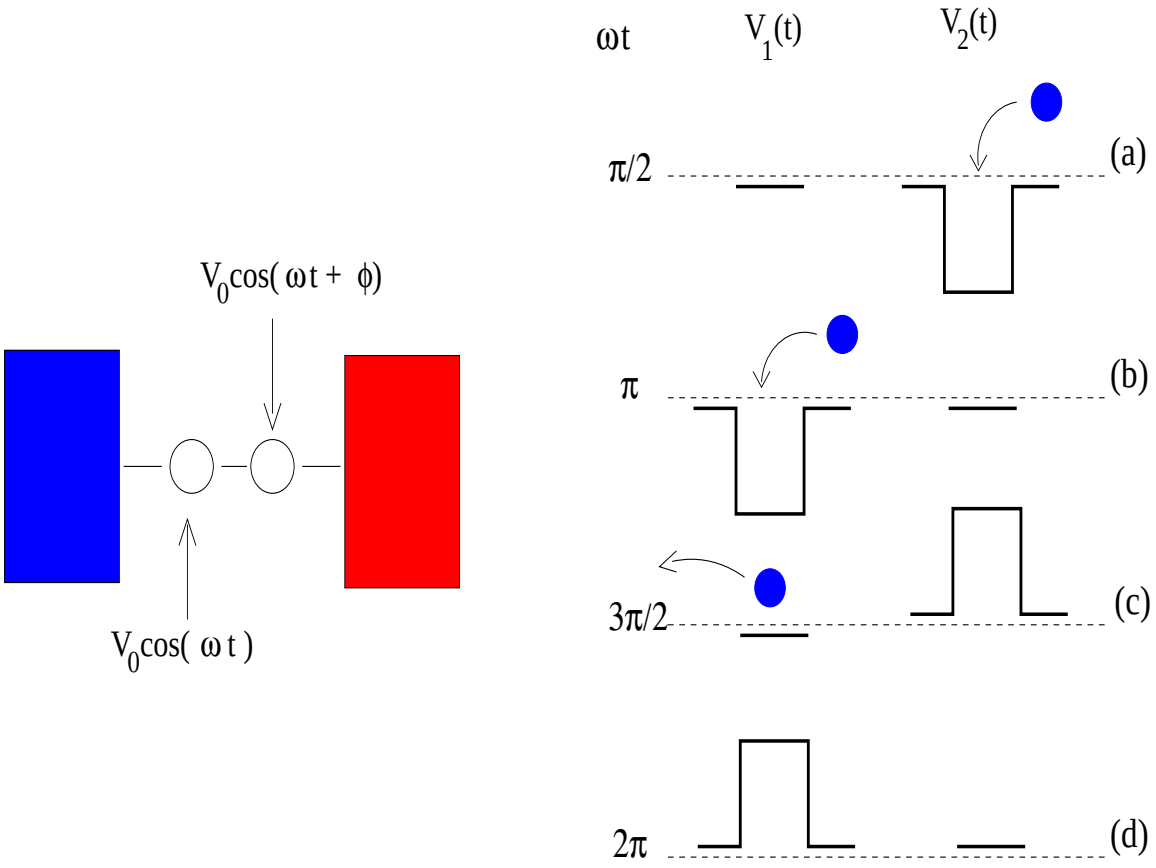

Figure 3.3: Two quantum dots in presence of oscillating voltages. Right hand figures show the two potentials at different times in a cycle. A net charge is transferred in one cycle.

was sent through the quartz crystal, and this produces travelling potential wells inside the nanotubes. It was found that an electron current can be generated across the nanotube as a function of the gate voltage. In this system, the transport of charge resembles the pumping of water by an Archimedean screw (see Fig. (3.5)). In the Archimedean screw, due to the chirality of the pump by rotating the handle water can be pumped to a higher level.

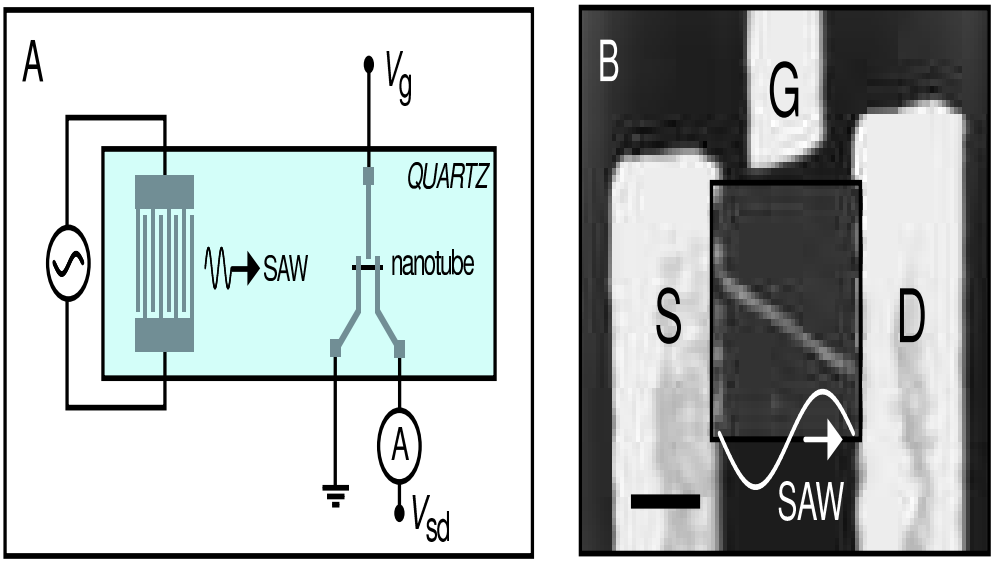

Figure 3.4: Schematic representation of the experimental assembly by Leek *et al.* [94].

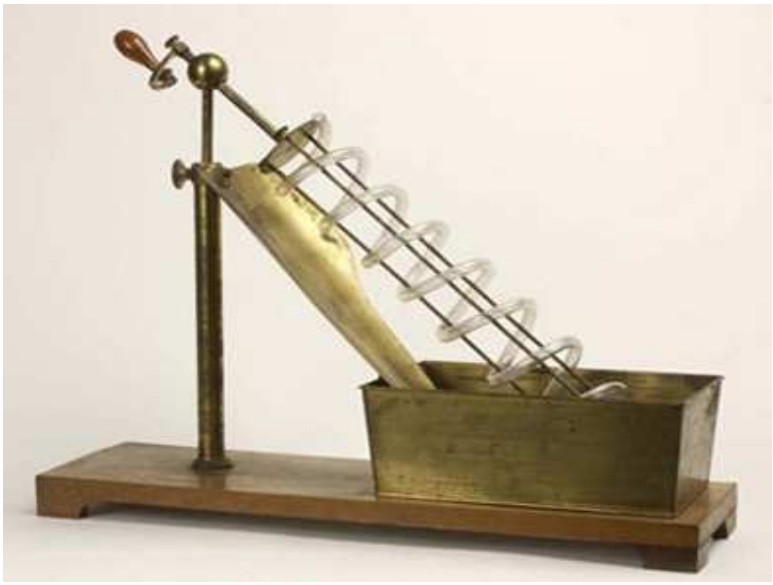

Figure 3.5: Archemedian screw.

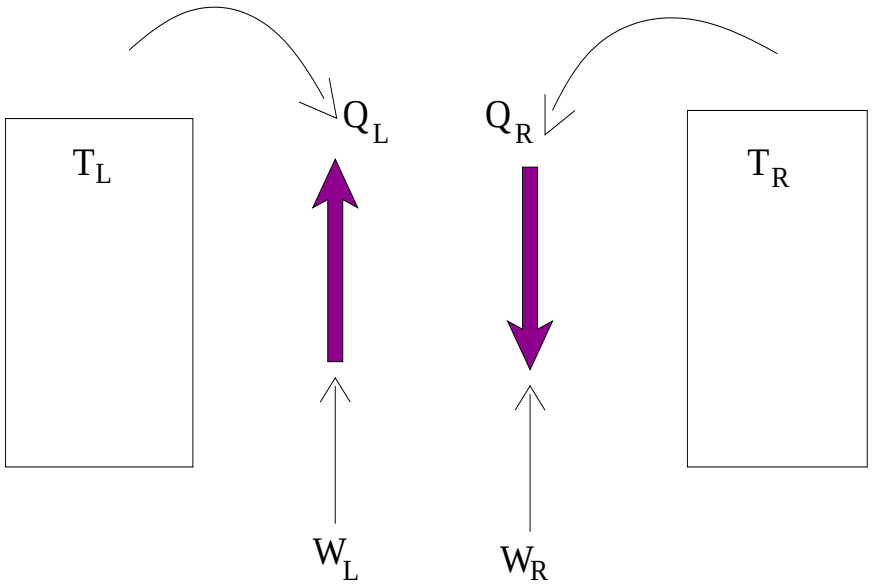

Figure 3.6: System of two Ising spins in contact with two heat baths and are driven by external time dependent magnetic fields.

Motivated by these quantum pump models, we examine classical models of heat pump which have the same basic design. We consider two different models:

1. A spin system consisting of two Ising spins each driven by periodic magnetic fields with a phase difference and connected to two heat reservoirs.

2. An oscillator system of two interacting particles driven by periodic forces with a phase difference and connected to two reservoirs.

In both cases we analyze the possibility of the models to work either as pumps or as engines. Our main result is that the spin system can work both as a pump and as an engine. On the other hand the oscillator model fails to perform either function.

3.2 Spin System

Our first model consists of two Ising spins driven by time-dependent magnetic fields $h_L(t)$ and $h_R(t)$ respectively and each interacting with separate heat reservoirs, see Fig. (3.6). The

Hamiltonian of the system is given by:

$$\mathcal{H} = -J\sigma_1\sigma_2 - h_L(t)\sigma_1 - h_R(t)\sigma_2 \,, \qquad \sigma_{1,2} = \pm 1, \tag{3.1}$$

where J is the interaction energy between the spins. The magnetic fields have the forms $h_L(t) = h_0\cos(\Omega t)$ and $h_R(t) = h_0\cos(\Omega t + \phi)$. The interaction of each spin with the heat baths is modeled by a stochastic dynamics. Here we assume that the time-evolution of the spins is given by Glauber dynamics [96], generalized to the case of two heat baths, with temperatures T_L and T_R. Thus the Glauber spin flip rates for the two spins, arising from the left and right reservoirs are respectively given by:

$$\begin{aligned} r^L_{\sigma_1\sigma_2} &= r\,(1 - \gamma_L\sigma_1\sigma_2)\,(1 - \nu_L\sigma_1) \\ r^R_{\sigma_1\sigma_2} &= r\,(1 - \gamma_R\sigma_1\sigma_2)\,(1 - \nu_R\sigma_2), \end{aligned} \tag{3.2}$$

where

$$\begin{aligned} \gamma_{L,R} &= \tanh(J/k_BT_{L,R}) \\ \nu_{L,R} &= \tanh(h_{L,R}/k_BT_{L,R}) \end{aligned} \tag{3.3}$$

and r is a rate constant. The master equation for evolution of the spin distribution function $\hat{P} = [P(+,+,t), P(-,+,t), P(+,-,t), P(-,-,t)]^T$ is then given by:

$$\frac{\partial\hat{P}}{\partial t} = \mathcal{T}\hat{P}\,, \tag{3.4}$$

where

$$\mathcal{T} = \begin{pmatrix} -r^L_{++} - r^R_{++} & r^L_{-+} & r^R_{+-} & 0 \\ r^L_{++} & -r^L_{-+} - r^R_{-+} & 0 & r^R_{--} \\ r^R_{++} & 0 & -r^L_{+-} - r^R_{+-} & r^L_{--} \\ 0 & r^R_{-+} & r^L_{+-} & -r^L_{--} - r^R_{--} \end{pmatrix}.$$

We define $\dot{Q}_L$, $\dot{Q}_R$ to be the rates (averaged over the probability ensemble) at which heat is absorbed from the left and right baths respectively while $\dot{W}_L$, $\dot{W}_R$ are the rates at which work is done on the left and right spins by the external magnetic field. These can be readily

expressed in terms of the spin distribution function and the various transition rates. Thus we find:

$$\begin{aligned}
\dot{Q}_L &= \sum_{\sigma_1,\sigma_2} P(\sigma_1,\sigma_2,t) r^L_{\sigma_1\sigma_2} \Delta E_1(\sigma_1,\sigma_2) \\
\dot{Q}_R &= \sum_{\sigma_1,\sigma_2} P(\sigma_1,\sigma_2,t) r^R_{\sigma_1\sigma_2} \Delta E_2(\sigma_1,\sigma_2) \\
\dot{W}_L &= -\langle\sigma_1\rangle\, \dot{h}_L = -\dot{h}_L \sum_{\sigma_1,\sigma_2} \sigma_1 P(\sigma_1,\sigma_2,t) \\
\dot{W}_R &= -\langle\sigma_2\rangle\, \dot{h}_R = -\dot{h}_R \sum_{\sigma_1,\sigma_2} \sigma_2 P(\sigma_1,\sigma_2,t)\,,
\end{aligned} \tag{3.5}$$

where

$$\begin{aligned}
\Delta E_1 &= 2\,(J\sigma_1\sigma_2 + h_L\sigma_1) \\
\Delta E_2 &= 2\,(J\sigma_1\sigma_2 + h_R\sigma_2)
\end{aligned} \tag{3.6}$$

are the energy costs in flipping the first and second spin respectively. The average energy of the system is given by

$$U = \langle\mathcal{H}\rangle = \sum_{\sigma_1,\sigma_2} \mathcal{H}(\sigma_1,\sigma_2,t)\, P(\sigma_1,\sigma_2,t). \tag{3.7}$$

Differentiating Eq. (3.7) with respect to time, we get

$$\dot{U} = \sum_{\sigma_1,\sigma_2} \dot{\mathcal{H}}(\sigma_1,\sigma_2,t)\, P(\sigma_1,\sigma_2,t) + \sum_{\sigma_1,\sigma_2} \mathcal{H}(\sigma_1,\sigma_2,t)\, \dot{P}(\sigma_1,\sigma_2,t). \tag{3.8}$$

Differentiating Eq. (3.1) with respect to time and using Eqs. (3.4) and (3.5) in Eq. (3.8), it is easy to verify the energy conservation equation:

$$\dot{U} = \dot{Q}_L + \dot{Q}_R + \dot{W}_L + \dot{W}_R. \tag{3.9}$$

From Floquet's theorem we expect probability distribution $\hat{P}$, at long times to be periodic with time period $\tau = 2\pi/\omega$. We will be interested in the following time averaged rates of

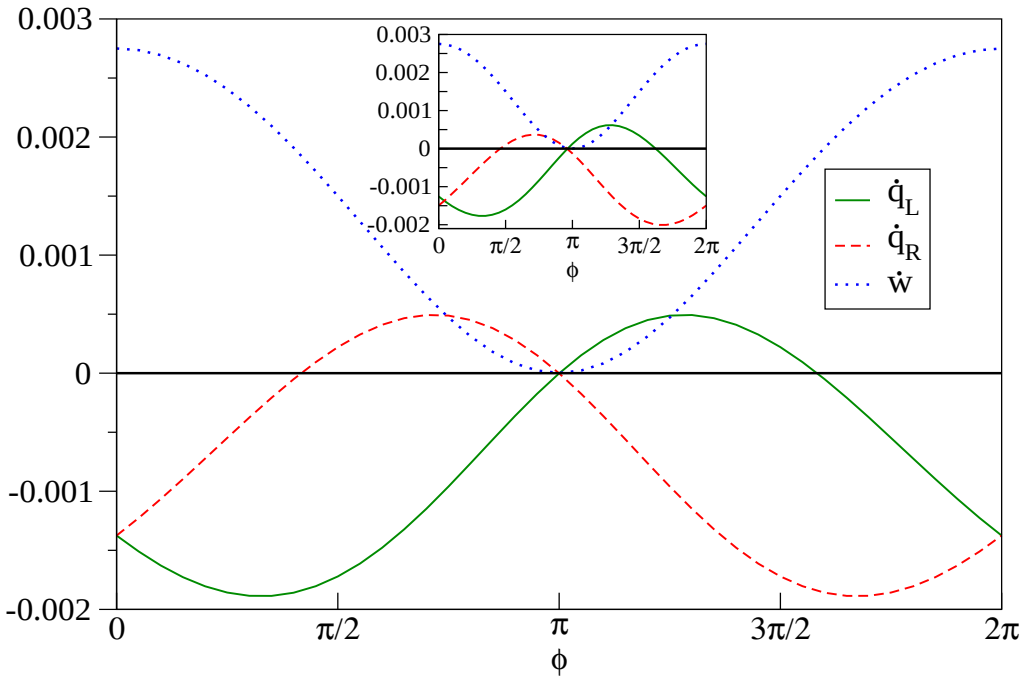

Figure 3.7: Plot of $\dot{q}_L$, $\dot{q}_R$, $\dot{w}$ versus ϕ with both baths at the same temperature. Inset shows the currents for the case where the right bath is slightly colder.

heat exchanges and work done, evaluated in the steady state:

$$\begin{aligned} \dot{q}_{L,R} &= \frac{1}{\tau}\int_0^\tau \dot{Q}_{L,R}\, dt\,, \\ \dot{w}_{L,R} &= \frac{1}{\tau}\int_0^\tau \dot{W}_{L,R}\, dt. \end{aligned} \tag{3.10}$$

We numerically solve the master equation Eq. (3.4) and then evaluate the various steady-state energy exchange rates $\dot{q}_{L,R}$ and $\dot{w}_{L,R}$. In all our numerical calculations we set $r = 0.5$ and $J/k_B = 1$ and all other quantities are measured in these units. In Fig. (3.7) we consider the parameter values $T_L = T_R = 0.5$, $h_0 = 0.25$, $\tau = 225$ and plot $\dot{q}_L, \dot{q}_R$ and $\dot{w} = \dot{w}_L + \dot{w}_R$ as functions of the phase ϕ. It can be seen that, for certain values of the phase, both $\dot{q}_L$ and $\dot{q}_R$ are negative while $\dot{w}$ is positive. Following our sign conventions, this means that all the work from the external driving is getting dissipated into the two baths. More interestingly we find that for certain values of the phase we can get $\dot{q}_L > 0$ and $\dot{q}_R < 0$ which means that there is heat flow *from* the left reservoir *to* the right reservoir. The direction of heat flow can be reversed by changing the phase. From continuity arguments it is clear that this model can also sustain heat flow against a small temperature gradient. Thus the inset of Fig. (3.7) shows

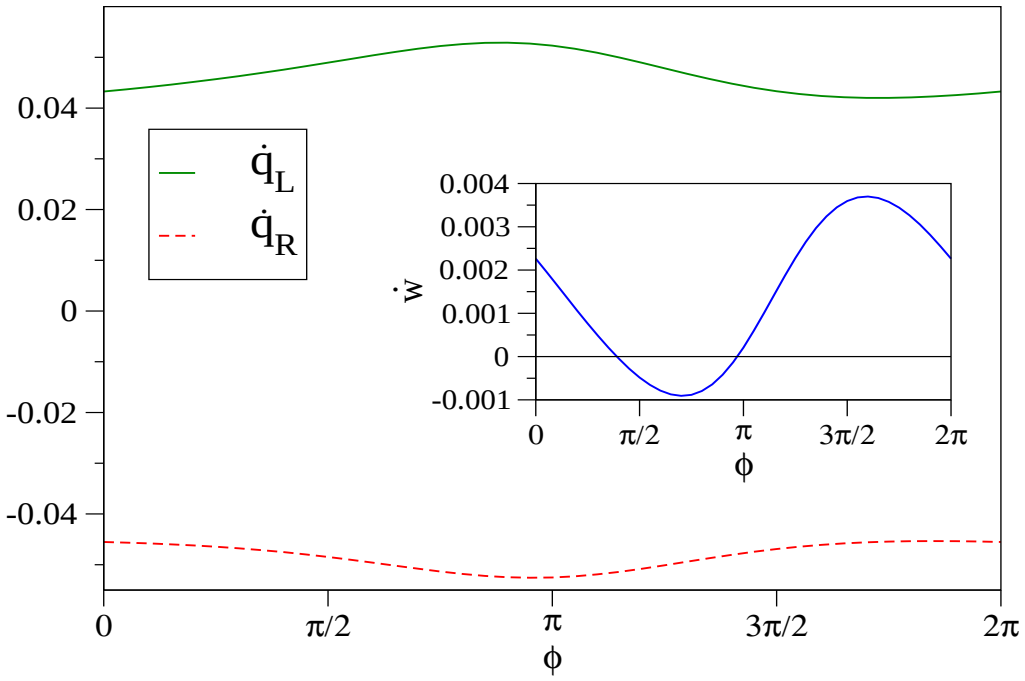

Figure 3.8: Plot of $\dot{q}_L$, $\dot{q}_R$, $\dot{w}$ versus ϕ for parameter values chosen such that the model performs as an engine.

the currents when the right reservoir is kept at a slightly lower temperature $T_R = 0.499$. In the absence of any driving we would get a steady current $\dot{q}_L = -\dot{q}_R = 1.41 \times 10^{-4}$ from the left to right reservoir. In the presence of driving and at a phase value $\phi = 2.2$ we get $\dot{q}_R = 3.674 \times 10^{-4}$, $\dot{q}_L = -1.025 \times 10^{-3}$ which means that heat flows *out* of the cold reservoir. Thus we see that our model can perform as a heat pump or a refrigerator. Similarly we find that the model can also perform like an engine and convert heat to work. This can be seen in Fig. (3.8) where we consider the parameter values $T_L = 1.0, T_R = 0.1$, $h_0 = 0.25$, $\tau = 190$. In this case we find that for certain values of ϕ we can have $\dot{w} < 0$ which means that work is being done on the external force. For typical values of parameters that we have tried we find that the efficiency of the engine is quite low. For example for Fig. (3.8) with $\phi = 0.7\pi$, we find $\eta = |\dot{w}|/\dot{q}_L = 1.75 \times 10^{-2}$.

Finally in Fig. (3.9) we plot the time-dependent energy transfer rates given by Eq. (3.5) for parameter values corresponding to the refrigerator and engine modes of operation. In both cases the initial configuration was chosen with $P(+,+,t=0) = 1$. At long times we

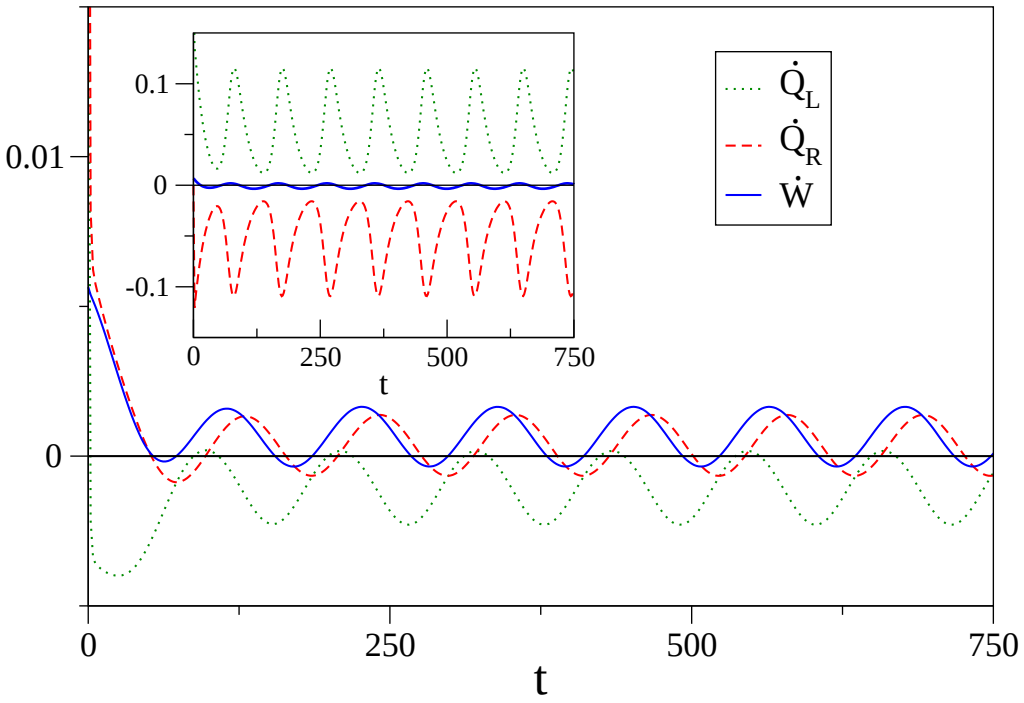

Figure 3.9: Plot of $\dot{Q}_L$, $\dot{Q}_R$, $\dot{W}$ as a function of time for parameters corresponding to pump and engine (inset).

see that all quantities vary periodically with time with the same period τ as the driving force. Fig. (3.9) corresponds to the parameter values $T_L = 0.5$, $T_R = 0.499$, $h_0 = 0.25$, $\tau = 225$ and $\phi = 2.2$ while the inset corresponds to the engine parameters $T_L = 1.0$, $T_R = 0.1$, $h_0 = 0.25$, $\tau = 190$ and $\phi = 2.2$.

3.3 Oscillator System

The second model of our engine consists of two particles which separately interact with two reservoirs kept at different temperatures (see Fig. (3.10)). The particles interact with each other and are also driven by two external periodic forces with a phase difference. We consider the system to be described by the Hamiltonian

$$\mathcal{H} = \frac{p_1^2}{2m} + \frac{p_2^2}{2m} + \frac{1}{2}kx_1^2 + \frac{1}{2}kx_2^2 + \frac{1}{2}k_c(x_1 - x_2)^2 - (f_L(t)\,x_1 + f_R(t)\,x_2). \qquad (3.11)$$

The two particles are acted on by external periodic forces given by $f_L(t) = f_0\cos(\Omega t)$ and $f_R(t) = f_0\cos(\Omega t + \phi)$ respectively, where ϕ is a phase difference. The effect of the heat baths

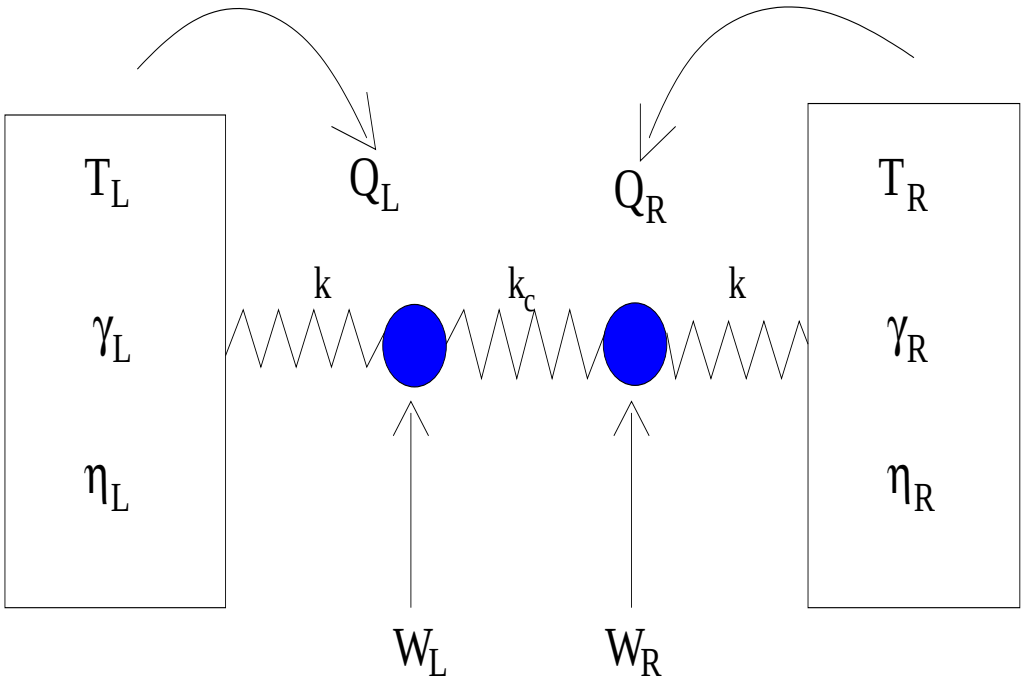

Figure 3.10: System of two Brownian particles in contact with two heat baths and are driven by external time dependent forces.

at temperatures T_L and T_R is modeled by Langevin equations. Thus the equations of motion are

$$\begin{aligned} m\ddot{x}_1 &= -(k+k_c)x_1 + k_c x_2 - \gamma\dot{x}_1 + \eta_L + f_L(t)\,, \\ m\ddot{x}_2 &= -(k+k_c)x_2 + k_c x_1 - \gamma\dot{x}_2 + \eta_R + f_R(t)\,, \end{aligned}$$

where the two noise terms are Gaussian and uncorrelated and satisfy the usual fluctuation-dissipation relations $\langle \eta_{L,R}(t)\eta_{L,R}(t')\rangle = 2k_B T_{L,R}\gamma\delta(t-t')$. Multiplying the two equations above by $\dot{x}_1$ and $\dot{x}_2$ respectively and adding them up we get:

$$\dot{\mathcal{H}} = (-\gamma\dot{x}_1 + \eta_L)\dot{x}_1 + (-\gamma\dot{x}_2 + \eta_R)\dot{x}_2 - \dot{f}_L(t)x_1 - \dot{f}_R(t)x_2, \tag{3.12}$$

which has the obvious interpretation of an energy conservation equation. Averaging over noise we get

$$\dot{U} = \dot{Q}_L + \dot{Q}_R + \dot{W}_L + \dot{W}_R, \tag{3.13}$$

where the various energy exchange rates have the same interpretations as in the previous discussion and are given by,

$$\begin{aligned}
\dot{Q}_L &= \langle(-\gamma\dot{x}_1 + \eta_L)\dot{x}_1\rangle \,, \\
\dot{Q}_R &= \langle(-\gamma\dot{x}_2 + \eta_R)\dot{x}_2\rangle \,, \\
\dot{W}_L &= -\langle \dot{f}_L x_1\rangle \,, \\
\dot{W}_R &= -\langle \dot{f}_R x_2\rangle. \qquad (3.14)
\end{aligned}$$

As before we define the average energy transfer rates in the steady state $\dot{q}_L, \dot{q}_R, \dot{w}_L, \dot{w}_R$. The present model being linear, it is straightforward to exactly compute these as we now show.

We first obtain the steady-state solutions of the equations of motion. We write the equations of motion in the following matrix form:

$$M\dot{X} = -\Phi X - \Gamma\dot{X} + \eta(t) + f(t), \qquad (3.15)$$

where $X = [x_1, x_2]^T$, $\eta = [\eta_L, \eta_R]^T$, $f = [f_0\cos(\Omega t), f_0\cos(\Omega t + \phi)]^T$, M and Γ are diagonal matrices with diagonal elements m and γ respectively and Φ is the force constant matrix. The steady state solution of this equation is:

$$\begin{aligned}
X(t) &= X_N(t) + X_D(t) \,, \\
\text{where } X_N(t) &= \int_{-\infty}^{\infty} d\omega e^{-i\omega t} G(\omega)\tilde{\eta}(\omega) \,, \\
X_D(t) &= Re[G(\Omega)\tilde{f}e^{-i\Omega t}] \,, \\
\text{with } G(\omega) &= [\Phi - \omega^2 M + i\omega\Gamma]^{-1} \,, \qquad (3.16)
\end{aligned}$$

and $\tilde{\eta} = \int_{-\infty}^{\infty} d\omega e^{-i\omega t}\ \eta(t)$, $\tilde{f} = \{1, e^{-i\phi}\}^T$. It is easy to see that the matrix $G(\omega)$ has two independent elements and we denote them as,

$$\begin{aligned}
A(\omega) = G_{11} &= G_{22} = [k + k_c - m\omega^2 - i\gamma\omega]/[(k + k_c - m\omega^2 - i\gamma\omega)^2 - k_c^2] \\
B(\omega) = G_{12} &= G_{21} = k_c/[(k + k_c - m\omega^2 - i\gamma\omega)^2 - k_c^2]. \qquad (3.17)
\end{aligned}$$

Using the above solution in Eq. (3.16), and after some bit of algebraic simplifications, we

obtain the following results:

$$\begin{aligned}
\dot{q}_L &= -\frac{f_0^2\Omega}{2}\,[\,A_I(\Omega) + B_I(\Omega)\cos(\phi) + D(\Omega)\sin(\phi)\,] + \frac{k_B\gamma k_c^2(T_L - T_R)}{2(mk_c^2 + (k+k_c)\gamma^2)}\,, \\
\dot{q}_R &= -\frac{f_0^2\Omega}{2}\,[\,A_I(\Omega) + B_I(\Omega)\cos(\phi) - D(\Omega)\sin(\phi)\,] + \frac{k_B\gamma k_c^2(T_R - T_L)}{2(mk_c^2 + (k+k_c)\gamma^2)}\,, \\
\dot{w}_L &= \frac{f_0^2\Omega}{2}\,[\,A_I(\Omega) + B_I(\Omega)\cos(\phi) - B_R(\Omega)\sin(\phi)\,]\,, \\
\dot{w}_R &= \frac{f_0^2\Omega}{2}\,[\,A_I(\Omega) + B_I(\Omega)\cos(\phi) + B_R(\Omega)\sin(\phi)\,], \qquad (3.18)
\end{aligned}$$

where $A_R,\ A_I,\ B_R,\ B_I$ are the real and imaginary parts of A and B respectively and $D(\Omega) = 2\gamma^2\Omega^2 k_c/Z(\Omega)$ where $Z(\Omega) = |(k+k_c-m\Omega^2-i\gamma\Omega)^2 - k_c^2|^2$. From the expressions in Eq. (3.18) it is clear that the heat transfer rates can be separated into deterministic parts (depending on the driving strength f_0) and noise parts (dependent on temperature of the two reservoirs). The work terms are temperature independent. We now note that the deterministic parts of $\dot{q}_L$ and $\dot{q}_R$, are both negative. This can be shown by using the facts that $A_I \geq 0$ and $A_I^2 - B_I^2 - D^2 = \gamma^2\Omega^2[(k + k_c - m\Omega^2)^2 + \gamma^2\Omega^2 - k_c^2]^2/Z^2 \geq 0$. This means that for $T_L > T_R$, we always get $\dot{q}_R < 0$ and hence we can never have heat transfer from the cold to the hot reservoir. Thus this *cannot* work as a heat pump. Also we note that while $\dot{w}_L$ and $\dot{w}_R$ can individually be negative, the total work done $\dot{w}_L + \dot{w}_R$ is always positive. This means that this model *cannot* work as an engine either. These conclusions remain unchanged even if we define work as $\dot{W}_L = \langle f_L\dot{x}_1\rangle$, $\dot{W}_R = \langle f_R\dot{x}_2\rangle$. In Fig. (3.11) we plot the dependence of the rates of heat transfer and work done in the system on the phase difference ϕ. The figures correspond to the parameter values $k = 2,\ k_c = 3,\ m = 1,\ f_0 = 1,\ \gamma = 1$ and $T_L = T_R = T$. The plots are independent of the temperature T. Note that the only effect of the driving is to pump in energy which is asymmetrically distributed between the two reservoirs. The asymmetric energy transfer into the baths is an interesting effect considering that there is no inbuilt directional asymmetry in the system.

In this model the heat baths and the external driving seem to act independently on the system. It is clear that the linearity of the model leads to this separability of the effects of the driving and noise forces and this could be the reason that the model is not able to function as a

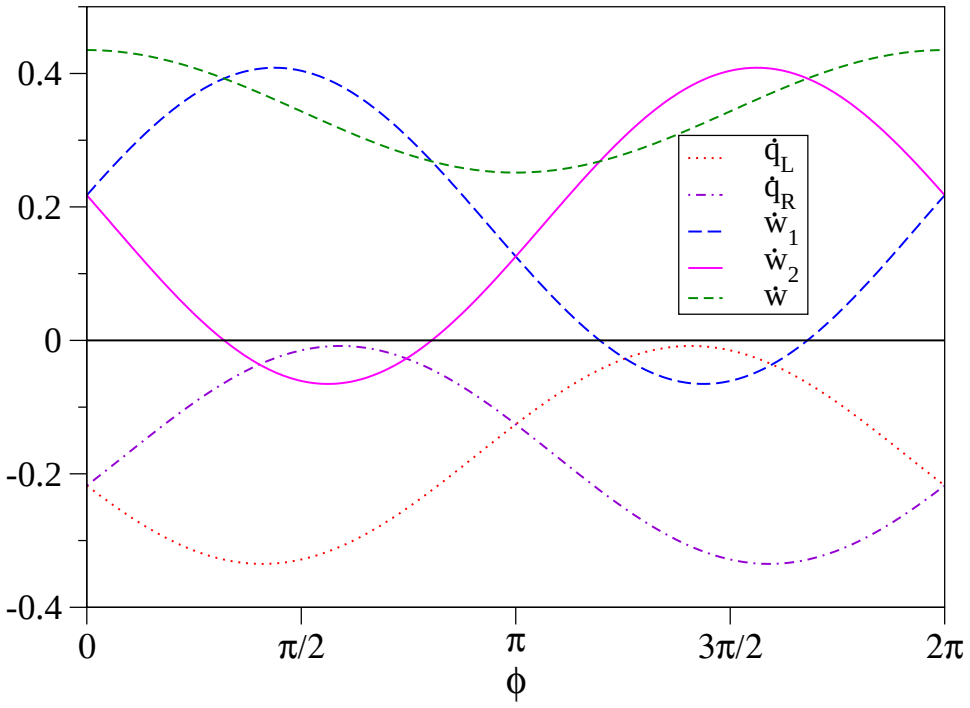

Figure 3.11: Plots of heat transfer and work done as a function of phase difference ϕ in the two particle model. Here $\Omega = 2\pi/3$.

heat pump. Hence it is important to consider the effect of non-linearity. We have numerically studied the effect of including a nonlinear part of the form $\alpha[x_1^4 + x_2^4 + (x_1 - x_2)^4]/4$, in the oscillator Hamiltonian. From simulations with a large range of parameter values we find that the basic conclusions remain unchanged and the model does not work either as a pump or as an engine. In Fig. (3.12) we show some typical results and see that here also even though two works w_L and w_R become negative, still total work done is always positive. Similarly heat transferred is always negative. In Fig. (3.13) we plot the total work done on the system, due to non-linearity we find that this work done now depends on the temperature unlike the linear model.

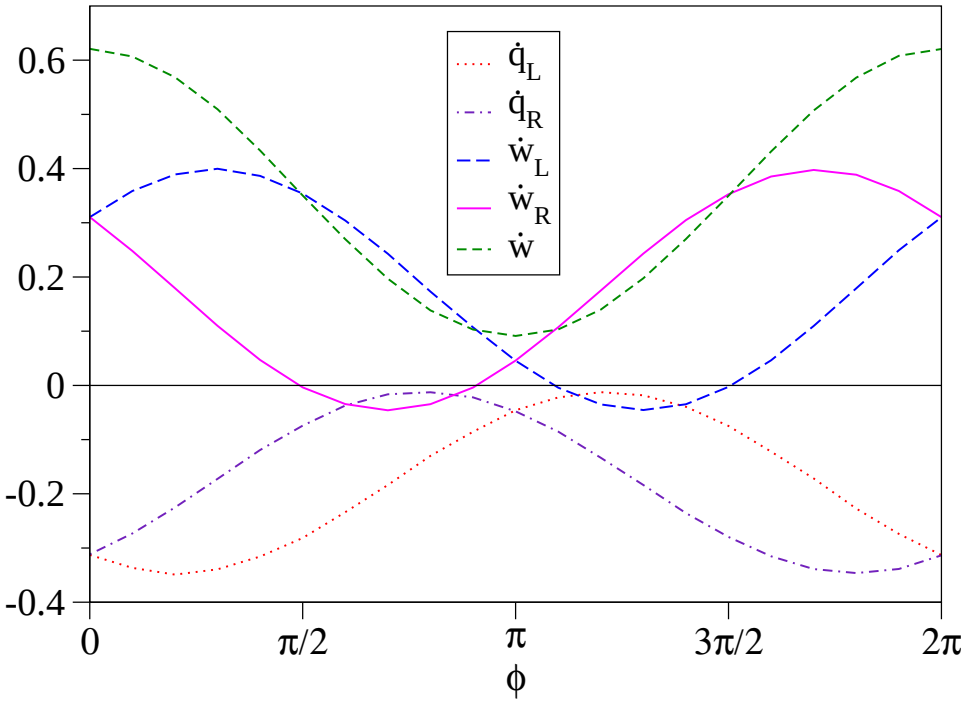

Figure 3.12: Plots of heat transfer and work done as a function of phase difference ϕ in the two particle model with non-linearity. Here $\Omega = 2\pi/3$ and other parameters same as in Fig. (3.11).

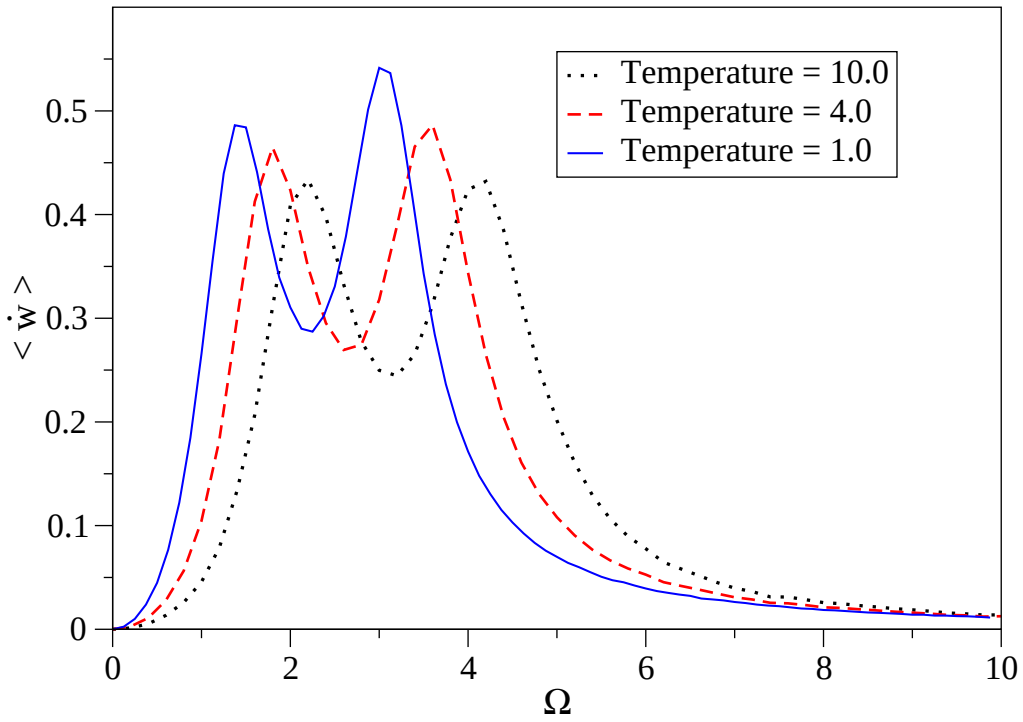

Figure 3.13: Plots of total work done as a function of frequency Ω in the two particle model with non-linearity. Here $\phi = \pi/2$ and other parameters same as in Fig. (3.11).

3.4 Conclusions

In conclusion, we have studied two models which have the same ingredients as those on which recent models of quantum pumps have been constructed. We find that the first model performs as a heat pump to transfer heat from a cold to a hot reservoir. Thus pumping is not an essentially quantum-mechanical phenomena. Also our model performs as an engine to do work on the driving force. It is useful to compare our model with the other well-studied microscopic model of a engine, namely the Feynman ratchet and pawl. Recent detailed studies have shown that this model can function both as an engine and as a refrigerator [53, 54]. One difference of this model from ours is that there is no periodic external driving. However this also means that in order for the model to work in a cyclic way, at least one of the degrees of freedom has to be a periodic (or angular) variable. This may not always be a desirable feature in realistic models. Surprisingly our second model, though apparently built on the same principles, fails to perform either as a pump or as an engine. We have also tried the double well potential of type, $-\frac{1}{2}\,kx_1^2 + \frac{1}{4}\,\alpha x_1^4 - \frac{1}{2}\,kx_2^2 + \frac{1}{4}\,\alpha x_2^4$, which resembles the two levels (in spin case). Though we have tried large range of parameter values, still it is not clear as to what are the necessary conditions for the pump model to work.

The important difference between microscopic models of heat engines, such as those studied here, and usual thermodynamic heat engines is that here the effects of thermal fluctuations are important. A second difference is that here the system is simultaneously in contact with both the cold and hot baths. The understanding of these microscopic models requires the use of non-equilibrium statistical mechanics and there are currently no general principles as in classical thermodynamics. It is clear that further studies are necessary to understand the pumping mechanism in simple models of molecular pumps and this can perhaps lead to more realistic and practical models of molecular pumps and engines.

4 Particle pump with symmetric exclusion process.

4.1 Introduction

The symmetric exclusion process (SEP) is one of the simplest and well studied models of a stochastic interacting particle system. In this model which can be defined on a d-dimensional hypercubic lattice, particles move diffusively while satisfying the hardcore constraint that two particles cannot be on the same site. A number of exact results have been obtained for this model, particularly in one dimension [95 – 97]. If the model is defined on a ring and conserves the total density, the system obeys the equilibrium condition of detailed balance in the steady state and thus does not support any net current. A lot of attention has also been given to non-equilibrium steady states of driven SEP in which the particles can enter or leave the bulk at the boundaries. For this model, the time-dependent correlation functions [100] and dynamical exponents have been obtained using the equivalence of the transition matrix (W-matrix) to the Heisenberg model [101]. Recently, large deviation functional and current fluctuations have also been calculated for the driven SEP [100 – 102]. Experimentally it has been shown that SEP can be used to model the diffusion of colloidal particles in narrow pores [103 – 108].

Here we study the SEP for the case where hopping rates are time-dependent. This is one of the few studies of a many-particle interacting stochastic model with time-dependent transition rates and as we demonstrate shows a lot of interesting behaviour. The initial motivation for this study comes from quantum pump models discussed in the previous chapter [85, 88, 90 – 92, 109 – 117]. We saw there that classical heat pumps could be built on simi-

lar principles. Here we investigate the question whether, by using similar driving protocols, particle pumping can be achieved in a classical stochastic model.

Classical pumping of particles in time-dependent stochastic models of non-interacting particles has earlier been studied [118 – 120] and seen in experiments [123]. Systems exhibiting pumping effect have often been modeled as Brownian ratchets in which non-interacting particles move in an external periodic potential and we have discussed various such models in chapter (1). Our model differs from such models in that here we are dealing with a many body particle system with interactions, and particle interactions seem necessary for the pumping effect.

We have studied the time-dependent SEP by simulations and also analytically by using perturbation theory. The first perturbation uses the driving amplitude as the small parameter. The other uses the inverse of driving frequency as a small parameter. Within this perturbative approach, we are able to obtain exact expressions for various physical quantities, and find very good agreement with simulation results. The most interesting result is that in the model with time-dependent rates at all sites, a $\mathcal{DC}$ current of order unity can be obtained. We note that the hopping rates though time-dependent, are still symmetric and hence our result is surprising.

4.2 Definition of Model

The model is defined on a ring with L sites (see Fig. (4.1)). A site $l = 1, 2, 3, ...L$ can be occupied by $n_l = 0$ or 1 particle and the system contains a total of $N = \rho L$ particles where ρ is the total density. A particle at site l hops to an empty site either on the left or right with equal rates given by:

$$\begin{aligned} u_l &= f_0 + f_1 \nu_l \\ \text{where } \nu_l &= \alpha_l \sin(\omega t + \phi_l) = \nu_l e^{i\omega t} + \nu_l^* e^{-i\omega t} \,. \end{aligned} \tag{4.1}$$

Here the site-dependent complex amplitudes are defined by $\nu_l = \alpha_l \, e^{i\phi_l}/2i$ with α_l as a real amplitude and f_1 is chosen such that all hopping rates are positive.

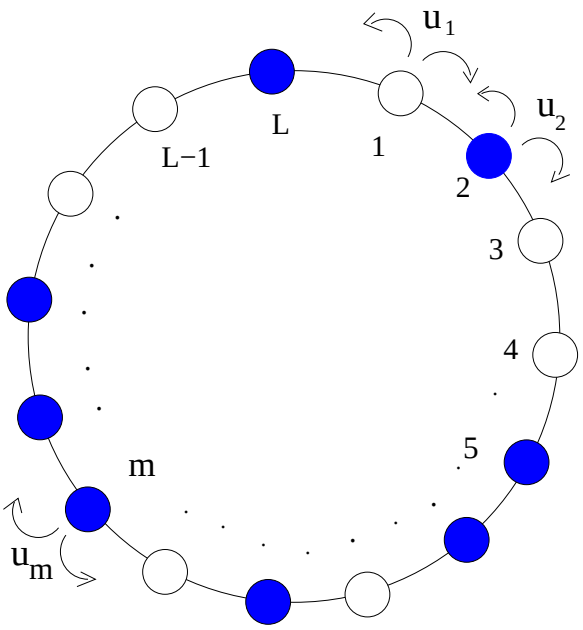

Figure 4.1: Schematic representation of the SEP model with periodic boundary conditions where a particle hops to next or previous unoccupied site with equal rates. Blue and white colors denote occupied and unoccupied sites respectively. For example particle at site 2 can hop to site 1 or 3 with equal probability where as particle at site 5 can hop to the previous site but not to the next site in this particular configuration.

A configuration of the system can be specified by the set $\{n_l\}$, $l = 1, 2, ...L$. Let us define $\mathbf{P}(t)$ as the probability vector in the configuration space, with elements $P(C, t)$ giving the probability of the system being in the configuration $C = \{n_l\}$ at time t. Then the stochastic dynamics of the many particle system is described by the master equation:

$$\frac{d\mathbf{P}(t)}{dt} = \mathbf{W}(t)\,\mathbf{P}(t) = \mathbf{W_0}\,\mathbf{P}(t) + \mathbf{W_1}(t)\,\mathbf{P}(t) \tag{4.2}$$

where $\mathbf{W}$ is the transition matrix, which we have split into a time-independent and a time-dependent part. One can also consider the time-evolution equations for m-point equal-time correlation functions $C_{l_1,l_2,l_3,....,l_m}(t) = \langle n_{l_1}...n_{l_m}\rangle = \sum_{\{n_l\}} n_{l_1}...n_{l_m} P(\{n_l\}, t)$. Thus, for example, the density $\rho_l(t) = \langle n_l\rangle$ and the two-point correlation function $C_{l,m}(t)$ satisfy the following

equations:

$$\frac{\partial \rho_l}{\partial t} + 2u_l\rho_l - u_{l-1}\rho_{l-1} - u_{l+1}\rho_{l+1} = u_l(C_{l-1,l} + C_{l,l+1}) - u_{l+1}C_{l,l+1} - u_{l-1}C_{l-1,l} \quad (4.3)$$

$$\begin{aligned} &\frac{\partial C_{l,m}}{\partial t} + 2(\,u_l + u_m\,)C_{l,m} - u_{l-1}\,C_{l-1,m} - u_{l+1}\,C_{l+1,m} - u_{m-1}\,C_{l,m-1} - u_{m+1}\,C_{l,m+1} \\ = \;& u_l\,(\,C_{l-1,l,m} + C_{l,l+1,m}\,) + u_m\,(\,C_{l,m-1,m} + C_{l,m,m+1}\,) - u_{l-1}\,C_{l-1,l,m} - u_{l+1}\,C_{l,l+1,m} \\ & -u_{m-1}\,C_{l,m-1,m} - u_{m+1}\,C_{l,m,m+1}, \quad \text{for} \quad |l-m| \neq 1 \\ &\frac{\partial C_{l,l+1}}{\partial t} + (\,u_l + u_{l+1}\,)C_{l,l+1} - u_{l-1}\,C_{l-1,l+1} - u_{l+2}\,C_{l,l+2} \\ = \;& u_l\;C_{l-1,l,m} + u_{l+1}\,C_{l,l+1,l+2} - u_{l-1}\,C_{l-1,l,l+1} - u_{l+2}\,C_{l,l+1,l+2}\,. \end{aligned} \quad (4.4)$$

From Floquet's theorem [124], it is expected that the long time state of the system (assumed to be unique) will be periodic in time with period $T = 2\pi/\omega$. Here we will be mainly interested in the *DC* current $\bar{J}$ defined as

$$\bar{J_l} = \frac{1}{T}\int_0^T J_{l,l+1}(t)\,dt, \quad (4.5)$$

where the current $J_{l,l+1}$ in a bond connecting sites l and $l+1$ is given by

$$J_{l,l+1} = u_l(\rho_l - C_{l,l+1}) - u_{l+1}(\rho_{l+1} - C_{l,l+1}) \quad (4.6)$$

and the local density $\rho_l = \langle n_l \rangle$. From the periodicity of the state and particle conservation, it follows that the *DC* current is uniform in space and therefore, using Eq. (4.6), we can write for the *DC* current:

$$\bar{J} = \frac{1}{LT}\int_0^T \sum_{l=1}^{L} J_{l,l+1}(t)\,dt \quad (4.7)$$

$$= \frac{f_1}{LT}\int_0^T \sum_{l=1}^{L} (v_{l+1} - v_l)C_{l,l+1}\,dt \quad (4.8)$$

Thus, to find the *DC* current, we need to compute 2-point correlation function $C_{l,l+1}(t)$. In this chapter, we will first develop a perturbation theory, for general v_l, and then apply it to some special cases.

Note that for $f_1 = 0$, the above model reduces to the homogeneous SEP with periodic

boundary conditions whose properties are known exactly. In this case the steady state is an equilibrium state which obeys detailed balance and hence the average current is zero (This result holds even when the u_l's are site dependent, but time independent). In the steady state, all configurations are equally probable i.e. $P(C) = 1/\binom{L}{N}$ when $f_1 = 0$. Then one can show that the density and correlation functions for the homogeneous SEP are given by:

$$\begin{aligned} \rho_l^{(0)} &= \rho = \frac{N}{L} \\ C_{l_1,l_2}^{(0)} &= \rho\frac{(N-1)}{(L-1)} \\ C_{l_1,l_2,l_3,....,l_m}^{(0)} &= \binom{L-m}{N-m}/\binom{L}{N}. \end{aligned} \tag{4.9}$$

4.3 Perturbation theory in f_1

For $f_1 \neq 0$, the knowledge of the exact steady state of homogeneous SEP enables us to set up a perturbation expansion in f_1 of various observables. We now describe this perturbation theory within which we calculate an expression for *DC* current $\bar{J}$ in the bulk of the system. A similar perturbation technique was developed for a two-state system in [125]. We expand various quantities of interest with f_1 as the perturbation parameter about the homogeneous steady state corresponding to $f_1 = 0$. Thus we write

$$\rho_l(t) = \langle n_l(t)\rangle = \rho + \sum_{r=1}^{\infty} f_1^r \rho_l^{(r)}(t) \tag{4.10}$$

$$C_{l,m}(t) = \langle n_l(t) n_m(t)\rangle = C_{l,m}^{(0)} + \sum_{r=1}^{\infty} f_1^r C_{l,m}^{(r)}(t)\,, \tag{4.11}$$

and similar expressions for higher correlations. Plugging in Eq. (4.11) into Eq. (4.8), we find that the lowest order contribution to $\bar{J}$ is at $O(f_1^2)$ and given by:

$$\bar{J}^{(2)} = \frac{f_1^2}{T\,L}\int_0^T \sum_{l=1}^{L} (\,v_l - v_{l+1}\,)\, C_{l,l+1}^{(1)}\, dt\,. \tag{4.12}$$

To develop our perturbation theory and finding $C_{l,m}^{(1)}$'s, we start with the time evolution equation for density $\rho_l(t)$ which is given by Eq. (4.3). Plugging in the expansions in Eqs. (4.10)

and (4.11), we get the following equation for the density $\rho_l^{(r)}$ at r^{th} order:

$$\begin{aligned}\frac{\partial \rho_l^{(r)}}{\partial t} &- f_0 \Delta_l \rho_l^{(r)} + 2\nu_l \rho_l^{(r-1)} - \nu_{l-1}\rho_{l-1}^{(r-1)} - \nu_{l+1}\rho_{l+1}^{(r-1)} \\ &= \nu_l (C_{l-1,l}^{(r-1)} + C_{l,l+1}^{(r-1)}) - \nu_{l-1} C_{l-1,l}^{(r-1)} - \nu_{l+1} C_{l,l+1}^{(r-1)}, \end{aligned} \tag{4.13}$$

where $\Delta_l g_l = g_{l+1} - 2g_l + g_{l-1}$ defines the discrete Laplacian operator. Thus the density at r^{th} order is obtainable in terms of density and two point correlation function at $(r-1)^{th}$ order. We check that at the zeroth order, we obtain the homogeneous SEP for which the density and all equal time correlations are given by Eq. (4.9). At first order, the above equation then gives:

$$\frac{\partial \rho_l^{(1)}}{\partial t} - f_0 \Delta_l \rho_l^{(1)} = r_0 \Delta_l \nu_l, \tag{4.14}$$

where $r_0 = \rho - C_{l,m}^{(0)}$. The solution for this equation is the sum of a homogeneous part which depends on initial conditions and a particular integral. At long times the homogeneous part vanishes while the particular integral has the following asymptotic form:

$$\rho_l^{(1)}(t) = A_l^{(1)} e^{i\omega t} + A_l^{*(1)} e^{-i\omega t}. \tag{4.15}$$

Substituting Eq. (4.15) in Eq. (4.14) we obtain the following equation for $\{A_l^{(1)}\}$:

$$(i\omega + 2f_0) A_l^{(1)} - f_0 A_{l-1}^{(1)} - f_0 A_{l+1}^{(1)} = r_0 (\nu_{l+1} - 2\nu_l + \nu_{l-1}) \,. \tag{4.16}$$

This can be written in matrix form as:

$$\hat{Z}(\omega) \;\; \mathbf{A} = -r_0 \; \hat{B} \, \mathbf{\Phi}, \tag{4.17}$$

where

$$\begin{aligned} Z_{lm} &= -f_0 \, \delta_{l,m+1} + (\, i\omega + 2f_0 \,) \, \delta_{l,m} - f_0 \, \delta_{l,m-1} \\ B_{lm} &= -\delta_{l,m+1} + 2 \, \delta_{l,m} - \delta_{l,m-1} \\ \mathbf{A} &= \{A_1^{(1)}, A_2^{(1)}, ..., A_L^{(1)}\}^T, \mathbf{\Phi} = \{\nu_1, \nu_2, ..., \nu_L\}^T, \end{aligned} \tag{4.18}$$

and periodic boundary conditions are implicitly taken. The above equation can be solved for **A** and we get:

$$\mathbf{A} = -r_0\, \hat{G}(\omega)\, \hat{B}\, \mathbf{\Phi}, \tag{4.19}$$

where $\hat{G}(\omega) = \hat{Z}^{-1}(\omega)$. Both $\hat{G}(\omega)$ and $\hat{B}$ are cyclic matrices and so can be diagonalized simultaneously. The eigenvalues of $\hat{Z}(\omega)$ are $i\omega + 4f_0 \sin^2(p\pi/L)$, while that of $\hat{B}$ are $4\sin^2(p\pi/L)$ with $p = 1, 2, ..., L$, and eigenvector elements are $e^{i2\pi pl/L}/L^{1/2}$. Hence $A_l^{(1)}$ can be written as:

$$A_l^{(1)} = -\frac{4r_0}{L} \sum_{m=1}^{L} \sum_{p=1}^{L} \frac{e^{-i\frac{2\pi p(l-m)}{L}} \sin^2(p\pi/L)}{i\omega + 4f_0 \sin^2(p\pi/L)}\, \nu_m, \tag{4.20}$$

which in the large L limit gives:

$$A_l^{(1)} = -\frac{r_0}{f_0}\, \nu_l + \frac{ir_0\omega}{f_0^2} \frac{1}{z_+ - z_-} \sum_{m=1}^{L} [\, z_-^{|m-l|} + z_-^{L-|m-l|}\,]\, \nu_m, \tag{4.21}$$

where, $z_- = y/2 - [(y/2)^2 - 1]^{1/2}$, $z_+ = 1/z_-$ and $y = 2 + (i\omega/f_0)$.

To compute the $O(f_1^2)$ contribution to $\bar{J}$, we need to evaluate $C_{l,m}^{(1)}$, which we now proceed to obtain. Inserting the perturbation series in Eqs. (4.10) and (4.11) into Eq. (4.4) we get the following equation for the correlation $C_{l,m}^{(r)}$ at r^{th} order for $|m - l| \neq 1$:

$$\begin{aligned}
\frac{\partial C_{l,m}^{(r)}}{\partial t} &- f_0\, (\, \Delta_l + \Delta_m\,)\, C_{l,m}^{(r)} + 2\nu_l\, C_{l,m}^{(r-1)} - \nu_{l-1}\, C_{l-1,m}^{(r-1)} - \nu_{l+1}\, C_{l+1,m}^{(r-1)} \\
&+ 2\nu_m\, C_{l,m}^{(r-1)} - \nu_{m-1}\, C_{l,m-1}^{(r-1)} - \nu_{m+1}\, C_{l,m+1}^{(r-1)} \\
&= \nu_l\, (\, C_{l-1,l,m}^{(r-1)} + C_{l,l+1,m}^{(r-1)}\,) + \nu_m\, (\, C_{l,m-1,m}^{(r-1)} + C_{l,m,m+1}^{(r-1)}\,) \\
&- \nu_{l-1}\, C_{l-1,l,m}^{(r-1)} - \nu_{l+1}\, C_{l,l+1,m}^{(r-1)} - \nu_{m-1}\, C_{l,m-1,m}^{(r-1)} - \nu_{m+1}\, C_{l,m,m+1}^{(r-1)},
\end{aligned}$$

while for $m = l + 1$:

$$\begin{aligned}
\frac{\partial C_{l,l+1}^{(r)}}{\partial t} &+ f_0\, (\, 2C_{l,l+1}^{(r)} - C_{l-1,l+1}^{(r)} - C_{l,l+2}^{(r)}\,) \\
&= \nu_{l+2}\, (\, C_{l,l+2}^{(r-1)} - C_{l,l+1,l+2}^{(r-1)}\,) + \nu_{l-1}\, (\, C_{l-1,l+1}^{(r-1)} - C_{l-1,l,l+1}^{(r-1)}\,) \\
&- \nu_l\, (\, C_{l,l+1}^{(r-1)} - C_{l-1,l,l+1}^{(r-1)}\,) - \nu_{l+1}\, (\, C_{l,l+1}^{(r-1)} - C_{l,l+1,l+2}^{(r-1)}\,).
\end{aligned} \tag{4.22}$$

At first order we get:

$$\begin{aligned}
\frac{\partial C^{(1)}_{l,m}}{\partial t} &- f_0(\Delta_l + \Delta_m) C^{(1)}_{l,m} = k_0(\Delta_l \nu_l + \Delta_m \nu_m)\,, \\
\frac{\partial C^{(1)}_{l,l+1}}{\partial t} &+ f_0\left(2C^{(1)}_{l,l+1} - C^{(1)}_{l-1,l+1} - C^{(1)}_{l,l+2}\right) = k_0(\nu_{l-1} + \nu_{l+2} - \nu_l - \nu_{l+1}),
\end{aligned} \tag{4.23}$$

where $k_0 = C^{(0)}_{l_1,l_2} - C^{(0)}_{l_1,l_2,l_3}$ and these are known from Eq. (4.9). The computation of even the homogeneous solution of the above set of equations is in general a nontrivial task because of the form of the equations involving nearest neighbor indices and requires a Bethe ansatz or dynamic product ansatz [99, 100]. However it turns out that the long time solution can still be found exactly and is given by:

$$C^{(1)}_{l,m}(t) = \frac{k_0}{r_0}[\rho^{(1)}_l(t) + \rho^{(1)}_m(t)] = A^{(1)}_{l,m} e^{i\omega t} + A^{*(1)}_{l,m} e^{-i\omega t}\,, \tag{4.24}$$

where $A^{(1)}_{l,m} = (k_0/r_0)(A^{(1)}_l + A^{(1)}_m)$. It is easily verified that this satisfies Eq. (4.23) for all l, m. To determine whether the system indeed has a product measure requires a more detailed analysis of the higher order terms in the perturbation series and higher correlations. We have verified that, at first order in perturbation theory, all correlation functions in fact have the same structure as the two-point correlation function in Eq. (4.24).

We now plug the solution in Eq. (4.24) into Eq. (4.12) for the average current in the system and after some simplifications obtain:

$$\bar{J}^{(2)} = -\frac{f_1^2}{L}\,\frac{k_0}{r_0}\,\sum_{l=1}^{L}\,(\,A^{*(1)}_{l+1}\nu_l \,+\, A^{(1)}_{l+1}\nu^*_l \,-\, A^{*(1)}_l \nu_{l+1} \,-\, A^{(1)}_l \nu^*_{l+1}\,)\,, \tag{4.25}$$

with $A^{(1)}_l$ given by Eq. (4.21). For any given choice of the rates ν_l, this general expression can be used to explicitly evaluate the net *DC* current in the system.

We now consider two special choices of the rates $\{\nu_l\}$.

(i) The choice $\alpha_1 = \alpha_L = 1$, all other $\alpha_l = 0$, and $\phi_1 = 0, \phi_L = \phi$ corresponds to the two-site pumping problem. In the limit of large L, this gives:

$$\bar{J}^{(2)} = \left(\frac{f_1}{f_0}\right)^2 \frac{k_0 \omega \sin\phi}{L}\,\mathrm{Re}[z_-]. \tag{4.26}$$

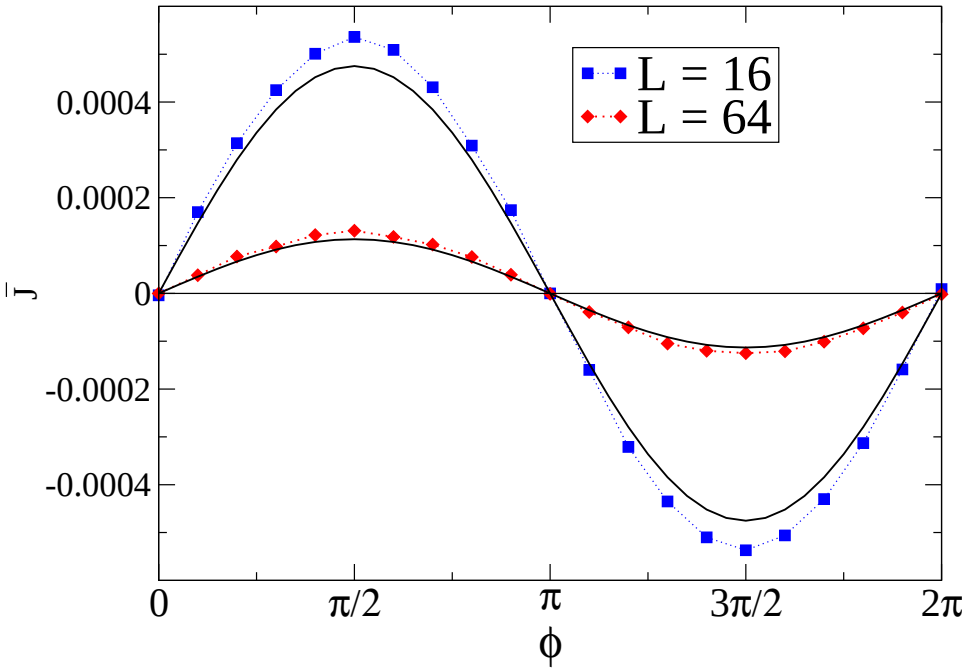

Figure 4.2: Plot of current $\bar{J}$ versus the phase difference ϕ. For parameters as in Fig. (4.4). The solid lines are from the perturbation theory.

Writing $z_+ = re^{i\eta}$, we find that for $\omega \ll \omega^* = 2f_0$, the magnitude $r \approx 1 + \sqrt{\omega/\omega^*}$ and the angle $\eta \approx \sqrt{\omega/\omega^*}$. In the opposite limit, $r \approx 2\omega/\omega^*$ and $\eta \approx \pi/2 - \omega^*/\omega$. Using $z_+ = 1/z_-$, we find that the current has the scaling form:

$$\bar{J}^{(2)} = \frac{f_1^2 k_0 \sin\phi}{f_0 L} G\left(\frac{\omega}{2f_0}\right), \tag{4.27}$$

where the scaling function $G(x) = 2x$ for $x \ll 1$ and $1/x$ for $x \gg 1$. We summarize the most interesting features of the above result. These are: (1) A *DC* current $\bar{J}$ is obtained, which decays with system size L as $\bar{J} \sim 1/L$. (2) The *DC* current $\bar{J}$ depends sinusoidally on the phase difference between rates at two sites. (3) The dependence of $\bar{J}$ on driving frequency ω shows a peak at a frequency ω^* with $\bar{J} \to 1/\omega$ as $\omega \to \infty$ and $\bar{J} \to \omega$ as $\omega \to 0$. The latter result means that a finite number of particles are circulated even in the adiabatic limit. We discuss this point in detail in Sec. (4.5). We have performed direct numerical simulations of the time-dependent SEP and compared them with our analytic results. We plot $\bar{J}$ versus phase difference ϕ and driving frequency ω in Figs. (4.2) and (4.3) respectively.

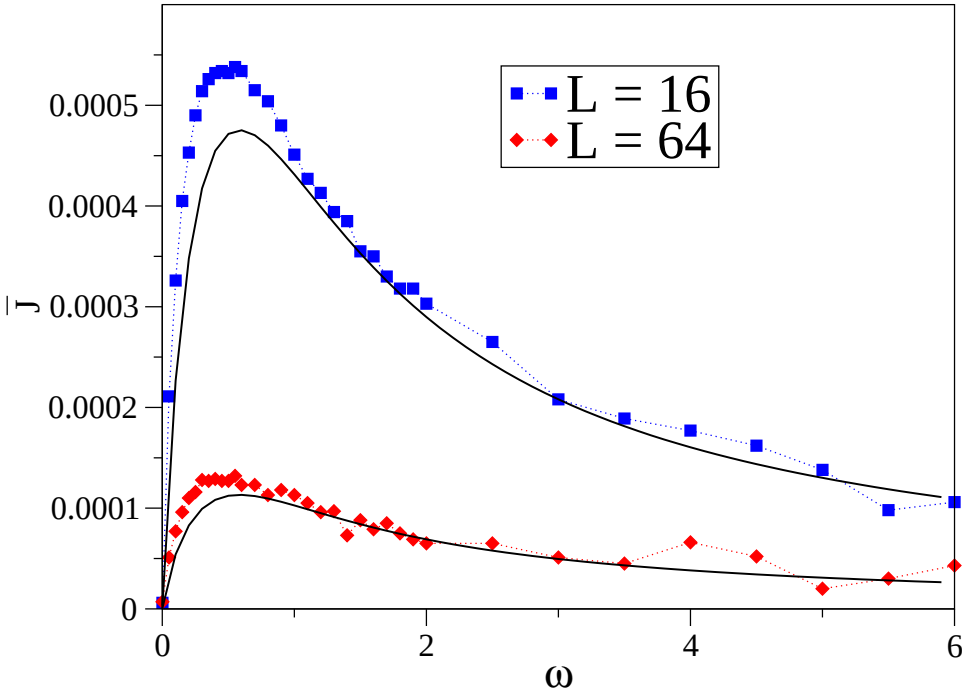

Figure 4.3: Plot of current $\bar{J}$ versus driving frequency ω for the same parameters as in Fig. (4.4). Solid lines are from perturbation theory.

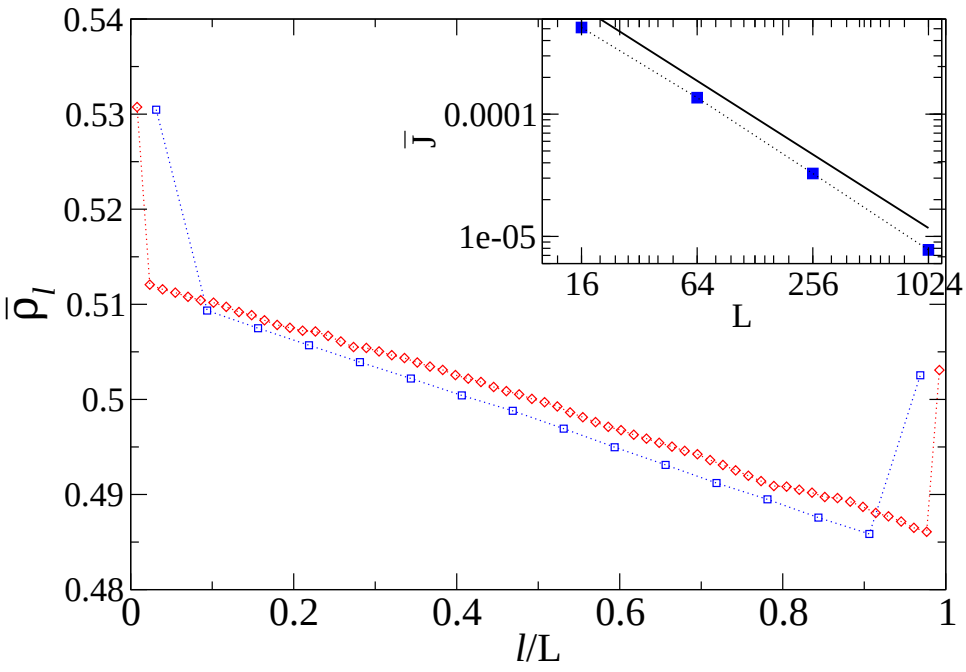

Figure 4.4: Plot of $\mathcal{DC}$ density $\bar{\rho}_l$ across the ring for $f_0 = 0.3$, $f_1 = 0.2$, $\omega = 0.2\pi$ and $\phi = \pi/2$ at half filling for two system sizes obtained from simulations. Inset: $\mathcal{DC}$ current (from simulations) $\bar{J} \sim 1/L$ as shown by solid line of slope -1.

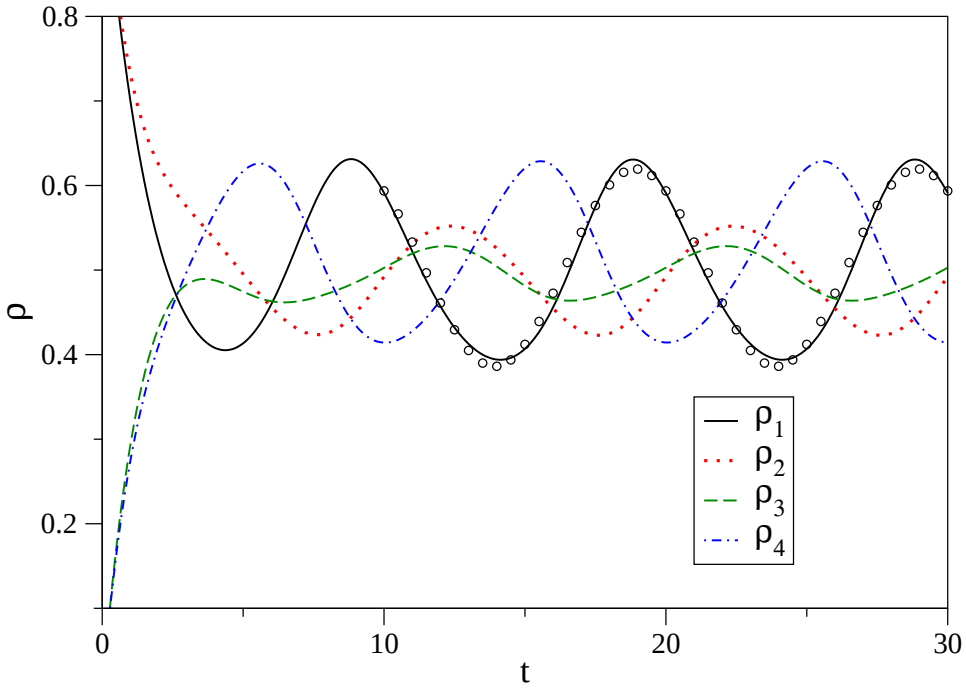

Figure 4.5: Plot of time-dependent densities at the four sites of a $L = 4$ lattice. In the initial configuration, sites 1 and 2 have one particle each and other sites are empty. The averages over one time period give: $\bar{\rho}_1 = 0.503493$, $\bar{\rho}_2 = 0.498702$, $\bar{\rho}_3 = 0.497417$, $\bar{\rho}_4 = 0.500388$ and $\bar{J} = 0.000514$. The points show the curve $\rho + f_1\rho_1^{(1)} + f_1^2\rho_1^{(2)}$. [Parameters: $f_0 = 0.4$, $f_1 = 0.1$, $\phi = \pi/2$ and $\omega = 0.2\pi$].

In the simulations we have also looked at the steady state density profiles. The results from simulation are shown in Fig. (4.4). The linear profile is expected since in the bulk of the system we have $J = -\nabla\rho$. From Eq. (4.15) it is clear that at first order correction, $\mathcal{DC}$ part $\bar{\rho}_l^{(1)}$ vanishes. Hence, we need to look at the higher order contribution, namely $\rho_l^{(2)}(t)$. This can be found exactly and has the form:

$$\rho_l^{(2)}(t) = \bar{\rho}_l^{(2)} + A_l^{(2)} e^{i2\omega\, t} \;+\; A_l^{*(2)} e^{-i2\omega\, t}. \tag{4.28}$$

The general expression for the $\mathcal{DC}$ part is given by:

$$\begin{aligned}
\bar{\rho}_l^{(2)} &= bl + h\,,\ l = 2, ..., L-1 \\
\bar{\rho}_1^{(2)} &= b + h + \frac{2}{f_0}\,\mathrm{Re}[\nu_1^*(A_{1,2}^{(1)} - A_1^{(1)})] \\
\bar{\rho}_L^{(2)} &= bL + h + \frac{2}{f_0}\,\mathrm{Re}[\nu_L^*(A_{L-1,L}^{(1)} - A_L^{(1)})]\,,
\end{aligned} \tag{4.29}$$

where the slope b of the linear density profile is given by

$$b = \frac{2}{L f_0} \, \mathrm{Re}[\nu_1^*(A_{1,2}^{(1)} - A_{1,L}^{(1)}) + \nu_L^*(A_{1,L}^{(1)} - A_{L-1,L}^{(1)})] \, , \tag{4.30}$$

and the intercept h can be found using the particle conservation condition $\sum_l \rho_l^{(2)} = 0$. This agrees with the form seen in results in Fig. (4.4). Finally in Fig. (4.5) we plot the density $\rho_l(t)$ as a function of time for $L = 4$ and $N = 2$ problem, which can be exactly solved numerically. As can be seen, the results from the perturbation theory match very well with the exact ones.

We also note that $\bar{J}$ is independent of f_0 for large x. This can be seen by writing the master equation as:

$$\frac{d\mathbf{P}}{d(\omega t)} = \frac{f_0}{\omega}\mathbf{W_0}\mathbf{P(t)} + \frac{f_1}{\omega}\mathbf{W_1}\mathbf{P(t)} \, . \tag{4.31}$$

For $\omega \gg f_0$, the first term on the right hand side can be neglected thus giving the probability distribution to be a function of f_1/ω.

(ii) The second case we consider is one where $\alpha_l = 1$ at all sites and $\phi_l = ql$, where $q = 2\pi s/L$ with $s = 1, 2...L/2$, so that there is a constant phase difference q between successive sites. In this case, $A_l^{(1)}$'s given by Eq. (4.20), evaluated at large L gives:

$$\begin{aligned} A_l^{(1)} &= \frac{ir_0}{2f_0} e^{iql} a \\ \text{where } a &= \frac{1 - \cos q}{y/2 - \cos q} \end{aligned} \tag{4.32}$$

and from Eq. (4.25) we get for the average current:

$$\begin{aligned} \bar{J}^{(2)} &= -\frac{f_1^2 k_0}{f_0} \sin q \, \mathrm{Im}[a] \\ &= \frac{2 \, f_1^2 \, k_0 \, \omega \, \sin q \, (1 - \cos q)}{[\, \omega^2 \, + \, 4 f_0^2 \, (1 - \cos q)^2 \,]} \, . \end{aligned} \tag{4.33}$$

Thus we see that for most values of q we get a finite current, even in the limit $L \to \infty$. For $q \sim 1/L$ and $q \sim \pi - 1/L$, the current goes to zero for large system size as $\bar{J} \sim L^{-3}$. From the current expression in Eq. (4.33), we can find out the value $q = q^*$, at which the current is a

maximum. By differentiating Eq. (4.33) with respect to q we get:

$$\cos(q^*) = (1 + \Omega^2) - \sqrt{(1 + \Omega^2)^2 - (1 - \Omega^2)}, \tag{4.34}$$

where $\Omega = \omega/2f_0$. It turns out that for large ω the maximum is at $q^* = 2\pi/3$, while for small frequencies we get $q^* \sim \sqrt{\omega}$. Also we find from Eq. (4.33) that in the adiabatic and fast drive limits, the currents are respectively given by:

$$\bar{J}^{(2)} \begin{cases} = \frac{f_1^2 k_0}{2 f_0^2} \cot(q/2)\, \omega & \omega/f_0 << (1 - \cos q) \\ = 2 f_1^2 k_0 \sin q (1 - \cos q)\, \frac{1}{\omega} & \omega/f_0 >> 1\ . \end{cases} \tag{4.35}$$

The perturbation theory results turn out to be quite accurate, as can be seen from the comparisons with simulation results, shown in Figs. (4.6) and (4.7), for different choices of q namely $q = \pi/2$ and $q = 2\pi/L$, for case (ii) discussed above. In these figures we have plotted the current for different system sizes and verify the $\bar{J} \sim L^0$ dependence and $\bar{J} \sim L^{-3}$ dependence for these two q's. Using the expression for k_0 in Eqs. (4.26, 4.33), we find that $\bar{J}^{(2)} \sim \rho^2(1 - \rho)$ which has a maximum at $\rho^* = 2/3$ and breaks particle-hole symmetry. This particle-hole asymmetry can be understood easily. From the definition of the model we see that, unlike the particles, the hopping rates of a hole are not symmetric: a hole at site l hops towards right with rate u_{l+1} and left with u_{l-1}. In Fig. (4.8) we have plotted simulation results for the average current as a function of particle density, for different system sizes, and find good agreement with our perturbative result, even at a relatively large value of f_1/f_0.

In simulations we have looked at the density profiles and find that the site wise density profile $\bar{\rho}_l$ in case (ii) is flat. This is unlike in case (i), where we found high densities at the two special sites and then a linear density profile in the bulk (see Fig. (4.4)). The flat density profile, for case (ii), is understood because here there are no special *pumping* sites. It is interesting that we can get current in the system even in the absence of Fick's law. We also note that even if the hop-out rates are made biased in one direction, like in the asymmetric exclusion process (ASEP), we can still get a current opposing this bias (for small biases).

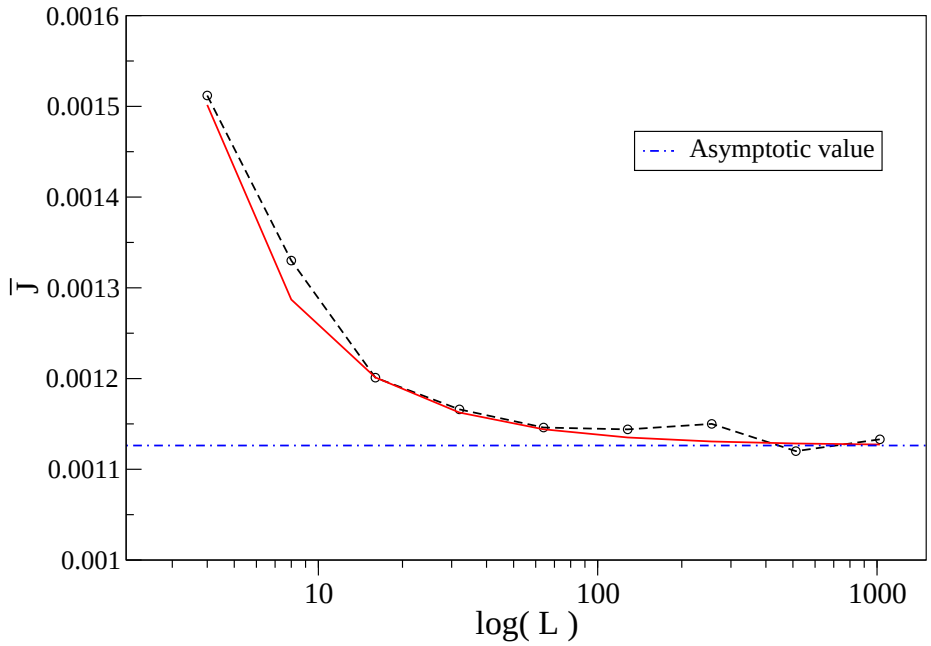

Figure 4.6: Plot of $\mathcal{DC}$ current $\bar{J}$ versus system size L for parameters $f_0 = 0.5$, $f_1 = 0.1$, $\omega = 0.2\pi$ and for $q = \pi/2$. Continuous line from perturbation theory and dotted line from simulations. $\bar{J}$ goes to a constant value can also be seen from Eq. (4.33) for this phase difference.

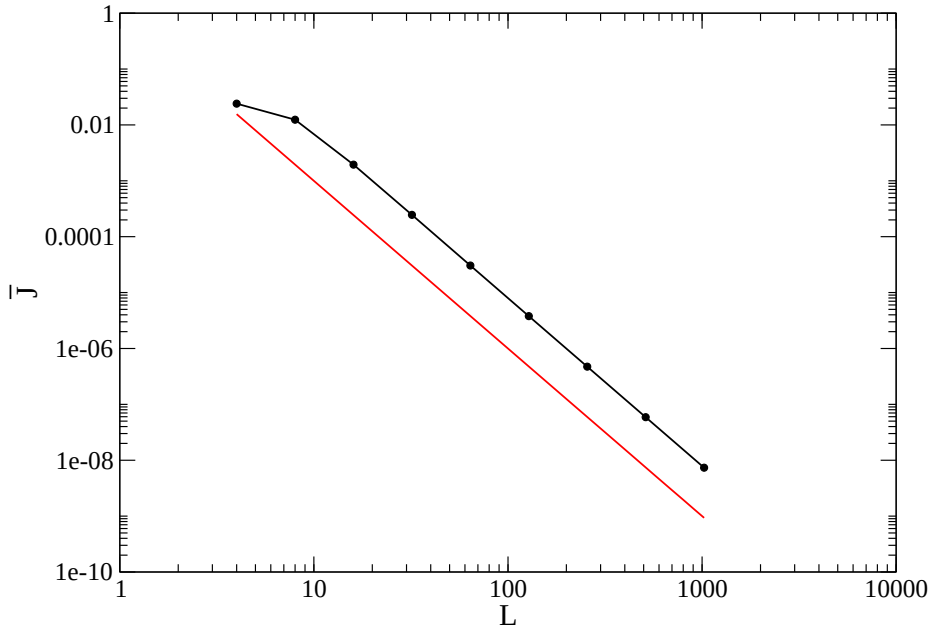

Figure 4.7: Log-log plot of $\mathcal{DC}$ current $\bar{J}$ (dotted line from Eq. (4.33), numerical values) versus system size L for $q = 2\pi/L$. The current decays as $1/L^3$ (continuous line) as predicted by Eq. (4.33). Parameter values are $f_0 = 0.5$, $f_1 = 0.4$, $\omega = 0.2\pi$.

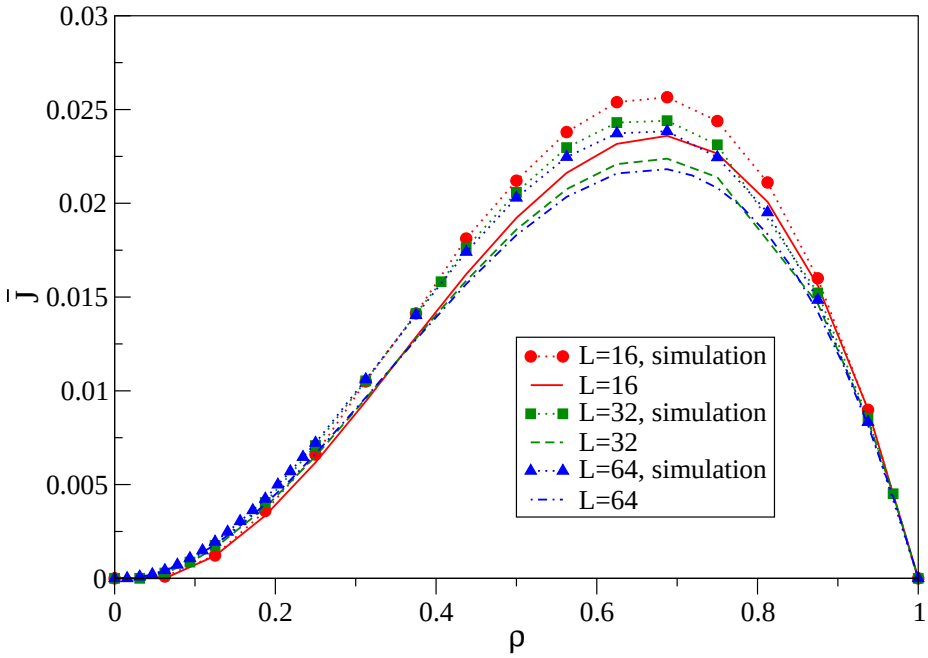

Figure 4.8: Plot of *DC* current $\bar{J}$ versus density $\rho = N/L$ for parameters $f_0 = 0.5$, $f_1 = 0.4$, $\omega = 0.2\pi$ and $\phi_l = \pi l/2$ for system sizes $L = 16, 32$ and 64. Both the results from simulations (symbols connected by dotted lines) and from the perturbation theory (lines) are plotted.

4.4 Perturbation theory in $1/\omega$

In this section, we find the *DC* current within sudden approximation following the procedure of [126]. Calling $\theta = \omega t$, the master equation Eq. (4.2) can be rewritten as

$$\frac{d\mathbf{P}(\theta)}{d\theta} = \frac{1}{\omega}\left[\mathbf{W_0} + \mathbf{W_1}(\theta)\right]\mathbf{P}(\theta) \tag{4.36}$$

which can be expanded in powers of $1/\omega$ by using $\mathbf{P}(\theta) = \sum_{n=0}^{\infty} \omega^{-n}\mathbf{P}^{(n)}(\theta)$ to give

$$\frac{d\mathbf{P}^{(0)}}{d\theta} = 0 \tag{4.37}$$

$$\frac{d\mathbf{P}^{(1)}(\theta)}{d\theta} - \mathbf{W_1}(\theta)\mathbf{P}^{(0)} = \mathbf{W_0}\mathbf{P}^{(0)} \tag{4.38}$$

and so on. From the zeroth order equation, we see that $\mathbf{P}^{(0)}$ is independent of θ. In fact, for $\omega \to \infty$, we expect the system to behave as the unperturbed homogeneous SEP for which $\mathbf{W_0}\mathbf{P}^{(0)} = 0$ is satisfied and as discussed in Section 4.2, all the elements of the vector $\mathbf{P}^{(0)}$ are known. Using this fact, the first order correction $\mathbf{P}^{(1)}$ can be found by integrating Eq. (4.38)

over θ. Following steps as those leading to Eq. (4.12), we now get an average current, $\bar{J_s}$, at order $O(1/\omega)$. This is given by:

$$\bar{J}_s^{(1)} = \frac{f_1}{2\pi\omega L}\int_0^{2\pi} d\theta \sum_{l=1}^{L}(v_{l+1}-v_l)C_{l,l+1}^{[1]} \tag{4.39}$$

where we have expanded the nearest neighbor correlation function $C_{l,l+1} = \sum_{n=0}^{\infty}\omega^{-n}C_{l,l+1}^{[n]}$ in powers of $1/\omega$ and again use the expression for $C_{l,l+1}^{[0]} = C_{l,l+1}^{(0)}$ given by Eq. (4.9). The first order correction to correlation function can be obtained by perturbatively expanding Eq. (4.4) and obeys the following simple equation:

$$\frac{dC_{l,l+1}^{[1]}}{d\theta} = f_1 k_0\,(v_{l+2}+v_{l-1}-v_l-v_{l+1})\,. \tag{4.40}$$

We now again discuss the two special choices of rates v_l, discussed in the previous section.

(i) In this case, only two sites have time-dependent hopping rates. Solving the equations above for the correlation function, we get:

$$C_{1,2}^{[1]} = f_1 k_0(\cos(\theta)-\cos(\theta+\phi)) + c_{1,2} \tag{4.41}$$

$$C_{L-1,L}^{[1]} = -f_1 k_0(\cos(\theta)-\cos(\theta+\phi)) + c_{L-1,L} \tag{4.42}$$

$$C_{L,1}^{[1]} = f_1 k_0(\cos(\theta)+\cos(\theta+\phi)) + c_{L,1} \tag{4.43}$$

where c's are constant of integration (which do not contribute to current). Using the above equations in the expression for $\bar{J}_s^{(1)}$, we finally obtain

$$\bar{J}_s^{(1)} = \frac{2f_1^2 k_0 \sin\phi}{\omega L}\,. \tag{4.44}$$

Thus, we find that to leading order in $1/\omega$ (and arbitrary f_1), the *DC* current is the same as the one obtained by taking large ω limit in the current expression Eq. (4.27) obtained from the f_1 expansion.

(ii) In this case with $\alpha_l = 1$ at all sites, the equations for the first order correlation functions can be solved for arbitrary phases ϕ_l, and we get:

$$C_{l,l+1}^{[1]} = k_0 f_1\left[\cos(\theta+\phi_l)+\cos(\theta+\phi_{l+1})-\cos(\theta+\phi_{l-1})\cos(\theta+\phi_{l+2})\right]\,. \tag{4.45}$$

Using these in the current expression and after some simplifications, we get:

$$\bar{J}_s^{(1)} = \frac{k_0 f_1^2}{\omega L} \sum_{l=1}^{L} \left[2\sin(\phi_{l+1} - \phi_l) - \sin(\phi_{l+1} - \phi_{l-1}) \right] . \tag{4.46}$$

Note that the above expression depends on the phase difference between nearest and next nearest neighbor sites. For $\phi_l = ql$, we recover the result stated in the second line of Eq. (4.35).

4.5 Adiabatic calculation

We now discuss an adiabatic calculation similar to that of Astumian for a two state model [123]. The model considered by Astumian consists of a single site connected to two reservoirs with input rates $\alpha_1(t)$, $\alpha_2(t)$ and output rates $\beta_1(t), \beta_2(t)$. The rate equation of the particle density at the site is given by:

$$\begin{aligned} \frac{dQ}{dt} &= I_1 + I_2 \\ \text{where } I_1 &= \alpha_1(1-Q) - \beta_1 Q, \quad I_2 = \alpha_2(1-Q) - \beta_2 Q \, . \end{aligned} \tag{4.47}$$

The instantaneous rates satisfy the conditions, $\alpha_1(t)/\beta_1(t) = \alpha_2(t)/\beta_2(t) = e^{\epsilon(t)}$ and $\alpha_2(t)/\alpha_1(t) = \beta_2(t)/\beta_1(t) = e^{u(t)}$. For low driving frequencies $Q(t)$ can be expanded about the instantaneous equilibrium solution $Q^{(0)}(t)$ as $Q(t) = Q^{(0)}(t) + \omega Q^{(1)}(t)$, where $Q^{(0)}$, $Q^{(1)}$ satisfy the following equations:

$$\alpha_1(1 - Q^{(0)}) - \beta_1 Q^{(0)} = \alpha_2(1 - Q^{(0)}) - \beta_2 Q^{(0)} = 0 \tag{4.48}$$

$$\frac{dQ^{(0)}}{dt} = -\omega(\alpha_1 + \beta_1 + \alpha_2 + \beta_2) Q^{(1)} \tag{4.49}$$

The instantaneous equilibrium solution, from Eq. (4.48) is:

$$Q^{(0)} = \frac{\alpha_1}{\alpha_1 + \beta_1} = \frac{1}{1 + e^{-\epsilon}} \, . \tag{4.50}$$

The net particle transport $\mathcal{N}$ (from reservoir 1 into system) over one period $T = 2\pi/\omega$ can be written as:

$$\begin{aligned} \mathcal{N} &= \int_0^T I_1 dt = -\int_0^T (\alpha_1 + \beta_1)\omega Q^{(1)} dt \\ &= \int_0^T \frac{\alpha_1 + \beta_1}{\alpha_1 + \beta_1 + \alpha_2 + \beta_2} \frac{dQ^{(0)}}{dt}\, dt = \int_C F\, dQ^{(0)}, \end{aligned}$$

$$\text{with} \quad F = \frac{1}{(1+e^{u})}\,, \tag{4.51}$$

and where $\int_C$ denotes the integral over a cycle.

In our case formally one can obtain an exact expression for the net particle transport. For this we start with the master equation $\partial\mathbf{P}/\partial t = \mathbf{W}(t)\mathbf{P}$. Let $\mathbf{P}^{(0)}(t)$ be the instantaneous equilibrium solution satisfying $\mathbf{W}(t)\mathbf{P}^{(0)} = 0$. Then, for slow rates ω, $\mathbf{P}(t)$ will have the form $\mathbf{P}^{(0)}(t) + \omega\mathbf{P}^{(1)}(t)$ where the correction is given by: $\omega\mathbf{P}^{(1)} = \mathbf{W}^{-1}\,\partial\mathbf{P}^{(0)}/\partial t$. The net particle transported across any bond in one time cycle, $\mathcal{N}$, can then be expressed as:

$$\mathcal{N} = \int_0^T dt \sum_C J(C)P(C,t) = -\int_0^{2\pi} dx \sum_{C,C'} J(C)\frac{\partial W^{-1}_{C,C'}(x)}{\partial x} P^{(0)}(C',x)\,, \tag{4.52}$$

where J refers to the current on any given bond. Thus we have a formal expression, for the net particle transported, in terms of an integral over an *equilibrium average* of some quantity. However this expression does not appear to have any simple physical interpretation and neither is it easy to obtain any explicit results, unlike the fast case treated in section (4.4). The above equation has to be interpreted carefully, since $\mathbf{W}$ has a zero eigenvalue and $\mathbf{W}^{-1}$ is not strictly defined.

4.6 Conclusions

Here we have considered a lattice model of diffusing particles with hard core interactions and shown that if the hopping rates at various sites are made time-dependent, but still symmetric, then a *DC* current can be generated in the system. Thus, a ratchet effect is obtained in the sense that a directed current occurs even though there is no applied external biasing

force. Unlike many other examples of models of classical ratchets, there is no asymmetric potential in our model. However asymmetry is incorporated in the modulation of the hopping rates, and this is best seen when we consider the case where the modulation is given by $v_l(t) = \sin(\omega t - ql)$. This of-course corresponds to a wave travelling in a *g*iven direction. A non-trivial aspect of the problem studied is the fact that the effect goes away as soon as we switch off the hard-core interactions. For non-interacting the *DC* current is given by $\bar{J} = (1/LT)\int_0^T dt \ \sum_{l=1}^{L} u_l\rho_l - u_{l+1}\rho_{l+1}$, and is seen to be exactly zero, for arbitrary choice of the time-dependent rates. On the other hand, having interactions in the system is not a sufficient condition to generate a *DC* current. For the models considered in this chapter, the hopping rate is site-wise symmetric. But if the hopping rates are symmetric bond-wise, *i.e.*, the hop rate $u_{l,l+1}$ from site l to $l+1$ is the same as that from $l+1$ to l, then the *DC* current is zero for any choice of phases ϕ_l. To see this, consider the density evolution equation obeyed by bond-wise symmetric SEP:

$$\frac{\partial \rho_l}{\partial t} = u_{l-1,l}(\rho_{l-1} - \rho_l) + u_{l,l+1}(\rho_{l+1} - \rho_l) \tag{4.53}$$

Unlike Eq. (4.3) for site-wise symmetric SEP, $\rho_l = \rho$ is a solution of the above equation for any choice of rates u_l. In fact, an inspection of the master equation shows that, even with a time-dependent **W**-matrix, all configurations are equally likely, thus leading to the zero current. Thus the exclusion process with bond-wise symmetric rates does not give the ratchet effect. It is not completely clear as to what are the necessary and sufficient conditions to get a directed current.

For the model considered here, since the equations for any *n*-point correlation function do not close, it does not seem simple to solve the model exactly. We have therefore studied the system analytically using a perturbation theory in the amplitude f_1 and the inverse frequency $1/\omega$. In this study, we have been able to obtain the *DC* current at order f_1^2 by solving the evolution equations for density and two point correlation function to order f_1. Also, we have been able to obtain results for large driving frequency by solving the correlation function alone by such perturbative approaches. Comparing with simulations we find that

the perturbative results turn out to be quite accurate.

Finally, we point out that an experimental realization of the effect observed in our model should be possible in colloidal systems. For instance, consider a colloidal suspension in an externally applied laser field. This constitutes a system of diffusive interacting particles in an external potential (generated by the laser field) of the form $V(x,t) = V_0 \sin(\omega t - qx)$. This system is similar to the model that we have studied. There are some differences, namely, in this case because the external field is space dependent, hence the effective hopping rates are not symmetric in the forward and backward directions. It would be interesting to study this model to see if a current can be generated here, and perhaps one can make detailed predictions for experimental observation.

Bibliography

[1] C. Bustamante, J. Liphardt and F. Ritort, Physics Today 43 (July 2005).

[2] M. J. Perrin, *Brownian Movement and Molecular Reality*, page 6 (Taylor and Francis, London, 1910).

[3] C. Jarzynski, Phys. Rev. Lett. **78**, 2690 (1997).

[4] C. Jarzynski, Phys. Rev. E **56**, 5018 (1997).

[5] E. G. D. Cohen, D. Mauzerall, J. Stat. Mech. P07006 (2004).

[6] C. Jarzynski, J. Stat. Mech: Theor. Exp. P09005 (2004).

[7] D. J. Evans, E G. D. Cohen, and G. P. Morriss, Phys. Rev. Lett. **71**, 2401 (1993).

[8] D. J. Evans and D. J. Searles, Phys. Rev. E **50**, 1645 (1994).

[9] G. Gallavotti and E. G. D. Cohen, Phys. Rev. Lett. **74**, 2694(1995).

[10] G. E. Crooks, Phys. Rev. E **60**, 2721 (1999).

[11] Udo Seifert, Phys. Rev. Lett. **95**, 040602 (2005)

[12] J. Kurchan, J. Phys. A: Math. Gen. **31**, 3719 (1998).

[13] J. L. Lebowitz and H. Spohn, J. Stat. Phys. **95**, 333 (1999).

[14] C. Maes, J. Stat. Phys. **95**, 367 1999.

[15] O. Narayan and A. Dhar, J. Phys. A: Math. Gen. **37** 63 (2004).

[16] R. van Zon and E. G. D. Cohen, Phys. Rev. Lett. **91**, 110601 (2003).

[17] R. van Zon, S. Ciliberto and E. G. D. Cohen, Phys. Rev. Lett. **92**, 130601 (2004).

[18] R. Marathe and A. Dhar, Phys. Rev. E **72**, 066112 (2005).

[19] J. Liphardt *et al.*, Science **296**, 1832 (2002).

[20] G. M. Wang *et al.*, Phys. Rev. Lett. **89**, 050601 (2002).

[21] K. Feitosa and N. Menon, Phys. Rev. Lett. **92**, 164301 (2004).

[22] S. Aumatre *et al.*, Eur. Phys. J. B **19**, 449 (2001).

[23] W. I. Goldburg, Y. Y. Goldschmidt and H. Kellay, Phys. Rev. Lett. **87**, 245502 (2001).

[24] N. Garnier and S. Ciliberto, Phys. Rev E **71**, 060101(R) (2005).

[25] F. Douarche *et al.*, Europhys. Lett. **70**, 593 (2005).

[26] G. Hummer and A. Szabo, Proc. Natl. Acad. Sci **98**, 3658 (2001).

[27] J. Gore, F. Ritort and C. Bustamante, Proc. Natl. Acad. Sci. **100**, 12564 (2003).

[28] R. F. Fox, Proc. Natl. Acad. Sci. **100**, 12537 (2003).

[29] S. Park *et al.*, J. Chem. Phys. **119**, 3559 (2003).

[30] T. Tome and M. J. de Oliveira, Phys. Rev. A **41**, 4251(1990).

[31] M. Rao, H. R. Krishnamurthy and R. Pandit, Phys. Rev. B **42**, 856 (1990).

[32] B. Chakrabarti and M. Acharyya, Rev. Mod. Phys. **71**, 847 (1999).

[33] S. W. Sides, P. A. Rikvold, and M. A. Novotny, Phys. Rev. E **57**, 6512 (1998).

[34] F. Ritort, C. Bustamante and I. Tinoco Jr., Proc. Natl. Acad. Sci. **99**, 13544 (2002).

[35] A. Imparato and L. Peliti, Europhys. Lett., **69**, 643 (2005).

[36] T. Speck and U. Seifert, Phys. Rev. E **70**, 066112 (2004).

[37] A. Dhar, Phys. Rev. E **71**, 36126 (2005).

[38] Petr Chvosta *et al.*, Phys. Rev. E **75**, 041124 (2007).

[39] Evzen Subrt and Petr Chvosta, J. Stat. Mech. P09019 (2007).

[40] A. M. Jayannavar and M. Sahoo, Phys. Rev. E **75**, 032102 (2007).

[41] S. Saikia *et al.*, Phys. Lett. A **369**, 367 (2007).

[42] M. Sahoo *et al.*, arXiv:0708.0496v2 (2007).

[43] P. Jop, A. Petrosyan, S. Ciliberto, EPL **81**, 5, 50005 (2008).

[44] S. Joubaud, N. B. Garnier, S. Ciliberto, EPL **82** 3, 30007 (2008).

[45] I. Dornic and C. Godrche, J. Phys. A **31**, 5413 (1998).

[46] T.J. Newman and Z. Toroczkai, Phys. Rev. E **58**, R2685 (1998).

[47] A. Dhar and S. N. Majumdar, Phys. Rev. E **59**, 6413 (1999).

[48] C. Chatelain, J. Stat. Mech: Theor. Exp. **18** P06005 (2006).

[49] R. Feynman, R. Leighton, and M. Sands, *The Feynman Lectures on Physics* (Adison-Wesley, Reading Massachussets, vol.1, chap. 46, 1966).

[50] J. M. R. Parrondo and P. Español, Am. J. Phys. **64**, 1125 (1996).

[51] M.O.Magnasco and G.Stolovitzky, J. Stat. Phys. **93**, 615 (1998).

[52] C. Jarzynski and O. Mazonka, Phys. Rev. E **59**, 6448 (1999).

[53] C. van den Broeck, R. Kawai, and P. Meurs, Phys. Rev. Lett. **93**, 090601 (2004).

[54] C. Van den Broeck and R. Kawai, Phys. Rev. Lett. **96**, 210601 (2006).

[55] A. L. R. Bug, B. J. Berne, Phys. Rev. Lett. **59** 948 (1987).

[56] R. Bartussek, P. Hanggi, J. G. Kissner, Europhys. Lett. **28** 459 (1994).

[57] N. G. van Kampen, Z. Phys. B **68**,135 (1987).

[58] A. M. Jayannavar, M. C. Mahato, Pramana-J. Phys. **45**, 369 (1996).

[59] N. G. van Kampen, IBM J. Res. Develop. **32** 107 (1988).

[60] K. Sekimoto, J. Phys. Soc. Jpn. **68**, 1448 (1999).

[61] M. Matsuo, S. Sasa, Physica A **276**, 188 (2000).

[62] J. D. Bao, Y. Abe, Y. Z. Zhuo, Physica A **265**, 111 (1999).

[63] R. H. Luchsinger, Phys. Rev. E **62**, 272 (2000).

[64] K. Sekimoto, Jr. Phy. Soc. Jpn. **66**, 1234 (1997).

[65] T. Hondou and F. Takagi, J. Phy. Soc. Jpn. **67**, 2974 (1998).

[66] H. Kamegawa, T. Hondou, and F. Takagi, Phys. Rev. Lett. **80**, 5251 (1998).

[67] F. Takagi and T. Hondou, Phys. Rev. E **60**, 4954 (1999).

[68] J. M. R. Parrondo and B. J. de Cisneros, Applied Physics A: Materials Science & Processing **75**, 179 (2002).

[69] I. M. Sokolov, Phys. Rev. E **60**, 4946 (1999).

[70] H. Sakaguchi, J. Phy. Soc. Jpn. **67**, 709 (1998).

[71] Y. Lee *et al.*, Phys. Rev. Lett. **91**, 220601 (2003).

[72] M. O. Magnasco, Phys. Rev. Lett. **71**, 1477 (1993).

[73] I. Derényi and T. Vicsek, Phys. Rev. Lett. **75**, 374 (1995).

[74] F. Jülicher, A. Ajdari, and J. Prost, Rev. Mod. Phys. **69**, 1269 (1997).

[75] P. Reimann, Phys. Rep. **361**, 57 (2002).

[76] R. D. Astumian, Science **276**, 917 (1997).

[77] R. D. Astumian and P. Hanggi, Phys. Today **55**, No. 11, 33 (2002).

[78] J. M. R. Parrondo, Phys. Rev. E **57**, 7297 (1998).

[79] O. Usmani, E. Lutz and M. Buttiker, Phys. Rev. E **66**, 021111 (2002).

[80] T. Feldmann, E. Geva, R. Kosloff, and P. Salamon, Am. J. Phys. **64**, 485 (1996).

[81] I. Derényi and R. D. Astumian, Phys. Rev. E **59**, 6219 (1999).

[82] A. Gomez-Marin and J. M. Sancho, Phys. Rev. E **71**, 021101 (2005).

[83] A. Gomez-Marin and J. M. Sancho, Phys. Rev. E **73**, 045101 (2006).

[84] M. C. Mahato, T. P. Pareek, and A. M. Jayannavar, International Journal of Modern Physics B **10**, 3857 (1996).

[85] R. D. Astumian and I. Dernyi, European Biophysics Journal **27**, 474 (1997).

[86] M. Buttiker, H. Thomas, and A. Pretre, Z. Phys. B. **94**, 133 (1994).

[87] P.W. Brouwer, Phys. Rev. B **58**, R10135 (1998).

[88] L. Arrachea, Phys. Rev. B **72**, 125349 (2005a).

[89] L. Arrachea, Phys. Rev. B **72**, 121306 (2005b).

[90] M. Strass, P. Hänggi, and S. Kohler, Phys. Rev. Lett. **95**, 130601 (2005).

[91] S. Kohler, J. Lehmann, and P. Hänggi, Phy. Rep. **406**, 379 (2005).

[92] A. Agarwal and D. Sen, J. Phys. Condens. Matter **19**, 046205 (2007).

[93] M. Switkes *et al.*, Science **283**, 1905 (1999).

[94] P. Leek *et al.*, Phys. Rev. Lett. **95**, 256802 (2005).

[95] D. Segal and A. Nitzan, Phys. Rev. E **73**, 026109 (2006).

[96] R. Glauber, Jr. Math. Phys. **4**, 294 (1963).

[97] T. Liggett, *Interacting particle systems* (Springer-Verlag, New York, 1985).

[98] B. Schmittmann and R. K. P. Zia, in *Phase transitions and Critical Phenomena, vol. 17,* edited by C. Domb and J. Lebowitz (Academic Press, London, 1995).

[99] G.M. Schütz, in *Phase transitions and Critical Phenomena*, edited by C. Domb and J. Lebowitz (Academic Press, London, 2000), pp. 3–242.

[100] J.E. Santos and G.M. Schütz, Phys. Rev. E **64**, 036107 (2001).

[101] R. B. Stinchcombe and G. M. Schütz, Phys. Rev. Lett. **75**, 140 (1995).

[102] H. Spohn, J. Phys. A **16**, 4275 (1983).

[103] B. Derrida, J. L. Lebowitz, and E. R. Speer, J. Stat. Phys. **107**, 599 (2002).

[104] B. Derrida, B. Douçot, and P.-E. Roche, J. Stat. Phys. **115**, 717 (2004).

[105] V. Gupta *et al.*, Chem. Phys. Lett. **247**, 596 (1995).

[106] K. Hahn, J. Kärger, and V. Kukla, Phys. Rev. Lett. **76**, 2762 (1996).

[107] V. Kukla *et al.*, Science **272**, 702 (1996).

[108] Q.-H. Wei, C. Bechinger, and P. Leiderer, Science **287**, 625 (2000).

[109] T. Chou, Phys. Rev. Lett. **80**, 85 (1998).

[110] T. Chou and D. Lohse, Phys. Rev. Lett. **82**, 3552 (1999).

[111] D. J. Thouless, Phys. Rev. B **27**, 6083 (1983).

[112] M. Büttiker, H. Thomas, and A. Prêtre, Z. Phys. B **94**, 133 (1994).

[113] I. Aleiner and A. Andreev, Phys. Rev. Lett. **81**, 1286 (1998).

[114] B. L. Altshuler and L. I. Glazman, Science **283**, 1864 (1999).

[115] P. Sharma and C. Chamon, Phys. Rev. Lett. **87**, 096401 (2001).

[116] O. Entin-Wohlman, A. Aharony, and Y. Levinson, Phys. Rev. B **65**, 195411 (2002).

[117] S. Watson, Phys. Rev. Lett. **91**, 258301 (2003).

[118] R. Citro, N. Andrei, and Q. Niu, Phys. Rev. B **68**, 165312 (2003).

[119] E. Sela and Y. Oreg, Phys. Rev. Lett. **96**, 166802 (2006).

[120] R.D. Astumian and I. Derenyi, Phys. Rev. Lett. **86**, 3859 (2001).

[121] N.A. Sinitsyn, I. Nemenman, Europhys. Lett. **77**, 58001 (2007).

[122] J. Ohkubo, J. Stat. Mech., P02011 (2008).

[123] R. D. Astumian, Phys. Rev. Lett. **91**, 118102 (2003).

[124] P. Jung, Phys. Rep. **234**, 175 (1993).

[125] R.D. Astumian and B. Robertson, J. Chem. Phys. **91**, 4891 (1989).

[126] P. Reimann *et al.*, Phys. Lett. A **215**, 26 (1996).